Mon. Not. R. Astron. Soc. **395,** 1409–1437 (2009) doi:10.1111/j.1365-2966.2009.14506.x

The death of massive stars – I. Observational constraints on the progenitors of Type II-P supernovae

S. J. Smartt,[1⋆] J. J. Eldridge,[2] R. M. Crockett[1] and J. R. Maund[3,4]

[1]*Astrophysics Research Centre, School of Mathematics and Physics, Queen's University Belfast, Belfast BT7 1NN*
[2]*Institute of Astronomy, The Observatories, University of Cambridge, Madingley Road, Cambridge CB3 0HA*
[3]*Department of Astronomy and McDonald Observatory, University of Texas, 1 University Station, C1400, Austin, TX 78712, USA*
[4]*Dark Cosmology Centre, Niels Bohr Institute, University of Copenhagen, Juliane Maries Vej 30, 2100 Copenhagen Ø, Denmark*

Accepted 2009 January 14. Received 2009 January 14; in original form 2008 September 2

ABSTRACT

We present the results of a 10.5-yr, volume-limited (28-Mpc) search for supernova (SN) progenitor stars. In doing so we compile all SNe discovered within this volume (132, of which 27 per cent are Type Ia) and determine the relative rates of each subtype from literature studies. The core-collapse SNe break down into 59 per cent II-P and 29 per cent Ib/c, with the remainder being IIb (5 per cent), IIn (4 per cent) and II-L (3 per cent). There have been 20 II-P SNe with high-quality optical or near-infrared pre-explosion images that allow a meaningful search for the progenitor stars. In five cases they are clearly red supergiants, one case is unconstrained, two fall on compact coeval star clusters and the other twelve have no progenitor detected. We review and update all the available data for the host galaxies and SN environments (distance, metallicity and extinction) and determine masses and upper mass estimates for these 20 progenitor stars using the STARS stellar evolutionary code and a single consistent homogeneous method. A maximum likelihood calculation suggests that the minimum stellar mass for a Type II-P to form is $m_{\rm min} = 8.5^{+1}_{-1.5}\,{\rm M}_{\odot}$ and the maximum mass for II-P progenitors is $m_{\rm max} = 16.5 \pm 1.5\,{\rm M}_{\odot}$, assuming a Salpeter initial mass function holds for the progenitor population (in the range $\Gamma = -1.35^{+0.3}_{-0.7}$). The minimum mass is consistent with current estimates for the upper limit to white dwarf progenitor masses, but the maximum mass does not appear consistent with massive star populations in Local Group galaxies. Red supergiants in the Local Group have masses up to $25\,{\rm M}_{\odot}$ and the minimum mass to produce a Wolf–Rayet star in single star evolution (between solar and LMC metallicity) is similarly 25–30 $\rm M_{\odot}$. The reason we have not detected any high-mass red supergiant progenitors above $17\,{\rm M}_{\odot}$ is unclear, but we estimate that it is statistically significant at 2.4σ confidence. Two simple reasons for this could be that we have systematically underestimated the progenitor masses due to dust extinction or that stars between 17–25 $\rm M_{\odot}$ produce other kinds of SNe which are not II-P. We discuss these possibilities and find that neither provides a satisfactory solution. We term this discrepancy the 'red supergiant problem' and speculate that these stars could have core masses high enough to form black holes and SNe which are too faint to have been detected. We compare the ^{56}Ni masses ejected in the SNe to the progenitor mass estimates and find that low-luminosity SNe with low ^{56}Ni production are most likely to arise from explosions of low-mass progenitors near the mass threshold that can produce a core-collapse.

Key words: stars: evolution – supergiants – supernovae: general – galaxies: stellar content.

1 INTRODUCTION

Stars which are born with masses above a critical threshold mass of around $8\,{\rm M}_{\odot}$ have long been thought to produce supernovae (SNe) when their cores collapse at a point when nuclear burning no longer provides support against gravity. SNe were first suggested to be a new class of astrophysical phenomena by Baade & Zwicky (1934) and since then detailed study has allowed them to be split into physical types: the thermonuclear explosions and core-collapse supernovae (CCSNe). The CCSNe form when their cores evolve to iron white dwarfs (WDs) and detailed stellar evolutionary

⋆E-mail: s.smartt@qub.ac.uk

models predict a minimum mass for this to occur of between 7 and 12 $M_{\odot}$ (Heger et al. 2003; Eldridge & Tout 2004b; Siess 2007; Poelarends et al. 2008). The CCSNe form a diverse group in terms of their spectral and photometric properties and the classification scheme has arisen primarily based on the appearance of their optical spectra, but also supplemented with their photometric behaviour (Filippenko 1997). There are the H-rich Type II SNe, which are subclassified into II-P (plateau light curves), II-L (linear decline light curves), IIn (narrow emission lines) and some peculiar events, generically labelled II-pec. The H-deficient SNe are split into Ib and Ic depending on whether He is visible and a hybrid class of IIb (Type II events which metamorphose into Ib SNe) has also been uncovered. The evolutionary stage of the progenitor star [i.e. its position in the Hertzsprung–Russell (HR) diagram and chemical composition of its atmosphere] very likely dictates what type of CCSN is produced.

Determining what types of stars produce which types of SNe and what mass range can support a CCSN is a major goal in modern studies of these explosions. The first attempts relied primarily on linking the results of stellar evolutionary models to the spectral (and photometric) evolution of the SNe (e.g. Chevalier 1976; Arnett 1980). More recently Hamuy (2003) and Nadyozhin (2003) have studied the light curves and ejecta velocities of II-P SNe to estimate the mass of the material ejected. These studies tend to favour quite large masses for progenitor stars, with Hamuy suggesting ranges of 10–50 $M_{\odot}$ and Nadyozhin 10–30 $M_{\odot}$. However, when SN 1987A exploded a new opportunity arose. The SN was in a galaxy close enough that its progenitor star could be easily identified. A blue supergiant star of around 15–20 $M_{\odot}$ was identified and it is clear that this object no longer exists (Gilmozzi et al. 1987; Walborn et al. 1989; Podsiadlowski 1992). The fact that it was a compact blue supergiant was a key factor in enabling the community to understand the event as a whole. A progenitor was also detected for the next closest explosion (SN 1993J in M81) and the binary nature of the progenitor helped understand the physical reason behind the II-b type given to the event (Podsiaklowski et al. 1993; Aldering, Humphreys & Richmond 1994).

Studies of the environments of CCSNe after discovery have been ongoing for many years with authors looking for correlations between the ages of star formation regions and the type of SNe that occur. For example, van Dyk (1992) and van Dyk, Hamuy & Filippenko (1996) suggested that there was no clear difference in the spatial distributions of Type Ib/c and Type II SNe compared to giant H II regions in their host galaxies. They concluded that they hence arose from parent populations of similar mass. However, recently both James & Anderson (2006) and Kelly, Kirshner & Pahre (2008) suggest that the stripped Type Ic SNe are more likely to follow regions of either high surface brightness or high Hα emission than Type II SNe. A larger sample of nearby core-collapse events and Hα correlations has been compiled by Anderson & James (2008) indicating that there is a progressive trend for Ib/c SNe to be associated with Hα emission regions, in the sense that Ic show the closest association with galactic Hα emission, then comes the Ib and then Type II. While these efforts are very valuable to discern differences in progenitor channel, it is difficult to assign definitive mass ranges to the progenitor systems from spatial correlations alone.

A much more direct way to determine the type of star that exploded is to search directly for progenitors in images of the host galaxies taken before explosion. The ease of access to large telescope data archives makes this search feasible for nearby events. There are now a number of groups around the world that are competitively searching for progenitor stars in such archive images. Particularly with the *Hubble Space Telescope* (*HST*) it has become possible to resolve massive stellar populations out to at least 20Mpc. In this case the information on each progenitor is much more detailed and quantitative than can be achieved with the unresolved environment studies, but there are fewer events which allow such a study.

Early work with *HST* concentrated on looking at the environments of SNe (Barth et al. 1996; Van Dyk et al. 1999). But it has now become possible to search directly for progenitor stars and carry out concerted campaigns on the nearest events. Three of the first Type II SNe to have excellent *HST* and ground-based pre-explosion images were the II-P SNe 1999gi, 1999em and 2001du (Smartt et al. 2001, 2002b, 2003; Van Dyk, Li & Filippenko 2003b). In all there was no detection of a progenitor, but meaningful limits were derived. Leonard et al. (2003b) and Leonard et al. (2002b) subsequently showed the importance of having reliable distances to the host galaxies of the SN progenitors in order to constrain the upper mass limits. Efforts to find progenitors continued (Smartt et al. 2003; Van Dyk, Li & Filippenko 2003a) until the first confirmation of a red supergiant progenitor of a Type II-P explosion in pre-discovery *HST* and Gemini-North images (Smartt et al. 2004). Unambiguous detections in *HST* images require the SN to be located on the pre-explosion images with accuracies of around 10 mas, which requires follow-up images of the SN to be taken at *HST* or corrected adaptive optics ground-based resolution (Gal-Yam et al. 2005; Maund & Smartt 2005; Crockett et al. 2008). The next clear and unambiguous detection of a progenitor star was also a red supergiant in NGC 5194 (SN2005cs; Maund, Smartt & Danziger 2005a; Li et al. 2006). The recent discovery of SN2008bk in NGC 7793 (3.9 Mpc) has produced detections in *IJHK* of a red progenitor star (Mattila et al. 2008). The near-infrared (NIR) spectral energy distribution (SED) of the SN2008bk progenitor is the best sampled SED yet of any red supergiant progenitor and matches a late M4I spectral type with moderate extinction of $A_V \simeq 1$ and an initial mass around 8–9 $M_{\odot}$. There have been claims of the detections of others such as 2004A (Hendry et al. 2006), 2004et (Li et al. 2005), 2006my and 2006ov (Li et al. 2007) and we review these in this paper. An additional method that has much to offer this field is locating SNe directly coincident with compact, coeval star clusters. If the age of the cluster can be determined then a main-sequence turn-off age, and turn-off mass can lead directly to an estimate of the progenitor star mass (e.g. 2004dj in NGC 2403 as studied by Maíz-Apellániz et al. 2004). The detection and characterization of progenitor stars has the potential to directly link the type of star to the SN explosion characteristics (e.g. the amount of ^{56}Ni synthesized in explosive O and Si burning and the total energy of the explosion) and also to set quantitative limits on progenitor mass ranges. The latter is of great interest to compare to the highest mass WD progenitors and to the stars that form neutron stars and black holes after core-collapse.

Work in this field has progressed substantially in the last 8 yr and compilations of progenitor properties have been made by Smartt et al. (2003); Gal-Yam et al. (2007a); Li et al. (2007); Kochanek et al. (2008). However, these compilations are somewhat ad hoc, incomplete and potentially biased as they do not define the selection criterion for inclusion rigorously. In addition the results are based on different methods for estimating the progenitor masses and upper limits (in terms of measurement and the theoretical models employed). The goal of this series of two papers is to define the selection criteria for inclusion (a volume- and time-limited survey) and to determine the physical parameters of the progenitor stars (luminosities and masses, or limits thereon) in a homogeneous and consistent way. Only then is it possible to reliably estimate the

population parameters. This paper specifically deals with the Type II SNe and all but two of the final sample of twenty have been confirmed as Type II-P. A companion paper will discuss the stripped SNe of types IIb, Ib and Ic which are drawn from the same volume- and time-limited survey.

In addition to the SNe with pre-explosion images we discuss in the paper there are three SNe with progenitor detections that fall outside either our time or volume definition. Those are SN 1987A, SN 1993J and SN 2005gl. Discussions of the first two are well documented in the literature (e.g. Walborn et al. 1989; Aldering et al. 1994; Van Dyk et al. 2002; Maund et al. 2004); 1987A will be discussed later in this paper and the implications of 1993J will be discussed in the second paper in this series. SN 2005gl is a Type IIn in NGC 266 at approximately 66 Mpc, hence although a progenitor is detected by Gal-Yam et al. (2007a) it does not fall within our distance limit. Gal-Yam et al. (2007a) suggest that this was a very massive star with $M_V \simeq -10.3$ and very likely a luminous blue variable (LBV). Although with only a detection in a single filter the blue colour is not confirmed, and there are not enough data to determine if the source was indeed variable. This is evidence that very massive stars do explode as bright SNe and is a point we will return to in the discussion.

This paper starts with defining the sample from which the targets with high-quality pre-explosion images are drawn. A consistent and homogeneous analysis method is then defined and justified. We then review previous detections (and add some new data) to build the data required for analysis and then statistically analyse the results. We follow this with an extensive discussion.

2 THE SAMPLE OF LOCAL UNIVERSE SUPERNOVAE

The observational data for this paper are compiled from many sources in the recent literature but the sample selection requires some justification and explanation if the later comparisons and discussions of physical parameters are to be meaningful. We have selected SNe for inclusion based on the following selection criteria, and we justify the choice of criteria where appropriate.

2.1 Definition and selection

We consider all core collapse SNe discovered in the 10.5 yr period between 1998 January 1 and 2008 June 30. The earlier date was chosen as the sensible start point for the concerted efforts to find SNe in archive pre-discovery images due to the fact that the local SN discovery rate had reached a significant level (van den Bergh, Li & Filippenko 2005), and we estimate the amount of imaging of nearby galaxies in the *HST* archive had become rich enough that coincidences were likely to occur. This was also the effective date of the start of concerted efforts to search for SN progenitors. Since the late 1990s our group (Smartt et al. 2001, 2002b), and others (e.g. Van Dyk et al. 2003a; Gal-Yam et al. 2005) have been systematically searching for pre-explosion images of core-collapse SNe in nearby galaxies. We have further restricted our sample to galaxies with recessional velocities less than 2000 km s^{-1}, effectively restricting us to a volume-limited sample. The recessional velocities, corrected for the infall of the Local Group towards the Virgo cluster, of all nearby galaxies hosting SNe were taken from the HyperLeda[1] (Paturel et al. 2003) data base. We emphasize that we have used the corrected velocities to apply the selection criterion of 2000 km s^{-1} and assuming $H_0 = 72$ km s^{-1} Mpc^{-1}, this local volume has a limit of 28 Mpc.

During this period, and in this volume, there have been 138 SN candidates discovered and all are listed in the Asiago,[2] CfA[3] and Sternberg Astronomical Institute[4] catalogues. Of course these are simply compilations of discoveries reported in the *International Astronomical Union* (IAU) Circulars and these catalogues normally list the discovery magnitudes and types reported in the first IAU announcement. It often happens that the SN classification is revised or refined with subsequent higher quality spectra, or longer monitoring. Both can reveal peculiarities and transformations, or simply give a more secure classification. In particular the subclassification of II-P can be added when significant light-curve information is gathered. Hence we have carefully checked the classification of each event, and have gone further and classified those SNe listed as 'II' into the subtypes II-P and II-L or IIn where possible. This was done using the following criteria in order. First, the refereed literature was searched and a classification taken from published photometric and spectroscopic results. Secondly, unpublished, professional spectra and light curves where taken from reliable sources such as those of the Carnegie Supernova Project (Hamuy et al. 2006) and the Asiago data archive (Turatto 2000). Thirdly, amateur light curves available on the web were checked and, if possible, a II-P classification was made if a clear and unambiguous plateau lasting longer than 30 d was recorded. The vast majority of II-P SNe have plateau phases lasting significantly longer than 30 d, in fact most are around 90–110 d (Hamuy 2003; Pastorello 2003; Pastorello et al. 2004) and there is no clear evidence that plateaus of shorter duration are particularly common. However, to observe such a long plateau necessarily means the SN must have been discovered close to explosion. This is often not the case, and we have chosen to take 30 d simply as an indicator that an extended plateau phase is evident. In all cases of our subclassifications of Type II SNe, we believe the designations not to be controversial or ambiguous and for only nine events classed as Type II were we unable to assign a subtype. In these cases the SNe were generally discovered late in the nebular phase. It is often difficult to distinguish Ib and Ic SNe from single spectra taken at an unknown epoch, and indeed there are six events for which authors have listed Ib/c classifications and we cannot improve on these classifications. All of the individual SNe are listed in Table A1. There are only two SNe which have not had a classification spectrum reported in the literature, 1998cf and 1999gs and these are ignored in the following frequency comparison.

We realize that the classifications into the standard bins are somewhat simplistic. In particular there are some SNe that show evidence of interaction with the circumstellar medium, which result in narrow lines (usually of H or He) superimposed on the spectrum. When narrow lines of H dominate the spectrum then the IIn designation is often used by the community, but some II-P and Ibc SNe do show evidence of this behaviour at a weaker level. The most striking example recently is that of the SN2006jc-like objects and the two examples in our sample are 2006jc and 2002ao (see Foley et al. 2007; Pastorello et al. 2007b, 2008b). These show broad lined spectra resembling Type Ic SNe (in that they do not exhibit H or He *in the high-velocity ejecta*), but have strong and narrow He emission lines

[1] http://leda.univ-lyon1.fr.

[2] http://web.pd.astro.it/supern/snean.txt.

[3] http://cfa-www.harvard.edu/cfa/ps/lists/Supernovae.html.

[4] http://www.sai.msu.su/sn/sncat/.

Table 1. The relative frequency of SNe types discovered between 1998 and 2008 (10.5 yr) in galaxies with recessional velocities less than 2000 km s^{-1}, and type taken from Table A1. The relative frequency of all types and the relative frequency of only core-collapse SNe are listed separately.

Type	No.	Relative (per cent)	Core-collapse only (per cent)
II-P	54	39.1	58.7
II-L	2.5	1.8	2.7
IIn	3.5	2.5	3.8
IIb	5	3.6	5.4
Ib	9	6.5	9.8
Ic	18	13.0	19.6
Ia	37	26.8	–
LBVs	7	5.1	–
Unclassified	2	1.4	–
Total	138	100	100
Total CCSNe	92	66	100

and weak Hα emission. This has led Pastorello et al. (2008b) to term this class of objects Ibn. However, rather than introducing this small and very specific class of events, we will class them as Ic SNe as this is a fair description of the underlying spectrum of the SN ejecta. Giving them a simple Ib label could be argued as being misleading in that they do not exhibit the broad, He absorption typical of this class of H-deficient events. The label Ibn is certainly a valid type for them but in this paper it is too specific to be a useful addition to the compiled subtypes. We will discuss these objects further in the second paper in this series which concerns the stripped events (Crockett et al., in preparation).

2.2 The relative frequencies of core-collapse SNe

In Table 1 we list the relative frequency of each subtype occurring in our sample. This is a volume-limited relative frequency rate of SN types. There may well have been undiscovered local SNe in this period, e.g. dust extinguished events, or events which exploded in solar conjunction which were missed at late times. The distance limit imposed ($\mu = 32.3$) and the range in the absolute magnitudes of each subtype (Richardson et al. 2002) would initially suggest that it is unlikely that there is a serious bias in the *relative number* of the different subtypes. However, there are two arguments which can be put forward against this. The first is if there is a substantial number of intrinsically faint SNe that may have gone undetected if they have typical magnitudes below about -13. The nature of the faint optical transient in M85 (Kulkarni et al. 2007; Ofek et al. 2008) is currently debated, and could conceivably be a core-collapse SN (Pastorello et al. 2007a, see Section 2.4). If a large number of intrinsically very faint SNe are evading discovery by current pointed surveys it could lead to a dramatic change in our understanding of the link between progenitor star and SN explosion. Secondly, there is an issue with the lack of Type Ia SNe discovered recently within 10 Mpc. In the 10.5 yr considered there are about 13 core-collapse that have been discovered within 10 Mpc (the exact number depends on some individual galaxy distance estimates and how strictly one enforces the distance limit; for a more in depth discussion see Kistler et al. 2008). But there have been no Type Ia SNe discovered and with a relative frequency of 27 per cent, one might have expected to have seen three to four SNe. The Poisson probability of this being a statistical fluctuation is not zero, but is small (2–5 per cent) and one could invoke the argument that there are more core-collapse SNe (perhaps of the fainter Type II) beyond 10 Mpc which are being missed and hence the relative rate of CCSNe/Ia is intrinsically much higher than we currently believe (also see Thompson et al. 2009).

van den Bergh et al. (2005) have presented a homogeneous sample of 604 recent SNe discovered (or recovered) by the Lick Observatory Supernova Search (LOSS) with the KAIT telescope (Filippenko et al. 2001). The galaxy search sample spans a much larger volume ($cz \lesssim 10\,000$ km s^{-1}) than we are considering and a significant majority of our sample in the overlapping time frames (∼85 per cent of the core collapse events between 1999 and 2004) are listed in the van den Bergh et al. summary of the LOSS survey. The ones which are not are predominantly more southern than $\delta = -30^{\circ}$. Hence our sample is very similar to that which would be obtained if one selected a distance- and time-limited sample from the discovered and recovered events of van den Bergh et al. (2005). The relative number of Type Ia SNe in the full LOSS catalogue is significantly higher than within our smaller volume (44 per cent compared to 27 per cent that we find here). This is very likely due to Type II-P SNe going undetected at the largest distances. At $cz \sim 10\,000$ km s^{-1}, with a moderate amount of foreground reddening at least half of the II-P distribution of Richardson et al. (2002) would be missed at the limiting magnitude of $R \sim 19$ of the KAIT survey. The Type Ib/c SNe appear slightly more abundant in our local sample (29 per cent of all core-collapse) compared to the van den Bergh et al. (2005) frequency (25 per cent), although the difference is not significantly greater than the expected Poisson scatter.

The nine SNe which were classed as Type II (and could not be further subclassified) can be split proportionally over the Type II subtypes, which assumes that that there was no particular bias underlying their poor observational coverage. As they were all discovered late in the nebular phase, this is likely to hold. We put eight in the II-P bin, and split the other one equally between the IIn and II-L, as they have equal numbers of confirmed types; hence the fraction which appears in Table 1. In a similar manner the six Ib/c SNe are split proportionately into the Ib and Ic bins based on the measured ratio of Ib:Ic = 7:14 (which comes from those events where a Ib or Ic classification seems secure). We did not include the two unclassified SNe in any of the rate estimates. Seven of the events originally announced as SNe in Table A1 have been shown to actually be outbursts of LBVs similar to those seen historically in Local Group LBVs such as η-Carinae and P-Cygni. These are 1999bw (Filippenko, Li & Modjaz 1999b), 2000ch (Wagner et al. 2004), 2001ac (Matheson & Calkins 2001), 2002kg or NGC 2403-V37 (Weis & Bomans 2005; Maund et al. 2006; Van Dyk et al. 2006), 2003gm (Maund et al. 2006), 2006fp (Blondin et al. 2006), 2007sv (Harutyunyan et al. 2007c). Hence we remove these from the rates of CCSNe since they are not true SN explosions. Table 1 lists the relative frequencies of core-collapse SNe. It is clear that the types II-L and IIn are intrinsically quite rare and the majority of core-collapse events are SNe II-P. Such a breakdown of subtypes has been suggested before (Cappellaro, Evans & Turatto 1999; Li et al. 2007) although this is the first time quantitative volume-limited statistics have been compiled and presented. The preliminary analysis by Li et al. (2007) of 68 LOSS only discovered events (within 30 Mpc) in 9 yr suggests 68:26:2:4 per cent breakdown between II:Ib/c:IIb:IIn. Perhaps the ratio of most interest is the Ibc/II ratio which has been used by previous studies to try to place constraints on progenitor populations (Prantzos & Boissier 2003; Eldridge 2007; Prieto, Stanek & Beacom 2008b). These three studies have estimated the ratio as a function of metallicity finding that, at approximately solar metallicity ($Z_{\odot}$), the ratio is

$N_{\rm Ibc}/N_{\rm II} \simeq 0.4 \pm 0.1$ (Poissonian uncertainty) and this goes down to around 0.1 at 0.3 $Z_\odot$ (although with fairly small numbers in each metallicity bin). The ratios at approximately $Z_\odot$ are fairly similar to what we find ($N_{\rm Ib/c}/N_{\rm II} = 0.45 \pm 0.13$) and as discussed below in Sections 4 and 5 our SN population is likely drawn from metallicities in the range 0.5–1.0 $Z_\odot$ due to the fact that nearby, high star formation rate galaxies are those that are most frequently monitored for SNe. A full analysis of the chemical composition of the sites of the SNe in this volume-limited sample would be desirable. We will discuss the SN rates more in Section 8.2.

The absolute rates of the different types in the standard SN units [1 SNu = 1 SN $(100\,{\rm yr})^{-1}$ $(10^{10}\ L^B_\odot)^{-1}$] is much more difficult to assess given that detailed knowledge of the sampling frequency for each galaxy and search strategy is required (see Cappellaro et al. 1999). The LOSS team will address this (Leaman, Li & Filippenko 2004) and will provide the best estimate of the local rates so far. While we cannot derive the SN rate in standard units, the numbers in Table 1 serve as a good guide to the relative numbers of SNe expected in future surveys, when used in conjunction with absolute magnitude distributions (assuming the local galaxy population is cosmically representative). If bias factors affecting the relative rate of discovery of the different types are minor, then these rates are a direct consequence of the initial mass function (IMF) combined with stellar evolution which is dependent on mass, metallicity, duplicity and initial rotation rate. The numbers of SNe we have tabulated give a lower limit on the number of types per $\rm Gpc^{-3}\ yr^{-1}$, which is at least a useful comparison to higher redshift estimates and also when considering the rates of gamma-ray bursts (GRBs) and X-ray flashes (XRFs). The volume enclosed by the 28 Mpc limit is $9.2 \times 10^{-5}\ \rm Gpc^3$; hence the local rate of CCSN explosions is likely to be $\geq 9.6 \times 10^4\ \rm Gpc^{-3}\ yr^{-1}$ and the local Ibc SN rate is $\geq 2.7 \times 10^4\ \rm Gpc^{-3}\ yr^{-1}$. The latter is in reasonable agreement with the $\sim 2 \times 10^4\ \rm Gpc^{-3}\ yr^{-1}$ put forward by Guetta & Della Valle (2007), based on the Cappellaro et al. (1999) rates and local galaxy luminosity functions.

One further point to bear in mind when considering the relative rates is the likely number of local SNe which are not discovered because they are in faint hosts which are not monitored. The Sloan Digital Sky Survey Data Release 5 (5713 $\rm deg^2$) contains about 2200 faint galaxies with $M_{\rm g} \gtrsim -17$ and with recessional velocities less than $2000\,{\rm km\,s^{-1}}$. Hence over the full 40 000 $\rm deg^2$ of sky, there are about 15 000 of these faint hosts within about 28 Mpc. These are generally not monitored by the LOSS and the amateur efforts, who typically target the most luminous 10 000 galaxies within about 100–140 Mpc. Young et al. (2008) estimate that such galaxies (with metallicities corresponding roughly to oxygen abundance <8.4 dex) would contribute about 5–20 per cent of the total star formation locally. Hence at least this fraction of core-collapse SNe are missing from the local samples and all of them are within faint hosts and potentially have low-metallicity progenitors. This could mean that very bright events like SNe 2005ap, 2006tf and 2008es (Quimby et al. 2007; Smith et al. 2008a; Gezari et al. 2009; Miller et al. 2009) found in blank-field searches (and faint hosts) could be missed. Although the true rate of such events appears to be quite small and likely less than ∼1 per cent (Miller et al. 2009). Discovery of these events locally should be possible with future all-sky surveys such as Pan-STARRS and LSST (for an estimate of rates see Young et al. 2008).

Of the 99 core-collapse SNe and LBV classified outbursts, the host galaxies of 46 of them were imaged by *HST* with either the Wide Field Planetary Camera 2 (WFPC2) or Advanced Camera for Surveys (ACS) *before* explosion. However, given the small field of view (FOV) of both of these cameras (2.6 and 3 arcmin, respectively) the site of the SNe did not always fall on the FOV of the cameras. Of these 46, only 26 had images of the SN site in the camera FOV, an overall hit rate of 26 per cent. A column is included in Table A1 which specifies whether or not the galaxy was observed by *HST* before explosion and if the SN falls on one of the camera FOVs. A further six have had high-quality ground-based images of the SN site taken before explosion and they are also included in this compilation. The observational sample for this paper and its companion studying the stripped events (Crockett et al., in preparation) is thus all of the core-collapse SNe which fulfil the above criteria and have good quality pre-explosion imagery. We have confirmed that there are no other SNe in Table A1 with *HST* pre-discovery images. We cannot make the same definitive statement about ground-based images given the amount of inhomogeneous imaging data around. But our manual searching of all well maintained large telescope archives suggests it is highly unlikely that further *high-quality* images of any of these events will surface, i.e. images with subarcsec resolution with the depth to detect a large fraction of the galaxy's massive stellar population. As such we have a well-defined sample in terms of distance and time. The rest of this paper focuses on the progenitor properties of the 20 Type II SNe listed in Table 2, of which 18 are confirmed II-P and two are of uncertain subtype (1999an and 2003ie). The other 12 SNe which are likely to have had stripped progenitors: 2000ds (Ib), 2000ew (Ic), 2001B (Ib), 2001ci (Ic), 2002ap (Ic), 2003jg (Ib/c), 2004gt (Ib/c), 2005ae (IIb), 2005V (Ibc), 2005cz (Ib), 2007gr (Ic), 2008ax (IIb), will be discussed in a companion analysis paper (Crockett et al., in preparation).

2.3 The relative frequencies of SN1987A-like events

In this volume-limited sample, there is only one SN which has been conclusively shown to be similar to SN1987A, that is SN1998A (Pastorello et al. 2005). SN1987A had a peculiar light curve and distinctly strong Ba II lines (probably a temperature effect) and an asymmetric Hα profile during its first ∼40 d of evolution and the community would have been very unlikely to miss such events as they would have created great interest. There is one other relatively nearby event that has a SN1987A-like appearance, which is 2000cb (Hamuy 2001) in IC1158. This one however has a $V_{\rm vir} = 2017\,{\rm km\,s^{-1}}$, which puts it just beyond our selection criteria. We shall see in Section 5.9 that Harutyunyan et al. (2008) suggest that a single spectrum of SN2003ie shows similarities to 1987A but it is not well studied enough to be definitive. Hence even if we would include 2000cb and 2003ie in our sample we can certainly say that 1987A events are intrinsically rare and probably less than around 3 per cent of all core-collapse events.

2.4 SN2008S and the M85 and NGC 300 optical transients

Recently three optical transients have been reported whose nature is still ambiguous and intensely debated. The optical transient in M85 reported by Kulkarni et al. (2007) was suggested by the authors to be a 'luminous red nova' which most likely arose from a stellar merger. However, this view was challenged by Pastorello et al. (2007a) who suggested a CCSN origin could not be ruled out. Since then two other optical transients of similar absolute magnitude have been discovered. One has been termed an SN (SN2008S; Stanishev, Pastorello & Pursimo 2008) although Smith et al. (2008c) suggest it could be an SN imposter and the outburst of a moderately massive star rather than a core-collapse. The other, in NGC 300 (Berger et al.

Table 2. The results of the homogeneous reanalysis of all the SN progenitors. The galaxies, their class, distance and extinction along the line of sight to the SNe are listed. The methods employed in the literature to determine distances are listed (TF = Tully–Fisher; Kin. = kinematic; Cep. = Cepheid; PNLF = planetary nebulae luminosity function; TRGB = tip of the red giant branch; Mean = mean of several methods which are detailed in Section 5. Kinematic distances are based on $H_0 = 72\,\mathrm{km\,s^{-1}\,Mpc^{-1}}$. The deprojected galactocentric radii are calculated as well as the radius with respect to the r_{25} value (the radius at which the surface brightness drops to 25 mag arcsec^{-1}). Oxygen abundances of the galactic ISM at the positions of the SNe are quoted ([O/H] = $12 + \log N_{\mathrm{O}}/N_{\mathrm{H}}$). The final estimated luminosities, or luminosity limits are in solar luminosity units. The ZAMS masses and upper mass limits as discussed in Section 5 are listed in the final column.

Supernova	SN Type	Galaxy	Galaxy class	Distance (Mpc)	Method	A_V	r_{G} (kpc)	r_{G}/r_{25}	[O/H] (dex)	$\log L/\mathrm{L}_\odot$ (dex)	ZAMS ($\mathrm{M}_\odot$)
1999an	II	IC 755	SBb	18.5 ± 1.5	TF	0.40 ± 0.19	4.7	0.82	8.3	<5.16	<18
1999br	II-P	NGC 4900	SBc	14.1 ± 2.6	Kin.	0.06 ± 0.06	3.1	0.69	8.4	<4.76	<15
1999em	II-P	NGC 1637	SBc	11.7 ± 1.0	Cep.	0.31 ± 0.16	1.6	0.28	8.6	<4.69	<15
1999ev	II-P	NGC 4274	SBab	15.1 ± 2.6	Kin.	0.47 ± 0.16	5.3	0.46	8.5	5.1 ± 0.2	16^{+6}_{-4}
1999gi	II-P	NGC 3184	SABc	10.0 ± 0.8	Mean	0.65 ± 0.16	3.1	0.30	8.6	<4.64	<14
2001du	II-P	NGC 1365	SBb	18.3 ± 1.2	Cep.	0.53 ± 0.28	14.7	0.53	8.5	<4.71	<15
2002hh	II-P	NGC 6946	SABc	5.9 ± 0.4	Mean	5.2 ± 0.2	4.1	0.45	8.5	<5.10	<18
2003gd	II-P	NGC 628	Sc	9.3 ± 1.8	Mean	0.43 ± 0.19	7.5	0.58	8.4	4.3 ± 0.3	7^{+6}_{-2}
2003ie	II?	NGC 4051	SABb	15.5 ± 1.2	TF	0.04	7.3	0.66	8.4	<5.40	<25
2004A	II-P	NGC 6207	Sc	20.3 ± 3.4	Mean	0.19 ± 0.09	6.7	0.79	8.3	4.5 ± 0.25	7^{+6}_{-2}
2004am	II-P	NGC 3034	Sd	3.3 ± 0.3	Cep.	3.7 ± 2.0	0.64	0.14	8.7	Cluster	12^{+7}_{-3}
2004dg	II-P	NGC 5806	SBb	20.0 ± 2.6	Kin.	0.74 ± 0.09	4.3	0.50	8.5	<4.45	<12
2004dj	II-P	NGC 2403	SABc	3.3 ± 0.3	Cep.	0.53 ± 0.06	3.5	0.37	8.4	Cluster	15 ± 3
2004et	II-P	NGC 6946	SABc	5.9 ± 0.4	Mean	1.3 ± 0.2	8.4	0.92	8.3	4.6 ± 0.1	9^{+5}_{-1}
2005cs	II-P	NGC 5194	Sbc	8.4 ± 1.0	PNLF	0.43 ± 0.06	2.7	0.22	8.7	4.25 ± 0.25	7^{+3}_{-1}
2006bc	II-P	NGC 2397	SBb	14.7 ± 2.6	Kin.	0.64	1.4	0.30	8.5	<4.43	<12
2006my	II-P	NGC 4651	Sc	22.3 ± 2.6	TF	0.08	4.4	0.37	8.7	<4.51	<13
2006ov	II-P	NGC 4303	SBbc	12.6 ± 2.4	TF	0.07	2.3	0.26	8.9	<4.29	<10
2007aa	II-P	NGC 4030	Sbc	20.5 ± 2.6	Kin.	0.09	10.3	0.91	8.4	<4.53	<12
2008bk	II-P	NGC 7793	Scd	3.9 ± 0.5	TRGB	1.0 ± 0.5	3.9	0.66	8.4	4.6 ± 0.1	9^{+4}_{-1}

2009; Bond et al. 2009), has not yet received an official SN designation, hence we refer to it as NGC 300 OT2008-1 (as in Berger et al. 2009). SN2008S has already been subject to a study of its pre-explosion environment and a detection of a source in *Spitzer* mid-IR images has been suggested to be a dust enshrouded red supergiant which is visually obscured (Prieto et al. 2008a). A similar dust dominated object has been found to be coincident with the optical transient NGC 300 OT2008-1 (Bond et al. 2009; Thompson et al. 2009). Thompson et al. (2009) suggested that all three could be the similar explosion of massive stars embedded in optically thick dust shells. The early studies of the evolution of SN2008S, NGC 300 OT2008-1 and their comparisons with M85OT2006-1 and other erupting systems have so far not favoured a core-collapse SN explanation for the physical source of the outburst (Smith et al. 2008c; Berger et al. 2009; Bond et al. 2009) The transients lack broad lines from high-velocity ejecta; their spectra are very slowly evolving and dominated by narrow H emission. Strangely they also do not appear to be similar to the V838 Mon variable system or M31 luminous red variable as initially suggested by both Kulkarni et al. (2007) and Bond, Walter & Velasquez (2008). Based on the mid-IR progenitor detections, Thompson et al. (2009) argue that the precursors may have been going through a short evolutionary phase which ends in a weak, electron capture SN. A full multi-wavelength study of the evolution of SN2008S from early to late times, and comparisons with the other two suggest there is some evidence for the SN explanation (Botticella et al., in preparation; Kotak et al. in preparation). All these studies reveal that the three objects are incredibly similar in their properties. As their nature is ambiguous and currently debatable, we will not consider them further in this paper. It is certain, however, that they are not normally Type II-P SNe.

3 THE STELLAR EVOLUTIONARY MODELS

As discussed above, observational and theoretical studies both now strongly suggest that the progenitors of type II-P are typically red supergiants. To estimate an initial mass for observed red supergiant progenitors we require stellar models to obtain a theoretical initial mass to final luminosity relation, as shown in Fig. 1. The stellar models we use were produced with the Cambridge stellar evolution code, STARS, originally developed by Eggleton (1971) and updated most recently by Pols et al. (1995) and Eldridge & Tout (2004a). Further details can be found at the code's web pages.[5] The models are available from the same location for download without restriction. The models are the same as those described in Eldridge & Tout (2004a) but here we use every integer initial mass from 5 to 40 $\mathrm{M}_\odot$ and integer steps of 5–10 $\mathrm{M}_\odot$ above.

As will be discussed in Section 4, we can estimate the metallicity of the exploding star from the nebular abundances in the discs of the host galaxies, hence we have calculated stellar evolutionary models for three metallicities; solar, Large Magellanic Cloud (LMC) and Small Magellanic Cloud (SMC) where we assume mass fractions of $Z = 0.02$, 0.008 and 0.004, respectively. All the models employ our standard mass-loss prescription for hydrogen-rich stars (Eldridge & Tout 2004b): we use the rates of de Jager, Nieuwenhuijzen & van der Hucht (1988) except for OB stars, for which we use the theoretical rates of Vink, de Koter & Lamers (2001).

In Fig. 1 we plot the range of luminosity for a star from the end of core helium burning to the model end point at the beginning of core neon burning (for a solar metallicity model). The beginning of core

[5] http://www.ast.cam.ac.uk/∼stars.

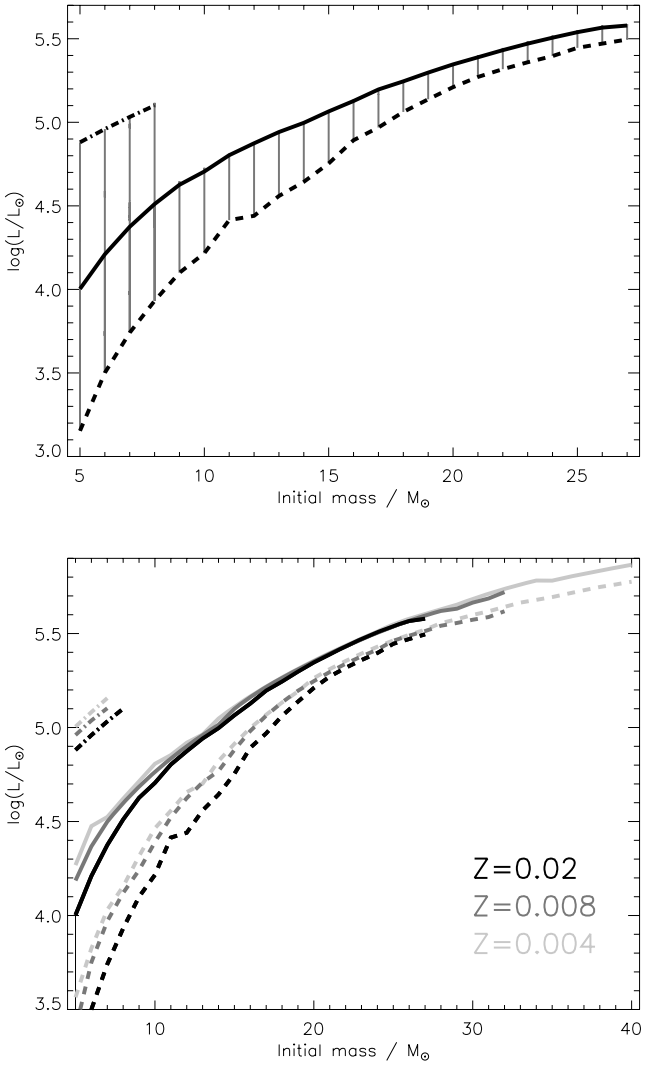

Figure 1. (a) The initial mass compared with the final luminosity of the stellar models for $Z = 0.02$. Each mass has the luminosity range corresponding to the end of He burning and the end of the model, just before core-collapse (these are the thin grey vertical lines). From a limit of luminosity an upper limit to the initial mass can be determined. The solid line is the luminosity of the model endpoint, the dashed line the luminosity at the end of core helium burning and the dash–dotted line is the luminosity after second dredge-up when the lower mass stars become AGB stars. (b) The same as (a) but with three metallicities shown for comparison, and with the vertical joining bars omitted for clarity. This illustrates that the choice of metallicity for the tracks is not critical, but we do use the most appropriate track to remove any systematic error.

neon burning is only a few years before core-collapse and this point is likely to be an accurate estimate of the pre-SN luminosity. The estimate of final mass from the observational limits will depend on uncertainties in these stellar models, which is a systematic that is difficult to constrain. To allow for this we assume that the range of reasonable luminosities for progenitor stars is somewhere between the end of core helium burning (dashed line in Fig. 1a) to the model end point at the beginning of core neon burning (solid line in Fig. 1a). For the lower mass stars that undergo the process known as second dredge-up to become asymptotic giant branch (AGB) stars, we also consider the luminosity before second dredge-up occurs. After second dredge-up the models have much higher bolometric luminosities but their observable characteristics are quite different to red supergiants (Eldridge, Mattila & Smartt 2007). We have previously shown that in the case of SN2005cs the progenitor could not have been a super-AGB star in the 5–8 $M_{\odot}$ range. Hence we assume throughout this paper that such stars are not the progenitors of the SNe discussed, and their positions in Fig. 1 are shown for completeness. A full discussion of this is given in Eldridge et al. (2007). In Fig. 1(b) we show the final luminosity ranges for the three metallicities, and the most appropriate metallicity for each SN is used when the initial masses are calculated in Section 5.

In Section 5, when we estimate a progenitor initial mass from Fig. 1, we will assume that the models are reliable enough to predict correctly that stars will undergo core-collapse after helium burning, so we use the full range of luminosities between the start of helium burning and the model endpoints in a conservative way. The mass estimate should be reasonable for all cases where the progenitor is a red supergiant.

4 METALLICITIES OF THE PROGENITOR STARS

As the stellar evolutionary tracks do differ slightly, to make sure that there are no underlying systematics in our analysis we require an estimate of the initial metallicity of the exploding star. There is good observational evidence now to show that mass-loss from massive stars is metallicity dependent, and that the lifetimes of stars in various phases as they evolve depend on metallicity (e.g. Massey 2003; Mokiem et al. 2007). Models predict that mass-loss and metallicity are driving forces behind stellar evolution (Heger et al. 2003; Meynet & Maeder 2003; Eldridge & Tout 2004b).

The most reliable determination of the metallicity of the progenitor star would be a measurement of the interstellar medium abundance in the galactic disc at the position of the event. In some cases the SNe have exploded in, or very close to, a previous catalogued H II region which has published spectroscopy and emission line fluxes. For these events we use these fluxes and calculate the nebular abundance of oxygen, using the strong-line method of the ratio of the [O II] λλ 3727 plus [O III] λλ 4959, 5007 to Hβ (see Bresolin 2008, for a discussion). Recently there has been much debate in the literature over which calibration to use to determine the nebular oxygen abundances from this method. Bresolin (2008) has shown that the calibration of Pilyugin & Thuan (2005) best matches the abundances determined in nearby galaxies where it is possible to measure the strength of the electron temperature sensitive lines and hence determine a simple empirical calibration for the strong-line method. The result is that the empirical determinations of Bresolin, Garnett & Kennicutt (2004) and the calibrations of Pilyugin & Thuan (2005) and Pettini & Pagel (2004) give significantly lower abundances (by a factor of 0.3–0.4 dex) than photoionization models (of Kewley & Dopita 2002, for example). Trundle et al. (2002) have shown that photospheric abundances of massive stars in M31 (B-type supergiants) are in much better agreement with the 'lower' metallicity scales of the P method employed by Pilyugin & Thuan (2005), and the empirical determinations from auroral lines. The recent downwards revision of the solar oxygen abundance to 8.66 ± 0.05 (Asplund et al. 2004; Asplund, Grevesse & Sauval 2005) and the agreement with all the other estimators of the Milky Way's interstellar medium (ISM) abundance at the solar radius (B stars, young F&G stars, H II regions, diffuse ISM) would also suggest that our adopted, lower, scale is appropriate (Sofia & Meyer

2001; Daflon, Cunha & Butler 2004; Simón-Díaz et al. 2006). Hence in this paper we will favour the calibrations of Bresolin et al. (2004) and Pilyugin & Thuan (2005) to determine nebular abundances.

Modjaz et al. (2008) have investigated the metallicities at the sites of Type Ic SNe and GRB-related SNe and show the importance of comparing abundances derived by self-consistent methods. By employing consistent abundance indicators they find that GRB related SNe tend to have significantly lower metallicities within their host galaxy environments than broad lined Type Ic SNe without GRBs. Their study illustrates the need to adopt consistent methods and compare abundances differentially.

We chose which stellar tracks to estimate the initial masses as follows. We use the observed present-day oxygen abundances as compiled by Hunter et al. (2007) for the Sun, LMC and SMC (8.65, 8.35, 8.05) to guide our choice of model. For those SNe which have estimated ISM oxygen abundances of [O/H] $\geq$ 8.4 we choose to use the $Z = 0.02$ metallicity tracks (solar). For those in the range $8.2 \leq$ [O/H] < 8.4 we use the $Z = 0.008$ tracks (LMC). We would have used the $Z = 0.004$ tracks for anything below [O/H] < 8.2 (SMC), but none of our targets have such low metallicity.

5 THE MASSES OF THE PROGENITORS OF TYPE II-P SUPERNOVAE

We expect that the progenitors of various subtypes of Type II SNe are hydrogen rich stars which have evolved from main-sequence stars of an approximate initial mass of $8\,M_{\odot}$ and above. If objects are detected in pre-explosion images then their colours and luminosities can be determined. If there is no star detected at the SN positions then the sensitivity of the images can be used to determine an upper luminosity limit and hence upper mass limit (see e.g. Smartt et al. 2003; Van Dyk, Li & Filippenko 2003c; Maund & Smartt 2005). In the papers presenting the original results, slightly different methods of determining the luminosity and mass limits from the pre-discovery images have been adopted. A mixture of 3 and 5σ limits have been quoted, uncertainties treated in varying manners, different stellar evolutionary models adopted and distances used which were not always the most recent and most accurate. In order to compare the sample as a whole, this calls for some homogenization, and we adopt the following method.

In the cases where there is no detection of a progenitor (13 in total) we determine the upper luminosity limit corresponding to the 84 per cent confidence limit. First, we take the 3σ detection limit for each pre-explosion image, where this is the detection magnitude in the filter system employed. To convert this to a bolometric luminosity one requires a measurement of extinction, distance and bolometric correction (with respect to the filter employed) for the progenitor. The 1σ uncertainties of these quantities are combined in quadrature to give a total 1σ uncertainty on the upper limit. If one assumes that the progenitor star was a red supergiant just prior to explosion then the bolometric and colour corrections for an M0 supergiant (Drilling & Landolt 2000) are appropriate. This assumption seems well justified as nearly all the SNe in our sample have been shown to be Type II-P, which require extended atmospheres physically similar to red supergiants (Chevalier 1976; Arnett 1980). Recent detections of the ultraviolet (UV) shock breakout from two Type II-P SNe determined the radii of the progenitor stars which adds further weight to the idea of the progenitors being red supergiants (Gezari et al. 2008; Schawinski et al. 2008). The uncertainty in the bolometric correction is taken to be ± 0.3 mag corresponding to the 1σ range of values for red supergiants between late K and late M type supergiants (Levesque et al. 2005). Assuming that the uncertainties are representative of a normal distribution of measurements, the 84 per cent confidence limit for the upper luminosity limit is 1σ above the best estimate, i.e. there is an 84 per cent chance that the progenitor stars have luminosities below this value given the individual uncertainties in the calculation. The 1σ distance and extinction errors are taken from the quoted sources as listed in the notes on the individual events below. These 84 per cent upper luminosity limits are then plotted on the final mass–luminosity plot discussed in Section 3. We determine the upper mass limit to be the maximum mass of a star which does not have part of its post-He burning track within the 84 per cent luminosity limit.

This method is equivalent to that previously employed by Smartt et al. (2003, 2002b) and Maund & Smartt (2005) (for example), in which an exclusion region of the HR diagram was determined as a function of effective temperature and an upper mass limit from the red supergiant region was determined. If an *I*-band (or *I*-band like) filter is employed both methods have the advantage of being fairly insensitive to the effective temperature of the assumed red supergiant progenitor as the peak of the stellar SED at this temperature range is $\sim$8300 Å (e.g. see figs 5 and 6 of Smartt et al. 2003). In all cases we have revised the distances to the galaxies to the most reliable, in our opinion, and most recent in the literature. Where no other distance is available we have calculated a kinematic distance estimate using the host galaxy radial velocity corrected for the Local Group infall into Virgo ($V_{\rm vir}$ from the HyperLEDA galaxy catalogue) and a value of the Hubble constant of $H_0 = 72\,{\rm km\,s^{-1}\,Mpc^{-1}}$. In such cases we employ an uncertainty of the local cosmic thermal velocity $187\,{\rm km\,s^{-1}}$ (Tonry et al. 2000), equivalent to ± 2.6 Mpc. If the value of H_0 adopted were either 65 or $85\,{\rm km\,s^{-1}\,Mpc^{-1}}$, the systematic effect on the distance scale would provide systematic luminosity differences of $+0.22$ and -0.36 dex for the five SNe which have kinematic host galaxy distances (1999br, 1999ev, 2004dg, 2006bc, 2007aa). We will discuss the effects of this systematic difference in Section 7. When determining the extinction in each wavelength band, we use the law of Cardelli, Clayton & Mathis (1989).

In the cases where we have a direct detection of the progenitor (five in total) the uncertainties in the luminosity are trivially determined and discussions of the individual events are listed below.

Two others (2004dj and 2004am) fall on bright, compact star clusters which are not resolved into individual stars (Maíz-Apellániz et al. 2004; Wang et al. 2005; Mattila et al. 2008; Vinko et al. 2008; Mattila et al., in preparation). These papers have determined the total cluster mass and age and hence the turn-off mass at the top of the main sequence. From this the mass of the progenitor has been determined. Hence the stellar mass determination is somewhat indirect and relies on the assumption that the time-scale of star formation in the cluster is significantly less than the current estimated age. The results are based on population synthesis codes which use different individual stellar evolutionary codes as input to those we have employed. The Maíz-Apellániz et al. (2004) and Vinko et al. (2008) results are based on the stellar synthesis codes STARBURST99 which uses the Geneva models (e.g. Schaller et al. 1992) as input, and the discussion in Section 6.1 indicates that the choice of stellar model does not introduce significant uncertainties. Hence although the analysis method, and hence mass determination, is different for these two events, we believe the mass estimates are worth including in this compilation. If they are left out, the main conclusions of this paper are not altered in any significant way.

5.1 1999an

IC755 is an SBb spiral with $M_B = -18.85$ (from HyperLEDA). As no direct abundance study of this galaxy has been done, we attempt to infer a probable abundance at the position of the progenitor from the O/H $- M_B$ relation of Pilyugin, Vílchez & Contini (2004). For galaxies in the range $-20 < M_B < -19$, the characteristic oxygen abundance (the oxygen abundance at a galactocentric distance of $r = 0.4r_{25}$) is typically in the range 8.5 ± 0.2 dex. The mean abundance gradient of this sample is -0.5 ± 0.3 dex$/r_{25}$. Hence at a deprojected distance of $0.8r_{25}$, the metallicity of the progenitor star of SN1999an can be approximated at 8.3 dex. This is somewhat uncertain given the large uncertainties on the gradient and the range of characteristic abundances and the error is likely to be ± 0.3 dex. However, it is the best estimate that can be derived with the current data in the literature.

There is no detection of a progenitor star in the WFPC2 pre-explosion images presented by Maund & Smartt (2005) and Van Dyk et al. (2003a). Both studies calculated similar sensitivity limits for the images, and we adopt the 3σ limit of Maund & Smartt (2005) of $m_{F606W} = 24.7$. Solanes et al. (2002) report a mean distance modulus for the host galaxy IC755 of $\mu = 31.33 \pm 0.18$ or $d = 18.45 \pm 1.5$ Mpc. Applying a line of sight extinction of $E(B-V) = 0.13 \pm 0.06$ (Maund & Smartt 2005) and assuming an M-type supergiant as the progenitor (for the colour correction between $F606W$ and Johnson V; see Maund & Smartt 2005) results in absolute upper limit of $M_V = -6.46 \pm 0.26$. For an M0 supergiant this corresponds to an upper luminosity limit of $\log L/\mathrm{L}_\odot = 5.00 \pm 0.16$, and an 84 per cent confidence limit of $\log L/\mathrm{L}_\odot = 5.16$. From Fig. 1 this implies an upper mass limit of $18\,\mathrm{M}_\odot$.

5.2 1999br

NGC 4900 is an SBc spiral, and similar to the case of IC755 discussed above it does not have a published abundance study. The same arguments as in Section 5.1 can be used (NGC 4900 has $M_B = -19.05$) to infer an oxygen abundance at the galactocentric radius of SN1999br ($0.69r_{25}$) of approximately 8.4 dex.

With no detection of a progenitor object at the SN position, Maund & Smartt (2005) place an upper limit on the magnitude of any progenitor of $m_{F606W} = 24.9$. This is significantly brighter than that of Van Dyk et al. (2003a) $m_{F606W} = 25.4$, and we adopt the former as the more conservative result. For the host galaxy (NGC 4900) only a kinematic distance modulus is available, with the Virgo infall corrected velocity giving $d = 14.1 \pm 2.6$ Mpc. The extinction to this event appears very low (Van Dyk et al. 2003a; Pastorello et al. 2004; Maund & Smartt 2005) and we adopt the foreground value quoted in these papers of $E(B-V) = 0.02 \pm 0.02$. As for SN1999an, we assume that the progenitor was a red supergiant and apply a colour correction and bolometric correction to determine an upper luminosity limit of $\log L/\mathrm{L}_\odot = 4.55 \pm 0.21$ and an 84 per cent confidence limit of $\log L/\mathrm{L}_\odot = 4.76$. From Fig. 1 this implies an upper mass limit of $15\,\mathrm{M}_\odot$.

5.3 1999em

van Zee et al. (1998) have published line strength measurements and abundances for 15 H II regions in NGC 1637. Using the calibration of Bresolin et al. (2004) we have redetermined the abundance gradient and at the galactocentric distance of SN1999em, the metallicity is 8.6 ± 0.1 dex. The nearest H II regions to 1999em are 510 and 794 pc, when deprojected, from the site of SN1999em and have oxygen abundances of 8.5 and 8.7 dex, respectively. Hence we adopt 8.6 dex.

The updated distance to NGC 1637 of $d = 11.7 \pm 1$ Mpc is taken from the Cepheid variable star estimate of Leonard et al. (2003b) and the reddening value of $E(B-V) = 0.1 \pm 0.05$ is adopted from Baron et al. (2000). Smartt et al. (2002b) present deep ground-based images of NGC 1637 before explosion in *VRI* filters and from these results we have determined a 3σ upper limit of $I = 23$. The I band is the most sensitive to red supergiant progenitors and between the supergiant spectral types of K2–M4 this corresponds to an upper luminosity limit of $\log L/\mathrm{L}_\odot = 4.54 \pm 0.15$, and an 84 per cent confidence limit of $\log L/\mathrm{L}_\odot = 4.69$. From Fig. 1 this implies an upper mass limit of $15\,\mathrm{M}_\odot$.

5.4 1999ev

NGC 4274 is an SBab spiral, and also has no abundance study of its H II regions. The same arguments as in Section 5.1 can be used (NGC 4274 has $M_B = -20.18$) to infer an oxygen abundance at the galactocentric radius of SN1999ev ($0.46r_{25}$) of approximately 8.5 dex.

SN1999ev was recovered in late, deep *HST* ACS images by Maund & Smartt (2005) and is coincident with a progenitor object found on a pre-explosion WFPC2 F555W image. Although Van Dyk et al. (2003a) originally suggested two other stars as possible progenitors, the *HST* follow-up clearly ruled this out and points to the object of magnitude $m_{\mathrm{F555W}} = 24.64 \pm 0.17$, at 4.8σ significance (Maund & Smartt 2005). There is no distance measurement to the galaxy NGC 4274 apart from a kinematic estimate, which is $d = 15.14 \pm 2.6$ Mpc, from HyperLEDA (Virgo infall corrected). Maund & Smartt (2005) determined the extinction to the nearby stellar population of $E(B-V) = 0.15 \pm 0.05$. We again assume that the progenitor was a red supergiant and apply a BC of -1.3 ± 0.3 to determine a final luminosity of $\log L/\mathrm{L}_\odot = 5.1 \pm 0.2$. The tracks in Fig. 1 imply the star would have been of mass $16^{+6}_{-4}\,\mathrm{M}_\odot$.

5.5 1999gi

Smartt et al. (2001) suggested that the H II region number three of Zaritsky, Kennicutt & Huchra (1994) at a position of 68″N 0″E is coincident with the star-forming region, or OB association that hosted SN1999gi. The calibration of Bresolin et al. (2004) using the R_{23} value of Zaritsky et al. (1994) gives an oxygen abundance of 8.6 dex.

A study of the progenitor site of SN1999gi was carried out by Smartt et al. (2001), but the distance to this galaxy was then improved in a compilation study of Leonard et al. (2002b) and Hendry (2006). Here we adopt the result in Hendry (2006) which is a mean of four estimates $d = 10.0 \pm 0.8$ Mpc, and the extinction of Leonard et al. $E(B-V) = 0.21 \pm 0.05$. The four distance methods detailed in Hendry (2006) are Tully–Fisher, expanding photosphere method (EPM), kinematic and the tertiary distance indicators of de Vaucouleurs (1979). The 3σ detection limit determined by Smartt et al. (2001) is $m_{F606W} = 24.9$, which results in an upper luminosity limit for an M-type supergiant of $\log L/\mathrm{L}_\odot = 4.49 \pm 0.15$, after the colour and bolometric corrections are applied. This gives an 84 per cent confidence limit of $\log L/\mathrm{L}_\odot = 4.64$ and, from Fig. 1, this implies an upper mass limit of $14\,\mathrm{M}_\odot$.

5.6 2001du

As discussed in Smartt et al. (2003) the H II region RW21 (Roy & Walsh 1997) is 1.5 arcsec from SN2001du, and it is likely the

metallicity of this region is representative of the progenitor star composition. The calibration of Bresolin et al. (2004) to the R_{23} value of Roy & Walsh (1997) gives an oxygen abundance of 8.5 dex.

The host galaxy NGC 1367 was observed as part of the *HST* Cepheid Key Project, hence the most accurate and recent distance estimate is taken from Paturel et al. (2002), $\mu = 31.31 \pm 0.15$. The extinction towards the SN was measured by three different methods by Smartt et al. (2003) to be $E(B-V) = 0.17 \pm 0.09$, giving $A_I = 0.25 \pm 0.13$, which is similar to that adopted ($A_I \simeq 0.2$) by Van Dyk et al. (2003c). Smartt et al. (2003) and Van Dyk et al. (2003c) presented pre-explosion images in the WFPC2 filters F336W, F555W, F814W and the most sensitive of these to red supergiants is the F814W. We determine the 3σ upper limit from the Smartt et al. results to be $I = 24$, similar to the sensitivity $m_{F814W} = 24.25$ of Van Dyk et al. (2003c). Between the supergiant spectral types of K2–M4 this corresponds to an upper luminosity limit of $\log L/\mathrm{L}_\odot = 4.57 \pm 0.14$, and an 84 per cent confidence limit of $\log L/\mathrm{L}_\odot = 4.71$. From Fig. 1 this implies an upper mass limit of $15\,\mathrm{M}_\odot$.

5.7 2002hh

None of the nine H II regions in NGC 6946 compiled by Pilyugin et al. (2004) are near the location of 2002hh. Hence we use the abundance gradient determined by Pilyugin et al. (2004) and the deprojected galactocentric radius of the SN position to determine the likely metallicity. As discussed above, the calibration of Pilyugin et al. (2004) is similar to the simple linear calibration of Bresolin et al. (2004), hence these should be on a similar scale. We determine an oxygen abundance of 8.5 dex.

A deep pre-explosion i'-band archive image of NGC 6946 from the Isaac Newton Telescope Wide Field Camera (INT–WFC) will be presented in a forthcoming paper (see Section 5.14). Although this SN suffered significant extinction, the proximity of the galaxy and the depth of the 3600-s i'-band image still places useful restrictions on the progenitor star. The 3600-s image is composed of 6×600-s exposures, with a final image quality of 1 arcsec. There is no object visible at the position of SN2002hh, and the 5σ detection limit for a point source was estimated to be $i_{\mathrm{CCD}} = 22.8$. This instrumental magnitude can be converted to a standard I using the well-calibrated colour transformations for the INT–WFC (Irwin & Lewis 2001).[6] We employ the reddening law determined in Pozzo et al. (2006) to estimate the extinction in the I band of $A_I = 2.1 \pm 0.3$. A distance of $d = 5.9 \pm 0.4$ Mpc is used which is a mean of the distance values from the compilation of Botticella et al. (in preparation) using the methods of Tully–Fisher, brightest supergiants, sosies, PLNF, EMP (applied to 1980K) and standard candle method (SCM) applied to SN2004et. SN2002hh appears to be a normal II-P, but behind a large dust pocket (Pozzo et al. 2006), hence we assume the progenitor was a red supergiant of type between K0 and M5. The falling bolometric correction combined with the rising intrinsic $(V-I)$ between K0 and M5 means that the bolometric luminosity limit stays approximately constant in this spectral range at $\log L/\mathrm{L}_\odot = 4.9 \pm 0.2$. Hence the 84 per cent confidence limit is $\log L/\mathrm{L}_\odot = 5.1$ and from Fig. 1 this implies an upper mass limit of $18\,\mathrm{M}_\odot$. We note that this is consistent with the progenitor mass of 16–18 $\mathrm{M}_\odot$ estimated by Pozzo et al. (2006) from the [O I] λλ6300, 6364 Å doublet.

[6] http://www.ast.cam.ac.uk/∼wfcsur/index.php.

5.8 2003gd

None of the previously catalogued H II regions in NGC 628, which have spectra and the R_{23} ratio measured, are particularly near the spatial position of SN2003gd. Hence we use the abundance gradient determined by Pilyugin et al. (2004) and the deprojected galactocentric radius of the SN position to determine the metallicity at this position. The parameters derived are in Table 2, with an abundance of 8.4 dex derived.

The progenitor star was detected by Smartt et al. (2004) and Van Dyk et al. (2003c), and an extensive compilation of distance measurements to NGC 628 and reddening towards the SN was carried out in Hendry et al. (2005). Those distance and extinction values determined were close to those employed in Smartt et al. (2004) to estimate the progenitor luminosity and mass. The Hendry et al. (2005) distance listed in Table 2 is a mean of the three methods: kinematic, brightest supergiants and SCM (applied to SN2003gd). The intrinsic $(V-I)_0 = 2.3 \pm 0.3$ colour is consistent with a supergiant in the spectral type range K5–M3, which Smartt et al. (2004) used to determine a luminosity of $\log L/\mathrm{L}_\odot = 4.3 \pm 0.3$. In the diagram of Fig. 1 the best value of 4.3 is closest to the termination point of the $7\,\mathrm{M}_\odot$ track, if we assume the progenitor did not go through second dredge-up. The uncertainties would bracket the $5\,\mathrm{M}_\odot$ and $13\,\mathrm{M}_\odot$ post-He burning tracks, hence we adopt the value $7^{+6}_{-2}\,\mathrm{M}_\odot$. Although the most likely value is below the lowest mass that is normally assumed possible to provide an iron core-collapse (8–10 $\mathrm{M}_\odot$; see Heger et al. 2003; Eldridge & Tout 2004b), the range of masses comfortably brackets the theoretically predicted limits.

5.9 2003ie

NGC 4051 is a Seyfert 1 galaxy of morphological type SABb and has no published abundance study of its H II regions. Hence we can estimate a probable abundance at the position of the progenitor as in Section 5.1. The galaxy has an $M_B = -20.3$, using our adopted distance and the corrected B-band magnitude given in HyperLEDA. At this magnitude the characteristic oxygen abundance (at a galactocentric distance of $r = 0.4r_{25}$) is approximately 8.5 ± 0.2 dex (Pilyugin et al. 2004). Again using the typical gradient of the galaxy sample (as in Section 5.1) of -0.5 ± 0.3 dex/r_{25}, the oxygen abundance at $0.66r_{25}$ is approximately 8.4 dex. As stated above this is quite uncertain (±0.3 dex) given the lack of detailed study of the galaxy but does show that it is unlikely to be a particularly low-metallicity environment. The SN was not studied in great detail by any group (as far as we know), but a single photospheric spectrum shows P-Cygni features of H I (Harutyunyan et al. 2008). The best match for the spectrum found by Harutyunyan et al. (2008) is that of 1998A, which itself appears like a 1987A-type event. Hence this event may not be a normal II-P SN and we have no light-curve information to consider. As we shall see below, the mass limits for the progenitor are not particularly restrictive and if the object were to be left out the conclusions of the paper would be unchanged.

The pre-explosion site of SN 2003ie was recovered in archive r'-band observations of NGC 4051 taken with the INT–WFC. This image was taken on 1999 November 11, with an exposure time of 900 s and image quality of 1.1 arcsec. We determined the position of SN 2003ie within an error circle of 0.17 arcsec (using an image of the SN from 2003 provided to us by Martin Mobberley). There is no progenitor object detected within this error circle and we derive a 3σ detection limit of $r' = 23$. This instrumental magnitude was converted to a standard R using the well-calibrated colour transformations for

the INT–WFC (Irwin & Lewis 2001),[7] giving $R = 22.65$. Pierce & Tully (1988) calculate the distance to the Ursa Major cluster to be 15.5 ± 1.2 Mpc using the Tully–Fisher method and we adopt this distance for NGC 4051. We have no measure of the internal extinction towards this SN and simply adopt the Galactic extinction value of $E(B - V) = 0.013$ (Schlegel, Finkbeiner & Davis 1998). We assume once again that the progenitor is a red supergiant and apply appropriate bolometric and colour corrections to determine a luminosity limit of $\log L/\mathrm{L}_\odot = 5.26 \pm 0.14$ and an 84 per cent confidence limit of $\log L/\mathrm{L}_\odot = 5.40$. From Fig. 1 this implies an upper mass limit of $24\,\mathrm{M}_\odot$.

5.10 2004A

There are no measurements of H II regions in NGC 6207 and we use the arguments presented in Hendry et al. (2006) to estimate the metallicity at the galactocentric distance of SN2004A. This paper based the results on typical abundance gradients measured by Pilyugin et al. (2004); hence again the estimate is on the same scale as the rest of the values. We point out that there is a typographical error in that paper, where R_{25} is quoted as 4 kpc, whereas it should be 8.6 kpc. However, repeating the same method, this does not change the calculated metallicity at the position of SN2004A which we estimate as 8.3 dex. The Hendry et al. (2006) distance listed in Table 2 is a mean of the three methods: kinematic, brightest supergiants and SCM (applied to SN2004A).

A faint object is detected at the position of SN2004A in Hendry et al. (2006), claimed as a 4.7σ detection in the $F814W$ filter, and it is not detected in the $F435W$ or $F555W$. If we assume this detection to be valid, it provides a blue limit for the colour of the progenitor and hence a star in the spectral range G5–M5. This gives a bolometric luminosity in the range $\log L/\mathrm{L}_\odot = 4.5 \pm 0.25$. In Fig. 1 this implies a best estimate of $7\,\mathrm{M}_\odot$, and the errors bracket the 5 and $13\,\mathrm{M}_\odot$ post-He burning tracks. Hence we adopt $7^{+6}_{-2}\,\mathrm{M}_\odot$. If the detection is not valid then the I-band detection sensitivity implies an 84 per cent confidence limit of $\log L/\mathrm{L}_\odot = 4.75$ and an upper limit of $13\,\mathrm{M}_\odot$.

5.11 2004am

There is no extensive published study of SN2004am to date, which is surprising given its proximity and the fact it is the only optically discovered SN in the starburst M82 (NGC 3034). However, it is clearly a II-P from the unfiltered magnitudes of Singer, Pugh & Li (2004) which stay constant for 76 d, and the spectrum of Mattila et al. (2004). Alignment of post-explosion NIR images and *HST* pre-explosion images shows that SN2004am is spatially coincident with the well-studied superstar cluster M82-L (Mattila et al., in preparation). The distance to M82 is assumed to be that of the M81 group, estimated from Cepheids in M81 (NGC 3031; Freedman et al. 2001).

A new study of M82-L has recently been carried out by Lançon et al. (2008) who modelled the integrated NIR 0.8–2.4 μm spectra. They used a population synthesis code (PÉGASE.2) and a new library of red supergiant observational and theoretical spectra to determine the age of M82-L. The fit to the overall SED and the individual molecular absorption features is impressive and gives an age estimate of 18^{+17}_{-8} Myr. With a lower than normal value of $R_V = 2.4$–2.7, Lançon et al. (2008) can also reproduce the optical SED of the cluster down to 6000 Å (the A_V value in Table 2 is taken from Lancon et al.). This age is somewhat younger than 65^{+70}_{-35} Myr that was first inferred by Smith et al. (2006) using only a limited range optical spectrum and the spectral synthesis code STARBURST99 (Leitherer et al. 1999). Lançon et al. (2008) point out that by using a low value of R_V they can reconcile the optical SED *and* the NIR molecular bands with the younger age and their updated spectral modelling technique and firmly exclude an age of 60 Myr. The cluster age provides quite a strong constraint on the mass of the progenitor star, assuming that the cluster formed coevally and the progenitor's age is similar to that of the cluster. The STARS models predict that the cluster ages correspond to lifetimes of stars of masses $12^{+7}_{-3}\,\mathrm{M}_\odot$. The models used in the population synthesis code of Lançon et al. (2008) were those of Bressan et al. (1993), which give very similar age–mass relationships to the STARS code (the uncertainty on the derived mass due to choice of code is within the error range).

In all of the above we have assumed solar metallicity for the stellar evolutionary tracks is appropriate. The fitting of Lançon et al. (2008) implies that this is appropriate. Also two recent papers have speculated on the abundances in the nuclear regions of M82, in environments close to super star cluster M82-L (Origlia et al. 2004; Smith et al. 2006). There is some uncertainty and difference in the abundances derived but the stellar abundances of red supergiants in these inner regions from Origlia et al. (2004) suggest a solar like oxygen abundance. The photospheric abundance in such objects are likely to be applicable to M82-L and the progenitor of SN2004am. Hence in the age estimations we chose the tracks close to 8.7 dex as the most appropriate.

5.12 2004dg

NGC 5806 is an SBb spiral, and also has no abundance study of its H II regions. The same arguments as in Section 5.1 can be used (NGC 5806 has $M_B = -19.86$) to infer an oxygen abundance at the galactocentric radius of SN2004dg ($0.56r_{25}$) of approximately 8.5 dex.

The pre-explosion site of SN 2004dg was imaged using both WFPC2 (2001 July 5) and ACS (2004 April 3) cameras onboard *HST* (the SN was discovered on 2004 July 31). The WFPC2 exposure times were 460 s in $F450W$ and $F814W$ filters. The ACS images had total exposure times of 700 s in $F658N$ and 120 s in $F814W$. We re-observed SN2004dg on (2005 March 10) with the ACS camera (in $F435W$, $F555W$ and $F814W$, as part of GO10187) and recovered the SN at transformed magnitudes of $B = 22.2$, $V = 20.8$, $I = 19.1$. Alignment of the two sets of images allowed us to locate the position of the SN on the pre-explosion images to within 0.015 arcsec (see Maund et al. 2005a; Crockett et al. 2008, for details of alignment procedures). Within this error circle there was no detection of a progenitor star in any of the image and filter combinations. A progenitor star was not detected at the SN position, therefore a 3σ detection limit of $m_{F814W} = 25.0$ was determined. There is no distance measurement to the galaxy apart from a kinematic estimate, which is $d = 20.0 \pm 2.6$ Mpc, from HyperLEDA (Virgo infall corrected). The total reddening towards SN 2004dg was estimated to be $E(B - V) = 0.24 \pm 0.03$, giving $A_I = 0.36 \pm 0.04$. Again we assume a red supergiant progenitor and find a luminosity limit of $\log L/\mathrm{L}_\odot = 4.28 \pm 0.17$ and an 84 per cent confidence limit of $\log L/\mathrm{L}_\odot = 4.45$. From Fig. 1 this implies an upper mass limit of $12\,\mathrm{M}_\odot$.

5.13 2004dj

As discussed in Section 5, SN2004dj fell on the compact star cluster identified by Maíz-Apellániz et al. (2004) and Wang et al. (2005) and the analysis used to determine a progenitor mass is different from

the direct identification and direct upper luminosity limits for the other SNe presented here. Maíz-Apellániz et al. (2004) determine an age of the compact star cluster of 14 Myr and hence a main-sequence mass of 15 $M_\odot$ for the progenitor. Wang et al. (2005) determine an age of around 20 Myr and hence a main-sequence mass of 12 $M_\odot$. A new and improved study by Vinko et al. (2008) using new UV observations of the cluster and extensive comparison of SEDs based on different model atmospheres and evolutionary tracks suggests a most likely turn-off mass (and hence progenitor zero-age main-sequence (ZAMS) mass) of between 12–20 $M_\odot$. This age (10–16 Myr) is consistent with the lack of Hα emission seen in the cluster spectrum of Vinko et al. (2008) and Humphreys & Aaronson (1987), as the ionizing O stars have died out. Hence we favour the older age and will adopt $15 \pm 3\,M_\odot$ as the progenitor mass (if we adopt $15^{+5}_{-3}\,M_\odot$ as suggested by Vinko et al. 2008, it does not affect any of the results below). The distance to NGC 2403 of 3.3 ± 0.3 Mpc is from the *HST* Cepheid Key Project (Freedman et al. 2001).

Maíz-Apellániz et al. (2004) adopted solar abundances in using the Geneva tracks of STARBURST99. On closer inspection this may be too high. We used the abundance gradient determined by Pilyugin et al. (2004) and the deprojected galactocentric radius of the SN position to determine the metallicity at this position of 8.4 dex. Although the H II regions in this galaxy have been studied extensively the only region which is physically close to the position of 2004dj is that of VS44 studied by Garnett et al. (1997), and even that is around 600pc from the cluster that hosted SN2004dj. The R_{23} ratio provided by Garnett et al. (1997) also gives an abundance of 8.4 dex with the calibration of Bresolin et al. (2004), in good agreement with the abundance gradient measurement. Although our oxygen abundance is below that employed by Maíz-Apellániz et al. (2004), this does not significantly affect the age (and hence turn-off mass) estimate when we compare STARS models of such different metallicities. We note that Vinko et al. (2008) favour a solar metallicity in their SED fits.

5.14 2004et

As discussed for SN2002hh (Section 5.7), there is no H II region near the galactic position of 2004et, which is some way from the centre of NGC 6946. We use the same method as for 2002hh to determine a metallicity typical for the galactocentric radius of 2004et of 8.3 dex. The adopted distance to NGC 6946 of $d = 5.9 \pm 0.4$ Mpc is discussed in Section 5.7.

Li et al. (2005) presented the detection of a candidate progenitor star of SN2004et in ground-based images from the Canada–France–Hawaii Telescope (CFHT) in both *UBVR* and $u'g'r'$ filters. They suggested it was a yellow supergiant as the *BVR* colours were matched with a G-type supergiant SED. From these colours and the models of Lejeune & Schaerer (2001), Li et al. (2005) determine a mass in the range $15^{+5}_{-2}\,M_\odot$.

However, it is now clear that the putative source detected by Li et al. (2005) was not a single star. Adaptive optics images of the site by Crockett et al. (2009) using Gemini-North show that the source breaks up into several stars. In addition *BVR* images taken 3 yr after explosion show identical colours to the pre-explosion object, indicating that the progenitor star was not detected in the pre-explosion frame. A deep i'-band image (the same image as discussed above for SN2002hh) does show a clear detection of a progenitor compared to the late-time *I*-band image. Crockett et al. (2009) use the i'-band detection (after converting to Johnson; $I = 22.06 \pm 0.12$) and limits on the *BVR* magnitudes to infer that the progenitor was a red supergiant with $(R - I)_0 > 1.80 \pm 0.22$. This implies an M4 spectral type or later, giving a bolometric magnitude of $M_{\rm bol} = -6.73 \pm 0.22$ and a progenitor luminosity of $\log L/L_\odot = 4.59 \pm 0.09$. Comparing this to stellar models of LMC metallicity, we estimate its initial mass to be $9^{+5}_{-1}\,M_\odot$ (as in Crockett et al. 2009).

5.15 2005cs

Maund et al. (2005a) have estimated the abundance at the galactocentric radius of SN2005cs in an identical manner as we have employed consistently in this paper, using the NGC 5194 abundance gradient of Bresolin et al. (2004), hence it is already on our common calibration scale. They determine 8.66 ± 0.11 dex, which we adopt in this paper.

The detection of the progenitor of SN2005cs is well documented by Eldridge et al. (2007), Li et al. (2006) and Maund et al. (2005a) which all give similar mass estimates in the range 7–10 $M_\odot$. Eldridge et al. (2007) have recently reanalysed all of the available photometry from the initial two discovery papers and suggested that the progenitor could not have been a super-AGB star that has gone through second dredge up. This analysis was done with the STARS code in an identical manner as this study and they found likely progenitor range of 6–8 $M_\odot$ (assuming a distance of 8.4 ± 1.0 Mpc). The Maund et al. (2005a) luminosity estimate for the progenitor is $\log L/L_\odot = 4.25 \pm 0.25$ and using the STARS tracks employed here this would suggest a mass of $7^{+3}_{-1}\,M_\odot$. If the closer distance of 7.1 ± 1.2 Mpc is chosen (from the mean of the compilation of Takáts & Vinkó 2006) then the best estimate of mass would reduce slightly to around 6 $M_\odot$. This would be rather low, but the uncertainty on the upper bound (3 $M_\odot$) would still place it comfortably within the normal theoretical ranges for core-collapse.

5.16 2006bc

NGC 2397 is an SBb spiral, and has no published abundance study of its H II regions. The same arguments as in Section 5.1 are employed (NGC 2397 has $M_B = -19.67$) to infer an oxygen abundance at the galactocentric radius of SN2006bc ($0.3r_{25}$) of approximately 8.5 dex.

The pre-explosion site of SN 2006bc was imaged using WFPC2 (2001 November 17) onboard *HST* with exposure times of 460 s in each of the F450W and F814W filters (the SN position fortunately fell on the PC1 chip). We re-observed SN2006bc on 2006 October 14 (as part of GO10498) with the ACS Wide Field Camera (WFC) in three filters *F*435*W* (1400 s), *F*555*W* (1500 s) and *F*814*W* (1600 s).[7] Aligning the before and after explosion images allowed us to locate the position of the SN on the pre-explosion images to within 0.024 arcsec (again see Maund et al. 2005a; Crockett et al. 2008, for details of alignment procedures). Within this error circle there was no detection of a progenitor star in any of the image and filter combinations. At the progenitor position we determined a 3σ detection limit of $m_{F814W} = 24.45$. There is no distance measurement to NGC 2397 apart from a kinematic estimate, which is $d = 14.7 \pm 2.6$ Mpc, from LEDA (Virgo infall corrected). The Galactic extinction is estimated to be $E(B - V) = 0.205$ (Schlegel et al. 1998). Assuming that the progenitor was a red supergiant we find a luminosity limit of $\log L/L_\odot = 4.23 \pm 0.20$ and an 84 per cent

[7] This constituted an ESA Photo Release: http://www.spacetelescope.org/news/html/heic0808.html.

confidence limit of $\log L/L_\odot = 4.43$. From Fig. 1 this implies an upper mass limit of $12\,M_\odot$.

5.17 2006my

SN2006my occurred at $r_G/r_{25} = 0.37$ almost exactly at the galactocentric radius of the characteristic oxygen abundance measured in NGC 4651 by Pilyugin et al. (2004). They measure a value of 8.7 dex at this position.

Li et al. (2007) claim the detection of a red supergiant progenitor of SN 2006my in pre-explosion *HST*/WFPC2 observations of NGC 4651. In order to determine the position of the SN on the pre-explosion *HST* images Li et al. (2007) aligned these images with ground-based observations of the SN from the CFHT. They derived an initial mass of $M = 10^{+5}_{-3}\,M_\odot$ for the object which they find coincident with the SN position.

However, in an improved analysis, Leonard et al. (2008) have shown that this is unlikely to be correct and the progenitor star is most likely not detected in the pre-explosion images. They used *HST* images of much higher resolution than CFHT which allows for object positions to be more accurately measured and ultimately leads to a more reliable transformation between the coordinate systems of the pre- and post-explosion images. They find that the offset between the SN and possible progenitor position is too large to support the claim that the two objects are associated (at about the 96 per cent confidence level). In a completely independent manner, we used similar data to carry out the same image alignment and the details of this analysis are presented in our companion paper (Crockett et al. 2009). Using the *HST* post-explosion to *HST* pre-explosion transformation, we also find that the progenitor object proposed by Li et al. (2007) is ∼74 mas from the transformed SN position. Given our total astrometric error this is approximately a 1.8σ separation. Hence we also find that this object is unlikely to be the progenitor of SN 2006my. Most likely it is not and the progenitor is undetected in the images, so we derive a 3σ detection limit of $m_{F814W} = 24.8$.

Solanes et al. (2002) have collected Tully–Fisher distance estimates for NGC 4651 from seven different sources and derive a mean distance modulus $\mu = 31.74 \pm 0.25$ (or $d = 22.3 \pm 2.6$ Mpc). As in Li et al. (2007) we apply only a correction for the Galactic extinction of $E(B-V) = 0.027$. Assuming that the progenitor star was a red supergiant we derive a luminosity limit of $\log L/L_\odot = 4.35 \pm 0.16$ and an 84 per cent confidence limit of $\log L/L_\odot = 4.51$. From Fig. 1 this implies an upper mass limit of $13\,M_\odot$.

5.18 2006ov

Pilyugin et al. (2004) redetermined the oxygen abundance gradient, and our calibrations are on this equivalent scale, hence we use the galactocentric radius $0.26r_{25}$ and abundance gradient of Pilyugin et al. to determine an oxygen abundance of 8.9 dex which is the highest in this sample.

Li et al. (2007) report the detection of a red supergiant progenitor of $M_{ZAMS} = 15^{+5}_{-3}\,M_\odot$ for SN 2006ov in archival *HST*/WFPC2 observations of NGC 4303. In this case the pre-explosion frames were aligned with *HST* observations of the SN in order to pinpoint the position of the progenitor on the archival images. Having performed point spread function (PSF) fitting photometry using HSTphot (Dolphin 2000) without detecting a progenitor star, it was noticed by Li et al. that a significant point source was still visible in the residual image close to the SN site. Li et al. (2007) suggest that this object in the residual image is in fact coincident with the SN position, and claim that by forcing HSTphot to fit a PSF at this position they detect an object of 6.1σ significance in the $F814W$ and $F450W$ observations.

We have repeated the alignment of the pre- and post-explosion *HST* observations and find exactly the same transformed SN position as in Li et al. (2007). We also find the same point source still visible in the residual image after performing PSF-fitting photometry using HSTphot. However, we measure the centre of this point source to be some ∼63 mas from the SN position, which given our total astrometric error is a 2.5σ separation. This casts significant doubt on the identification of this object as the SN progenitor. Furthermore, we are unable to reproduce the photometry results of Li et al. (2007) by forcing HSTphot to fit at the transformed SN position. Rather we find detections of the highest significance (∼6.0σ in $F814W$ and ∼4.4σ in $F450W$) when we force a fit at our own measured position of this point source, which as we have already said is not coincident with the SN position. A more detailed discussion of this analysis are presented in Crockett et al. (2009).

Since we cannot confirm that this object is the progenitor of SN 2006ov we derive a 3σ detection limit of $m_{F814W} = 24.2$.

Li et al. (2007) derive a mean distance modulus for NGC 4303 (M61) of $\mu = 30.5 \pm 0.4$ (or $d = 12.6 \pm 2.4$ Mpc) from two Tully–Fisher distance estimates, and that value is adopted here. We apply only a correction for the Galactic extinction of $E(B-V) = 0.022$. Again assuming that the progenitor star was a red supergiant we derive a luminosity limit of $\log L/L_\odot = 4.09 \pm 0.2$ and an 84 per cent confidence limit of $\log L/L_\odot = 4.29$. From Fig. 1 this implies an upper mass limit of $10\,M_\odot$.

5.19 2007aa

NGC 4030 is an Sbc spiral with no study of its H II regions published. The same arguments as in Section 5.1 can be used (NGC 4030 has $M_B = -20.7$) to infer an oxygen abundance at the galactocentric radius of SN2007aa ($0.91r_{25}$) of approximately 8.4 dex.

The pre-explosion site of SN 2007aa was imaged using WFPC2 (2001 July 30) with exposure times of 460 s in each of the $F450W$ and $F814W$ filters. We determined the position of SN 2007aa on these images using a ground-based image of 0.8 arcsec resolution taken with the AUX Port camera on the William Herschel Telescope on 2007 March 11 in the *I*-band filter. Alignment of this image with the pre-explosion frames produced an error circle of 0.07 arcsec for the SN position on the $F450W$ and $F814W$ images. No object was detected within this region and hence a 3σ detection limit of $m_{F814W} = 24.44$ was determined. A kinematic distance estimate of $d = 20.5 \pm 2.6$ Mpc for NGC 4030 was calculated from its recessional velocity (Virgo infall corrected) as recorded in LEDA. Extinction due to the Milky Way is estimated to be $E(B-V) = 0.026$ (Schlegel et al. 1998). Assuming the progenitor was a red supergiant we find a luminosity limit of $\log L/L_\odot = 4.38 \pm 0.15$ and an 84 per cent confidence limit of $\log L/L_\odot = 4.53$. From Fig. 1 this implies an upper mass limit of $12\,M_\odot$.

5.20 2008bk

SN2008bk was recently discovered in NGC 7793 a nearby galaxy with two distance modulus estimates of $\mu = 27.96 \pm 0.24$ (Karachentsev et al. 2003) determined from the tip of the red giant branch and $\mu = 28.01$ from a Tully–Fisher distance in LEDA. We will adopt the distance modulus of $\mu = 27.96 \pm 0.24$ ($d =$

3.9 ± 0.4 Mpc). The galaxy is part of the oxygen abundance gradient study of Pilyugin et al. (2004). The galactocentric radius $0.66r_{25}$ and the abundance gradient imply an oxygen abundance of between 8.2 and 8.4 dex at the SN position (Mattila et al. 2008), hence we adopt the LMC-type metallicity.

The galaxy has a wealth of pre-discovery images available from the Very Large Telescope (VLT), with optical *BVI* images from FORS1 and NIR *JHK* images from HAWK-I and ISAAC. We have shown in a recent letter that SN2008bk is exactly coincident with a bright, red, source detected in the *IJHK* bands, using high-resolution K_s-images from the NACO system (Mattila et al. 2008). Although the foreground extinction towards the galaxy is low and the early observations of the SN appear to show no signs of significant extinction, Mattila et al. (2008) show that the progenitor SED can be fitted with a late-type M4I spectral type with a visual extinction of $A_V = 1.0 \pm 0.5$. Using methods which are entirely consistent with our approach in this paper, Mattila et al. (2008) have estimated the luminosity and mass of this red supergiant. The distance of 3.9 ± 0.4 Mpc and $A_V = 1.0 \pm 0.5$ results in $M_K = -9.73 \pm 0.26$. Levesque et al. (2005) show that using M_K to determine $M_{\rm bol}$ is preferable to using the optical bands. The best-fitting SED of around M4I would correspond to $T_{\rm eff} \simeq 3550 \pm 50$ K and a bolometric correction $\mathrm{BC}_K = +2.9 \pm 0.1$ (both from the Levesque et al. scale). This results in $\log L/\mathrm{L}_\odot = 4.63 \pm 0.1$ and from Fig. 1 (at LMC metallicity) this corresponds to a mass of $9^{+4}_{-1}\,\mathrm{M}_\odot$.

6 SYSTEMATIC UNCERTAINTIES IN THE DETERMINATION OF STELLAR MASS

6.1 Stellar evolution models

The luminosity estimates and limits used to determine stellar masses are obviously dependent on the stellar model used. Hence it is necessary to compare our stellar models to other contemporary models of massive stars. The constituent physics of modern codes is mostly identical, using the same nuclear reaction rates and opacity tables. The differences come from the adopted mass-loss rates, the numerical schemes employed to solve the stellar structure equations and the treatment of mixing, convection and rotation in the codes (see Langer & Maeder 1995; Stancliffe 2006, for example). Here we illustrate the differences between our models and those of Schaller et al. (1992), Hirschi, Meynet & Maeder (2004) and Heger & Langer (2000). We consider three details of the end points of the stellar models, these are the final luminosity, the final effective temperature and the stellar lifetimes in Figs 2–4.

One detail to note first is that the Geneva rotating models (Hirschi et al. 2004) predict a smaller maximum initial mass for red supergiant progenitors of $22\,\mathrm{M}_\odot$ rather than the $27\,\mathrm{M}_\odot$ from the STARS models, while the non-rotating Geneva models (Schaller et al. 1992) predict a maximum initial mass for red supergiant progenitors of $34\,\mathrm{M}_\odot$. Beyond these masses the codes predict the stars will end as H-deficient WR stars (depending on the mass-loss recipe employed). One other noticeable feature is that only the STARS models follow the process of second dredge-up and produce massive AGB stars at low masses. This is because the other models have been stopped before it could occur. Second dredge-up is found at similar masses in other codes specifically designed to follow this stage (e.g. Siess 2006, 2007; Poelarends et al. 2008).

In Fig. 2 the difference in final luminosities between models is illustrated. The model sets with the greatest difference with our M–$\log L/\mathrm{L}_\odot$ relation are the non-rotating Geneva and Heger & Langer models, while their rotating models have reasonable agreement with

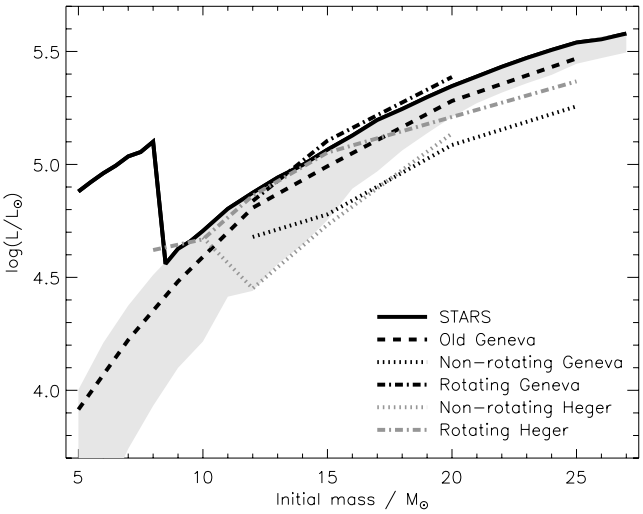

Figure 2. The initial mass compared with the final luminosity of the STARS and Geneva stellar models. For each mass we plot the luminosity at the end of the model, just before core-collapse. For the STARS models this is up to the beginning of neon burning. The old Geneva models end after core carbon burning. For the newer Geneva models both end at silicon burning. The grey-shaded region represents the range of luminosity for the STARS models from the end of core helium burning to the luminosity at the onset of core neon burning (see Section 3 and Fig. 1)

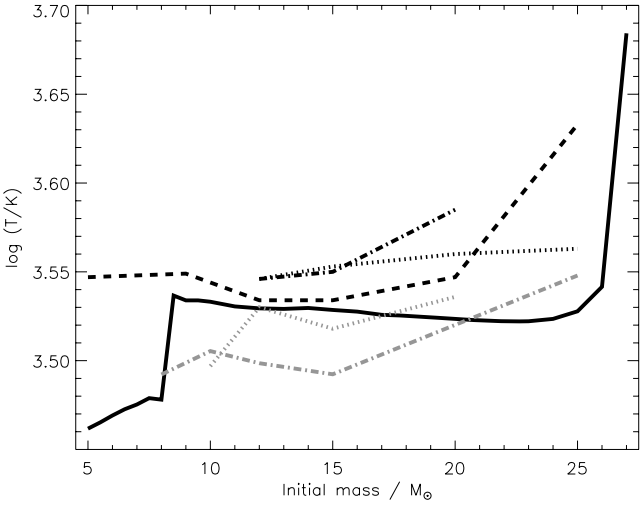

Figure 3. Similar to Fig. 2 but with initial mass versus effective temperature at the end of the stellar model.

the STARS models and with the older Schaller et al. (1992) models. The main reason for the relationships not being exactly similar is because of different assumptions of mixing in the stellar models and also the tracks end at different points in the stars' evolution. For example, the old Geneva models have lower luminosities than the STARS models because they end after core carbon burning while the STARS models progress slightly further to the beginning of neon burning and we find the luminosity grows after core carbon burning. Also the Geneva $9\,\mathrm{M}_\odot$ models end after core helium burning and therefore it underestimates the final core mass and luminosity.

The newer Geneva models differ in the treatment of mixing and convection in the models which affects the vigour of the nuclear burning in the stars and therefore the luminosity. For example, they use a smaller overshooting parameter than the older Geneva models

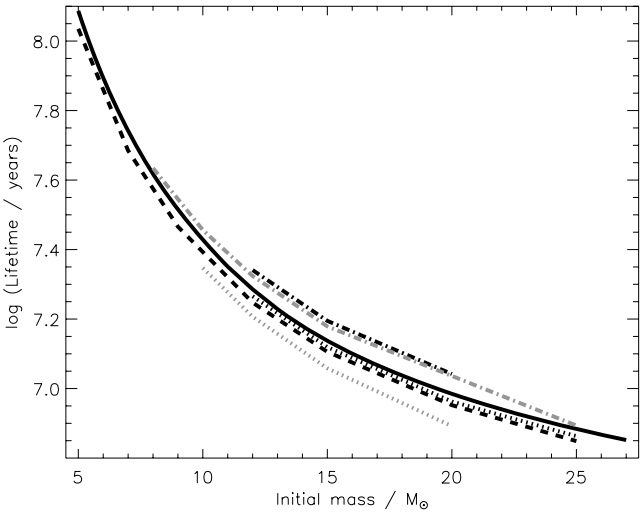

Figure 4. Similar to Fig. 2 but with initial mass versus lifetime to the end of the stellar model.

as mixing is now also provided by the rotation. Thus the rotating models agree with our final luminosities but the non-rotating star luminosities are 0.3 dex lower. We emphasize that the new non-rotating models are artificially pushed to lower luminosities as the mixing efficiencies (from overshooting) have been significantly reduced. Otherwise employing the same mixing parameters as previously employed *and* adding rotational mixing would push all the luminosities too high to be consistent with observed HRDs.

In general the uncertainty in final luminosity due to the assumption of a certain set of stellar models is typically 0.1 dex between our STARS models and the most up to date rotating models. However, the issue of how much mixing is included and by which mechanism can lead to an uncertainty of up to 0.3 dex. This does not pose a major problem to our estimates as we are using the luminosity at the end of core helium burning to estimate the 84 per cent confidence upper mass limits. In Fig. 2 one can see that the grey area (which highlights the region in the STARS code between end of core He burning and the end of the model as discussed in Section 3) brackets nearly all the tracks.

While the initial mass to final luminosity is uncertain the final helium core mass to final luminosity relationship is much tighter. This is because the size of the helium core is the major factor in determining a red supergiants luminosity. To remain consistent with progenitor masses measured from cluster turn-off ages and with previous studies we have determined *initial masses* ($M_{\rm i}$) for our progenitors. Helium core masses ($M_{\rm He\,core}$) can then be estimated from these by using the following relation determined from the STARS stellar models:

$$M_{\rm He\,core} = (0.830 \pm 0.168) + (0.053 \pm 0.027)M_{\rm i} + (0.015 \pm 0.001)M_{\rm i}^2. \quad (1)$$

The surface temperatures in Fig. 3 show that the final predicted effective temperatures are all within 0.05 dex with the Heger & Langer (2000) models being the coolest. At higher masses the temperature sharply increases as the hydrogen envelopes in these cases are low mass ($<0.5\,{\rm M}_{\odot}$) as the star is stripped due to mass-loss. These temperatures are highly sensitive to the boundary conditions in the stellar models as well as the opacities used, so it is not easy to simply identify the reason for the differences between the models. But the uncertainty (± 200 K) is well below the uncertainty in the surface temperature implied from spectral types of observed SN progenitors (typically ± 500 K, from the colour spectral type estimates).

The stellar lifetimes in Fig. 4 also show close agreement. The most discrepant are the rotating Geneva models. Rotation increases the hydrogen burning lifetime considerably by mixing fresh hydrogen into the core and extending the hydrogen burning lifetime of the star. The increase, however, is less than 0.1 dex and therefore masses derived from lifetimes (i.e. turn-off masses for 2004am and 2004dj) are consistent between stellar models.

Hence we conclude that the use of different stellar models are unlikely to have a significant effect on the estimated masses and mass limits we have derived, especially if a single method is employed and all masses are derived on a homogeneous scale. Furthermore, while the initial masses may be somewhat dependent on the choice of single star models, the final helium core masses that our initial mass corresponds to should be reliable.

6.2 Extinction determinations

It is likely that our largest source of error comes from the extinction that we assume is applicable to the line of sight towards each SN. This is not likely to be a simple systematic effect that would change all the mass estimates and limits by a constant. However, we need to consider if we are consistently underestimating the extinction towards the progenitor stars and by what magnitude.

The extinctions which have been estimated for each of the progenitor stars come from several methods. All of these suffer from their own uncertainties and problems and in general we favour taking the mean of different results. The rationale is that no single method is clearly superior to the others and a mean of several, possibly problematic, estimates is better than adopting one. The extinctions have been estimated by some of the following techniques: measurements of the Na I ISM absorption lines and calibrating this using Turatto, Benetti & Cappellaro (2003); comparing the early continuum slopes to the well-observed and reliably modelled 1999em and also to unphysically hot blackbody continua; fitting stellar SEDs to the surrounding massive star population within about 10–100 pc; and if the SN exploded within an H II region or compact cluster then using the value determined from the nebular emission lines or the cluster SED. An example of the applications of all of these methods applied to SN2001du can be found in Smartt et al. (2003). In the latest case of SN2008bk there is no accurate extinction measurement towards the SN yet and Mattila et al. (2008) have employed $A_V = 1.0$ to fit a late-type M4I to the observed *IJHK* progenitor colours. An extinction of less than this results in a star which is intrinsically too red to be compatible with known massive red supergiants. We do not revisit the reliability of every method applicable to each event as this is dealt with in the relevant references cited in the subsections for the events above. However, we should consider if these methods as a whole are applicable and what are the likely sources of error.

The primary concern is our assumption that the extinction towards the SN (and surrounding stellar population) is directly applicable towards the line of sight to the progenitor. Two methods probe the intervening line of sight directly to the SN. However, the early soft X-ray, UV–optical flash of the explosion could conceivably have photoevaporated substantial circumstellar dust close to the progenitor (Dwek 1983). Waxman & Draine (2000) have suggested that the X-ray and UV afterglow of a GRB could photoevaporate a large cavity surrounding the progenitor star. Scaling the GRB energy to the observed flux from recent shock breakouts observed for Type II-P and Ibc SNe, Botticella et al. (in preparation) have

estimated how much dust could conceivably be destroyed in a dense circumstellar envelope. It would appear that it is quite possible for such a UV, soft X-ray flash to destroy dust masses that could provide several tens of magnitudes of extinction in the optical V band.

This is of obvious concern when one considers that the observations of luminous red supergiants in the Magellanic Clouds, the Galaxy and the Local Group are known to produce large quantities of dust (Massey et al. 2005; van Loon et al. 2005). A histogram of extinctions towards optically selected red supergiants in the LMC and SMC clusters by Levesque et al. (2006) suggests that RSGs tend to be redder (by on average $A_V \simeq 0.4$ mag) compared to the extinctions towards the other OB stars in their stellar associations. The mean extinction towards LMC and SMC RSGs is 0.60 and 0.73 mag, respectively. The mean extinction that has been determined towards our SN progenitors is 0.7 ± 1.1 (from Table 2) and the large standard deviation is due to 2002hh with $A_V = 5.2$. In this calculation we have left out 2004am which clearly suffers from high extinction in line of sight in M82; its host cluster is heavily reddened hence its high A_V is unlikely to be due to CSM dust shells (see Section 5.11). This simple comparison would suggest there is no clear difference in the extinctions of the two samples. If we further exclude 2002hh (as an anomalously high extinction object), we have a mean extinction towards the 18 progenitors of 0.44 ± 0.34. In Fig. 5 we show the histogram of our A_V estimates towards the likely red supergiant progenitors and compare them to the LMC and SMC combined population (disregarding the two highest values for 2004am and 2002hh). There is some evidence to suggest that we have more progenitors in the lowest bin 0 −0.2 mag than would be typical for RSG progenitors. This is not unexpected as for several of our SNe we have been forced to adopt the extinction towards the host galaxy alone due to lack of additional information. Given the low numbers of objects and the differences in the sample size, the distribution between 0.2–4.0 does not appear to be a major cause for concern. There are five events for which we adopt a low (foreground Milky Way component only) extinction of $A_V < 0.1$. If these have been underestimated by $A_V \simeq 0.3$ mag, that would bring the mean A_V of the progenitor sample into line with the SMC/LMC RSG populations. In doing so the luminosity and mass limits for each event would increase by: 1999br ($\log L/L_\odot = 4.88$, $<16\,M_\odot$); 2003ie, ($\log L/L_\odot = 5.49$, $<27\,M_\odot$); 2006my, ($\log L/L_\odot = 4.55$, $<13\,M_\odot$); 2006ov ($\log L/L_\odot = 4.35$, $<11\,M_\odot$); 2007aa ($\log L/L_\odot = 4.6$, $<13\,M_\odot$). This does not affect the lower mass limit that we derive below for the sample from the maximum likelihood analysis and has a minimal affect on the maximum mass as we shall see (Section 7).

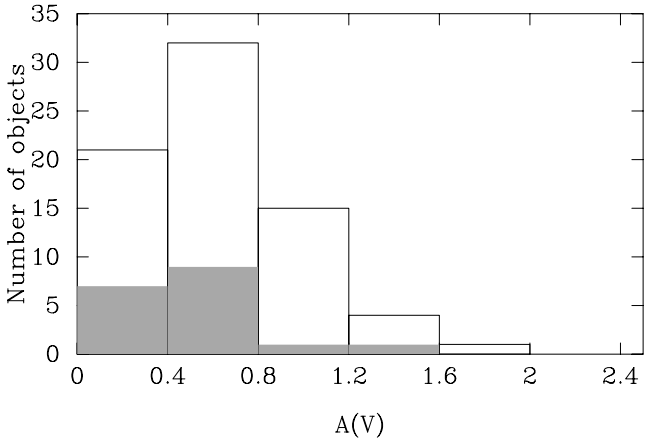

Figure 5. Histogram of the A_V values adopted for the progenitor stars (shaded bars) compared to A_V values of red supergiants in the LMC and the SMC from Levesque et al. (2006) (open bars). There are 18 SN progenitors plotted here in the shaded bars (2004am and 2002hh were excluded as explained in the text), and 73 RSGs from the combined SMC and LMC samples.

The extinction remains the major source of uncertainty and there exist populations of dusty red supergiants which are obscured in the visual and near-IR (often by ∼10 mag in the V band) and are mid-IR bright as their optically thick dust shell is heated by the stellar luminosity and this light is reprocessed into thermal mid-IR emission from dust grains (Loup et al. 1997; van Loon et al. 2005, 2006). These would not appear in the Massey & Olsen (2003) and Massey (2002) sample as they are too faint optically. However, the relative numbers of red supergiants (*excluding* AGB stars, which are below the mass threshold to produce SNe) which are visually obscured (e.g. objects similar to those in van Loon et al. 1998, 2005) and those which suffer moderate extinctions (the optically detectable stars in Massey & Olsen 2003) is unknown. Such a study to quantify the latest stages in stellar evolution in a complete manner would be highly desirable and the Magellanic Clouds would appear to be an excellent laboratory. Clearly we do see a large population of RSGs with low moderate extinctions as shown by Levesque et al. (2006) and Massey & Olsen (2003), and we suggest that our progenitors are part of this population. How many dust obscured RSGs which are missing from optical and near-IR surveys remains to be seen.

Additionally if a mass-loss mechanism (such as pulsations) occurs during the final stages of evolution of most massive stars as core-collapse approaches one might envisage that the progenitors become systematically more obscured. This would invalidate the comparison with the LMC RSG population. Such severe mass-loss is not well constrained observationally or theoretically but if it occurred frequently one would expect to see signatures of circumstellar gas as well as dust. The Type II-P tend to be low-luminosity radio and X-ray emitters and tend not to show narrow hydrogen or helium lines suggestive of CSM shells (Chevalier, Fransson & Nymark 2006).

While there is no clear evidence that dense dust shells form around II-P progenitors, we at present cannot rule out some visual obscuration due to an optically thick dust shell which was then evaporated by a soft X-ray, UV and optical flash at shock breakout. This has been suggested as a possible mechanism for SN2008S (Prieto et al. 2008a), see Section 2.4.

7 MAXIMUM LIKELIHOOD ANALYSIS OF THE MASSES OF PROGENITOR STARS

Using the measurements of progenitor masses in Table 2 it is possible to estimate parameters that describe the progenitor population. The three parameters of the progenitors that we are interested in are the minimum initial mass for a Type II-P SN, the maximum initial mass and the IMF of the population.

Estimating these from a small sample is not difficult but the relatively small number of data points can restrict the accuracy with which one can constrain the most probable values. We therefore use the unbinned maximum likelihood method, e.g. Jegerlehner, Neubig & Raffelt (1996). For a large number of objects this effectively becomes a χ^2 method. The likelihood is defined to be

$$\mathcal{L} = \prod P_i(m), \tag{2}$$

where P_i is the probability of the ith event to have mass m. We must define a function for the probability of each event, P_i, and then maximize the likelihood to find the parameters that give the most probable set of events.

To make the maximization more straightforward we first take the natural logarithm of the likelihood function and so we are required to calculate a sum rather than a product,

$$\ln \mathcal{L} = \sum \ln P_i(m). \tag{3}$$

The probability function that describes the probability that a progenitor will have mass m within a certain mass range is essentially the IMF. We do need to treat the detections and the non-detections differently. For non-detections we adopt the probability function,

$$P_i = \int_{m_{\rm min}}^{m_{i,\rm limit}} \frac{m^{\Gamma-1}}{(m_{\rm min}^{\Gamma} - m_{\rm max}^{\Gamma})} {\rm d}m, \tag{4}$$

where Γ is the value of the IMF, Salpeter being -1.35, $m_{\rm min}$ is the minimum mass for a Type II-P SN, $m_{\rm max}$ is the maximum mass for a Type II-P SN, and $m_{i,\rm limit}$ is the upper mass limit for the ith non-detection. If $m_{\rm max}$ is less than $m_{i,\rm limit}$ we set $P_i = 1$. If $m_{\rm min}$ is greater than $m_{i,\rm limit}$ we set $P_i = 0.16$ because our mass limits are 84 per cent confidence limits so there is a chance that the progenitor could be more massive.

For detections the case is more complicated. The errors for the progenitor luminosity are roughly Gaussian, but converting to an initial mass affects the distribution. We first take the best estimated mass, m_j, as the most probable value for each detection. Then above this mass we integrate the IMF up to the upper uncertainty on the mass estimate, $m_{j,\rm high}$. Below m_j we assume the probability distribution is a straight line going to zero at the lower uncertainty on the mass limit, $m_{j,\rm low}$. While these error distributions are somewhat arbitrary they avoid skewing the overall distribution to higher or lower masses as happens when using a Gaussian distribution to describe the uncertainties. We have experimented with different probability functions for detection, e.g. using triangular and rectangular error functions at the low and high uncertainty limits. The $m_{\rm max}$ and $m_{\rm min}$ would typically vary by $\approx 1\,{\rm M}_{\odot}$ which is within the uncertainty we derive for these parameters. We feel our chosen method for describing the probability function in the case of detections is the best representation of the asymmetric errors on the mass estimates. Hence for detections we use the following probability distribution

$$P_j = \int_{m_{j,\rm low}}^{m_j} \frac{(m - m_{j,\rm low}) m_j^{\Gamma-1}}{(m_j - m_{j,\rm low})(m_{\rm min}^{\Gamma} - m_{\rm max}^{\Gamma})} {\rm d}m + \int_{m_j}^{m_{j,\rm high}} \frac{m^{\Gamma-1}}{(m_{\rm min}^{\Gamma} - m_{\rm max}^{\Gamma})} {\rm d}m. \tag{5}$$

If $m_{j,\rm low}$ is lower or higher than $m_{\rm min}$ and $m_{\rm max}$ then the integral is truncated within these limits.

We calculate the likelihood using the masses for the SN progenitors listed in Table 2 and allow $m_{\rm min}$ and $m_{\rm max}$ to vary, while fixing the IMF slope to Salpeter ($\Gamma = -1.35$). Originally we attempted to let the IMF vary as well as the maximum and minimum mass values but find it constrains the IMF only very weakly and we chose to fix it at three different values, as justified below.

Furthermore we estimate the confidence regions from

$$\ln \mathcal{L}_{\rm max} - \ln \mathcal{L} = \frac{1}{2}\chi, \tag{6}$$

where for two parameters, when $\chi = 2.3$, 4.6 and 6.2 we have the 68, 90 and 95 per cent confidence regions (Press et al. 1992).

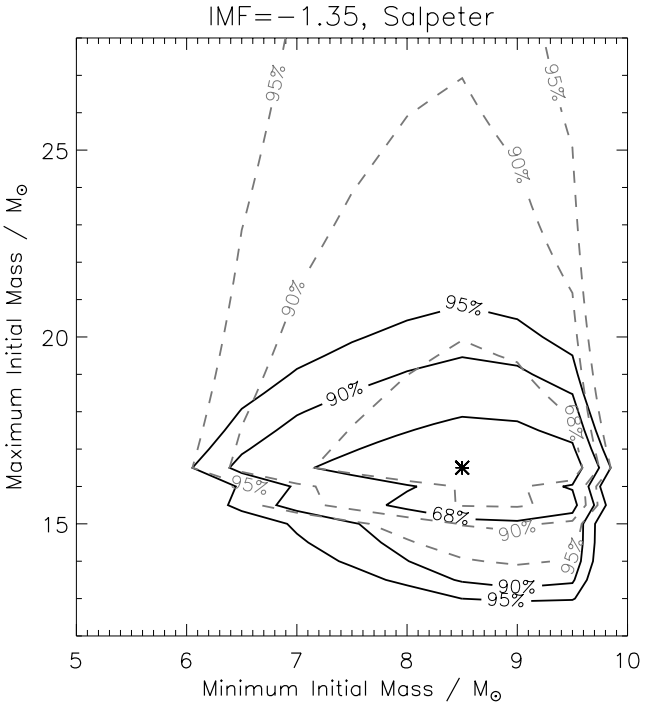

Figure 6. Plot of the likelihood function for the mass ranges of Type II-P progenitors. The star indicates the parameters with the highest likelihood and the contours the confidence regions. The dotted grey lines show the results using the seven detections only, which results in a lower mass limit of $8.5\,{\rm M}_{\odot}$. The solid black lines show the contours using the fixed lower limit and allowing the maximum mass to vary.

We first estimate $m_{\rm min}$ and $m_{\rm max}$ using the seven detections only (without incorporating the upper limits). The results can be seen in dashed contours in Fig. 6. The parameters we estimate are $m_{\rm min} = 8.5^{+1}_{-1.5}\,{\rm M}_{\odot}$ and $m_{\rm max} = 16.5^{+4}_{-1.0}\,{\rm M}_{\odot}$. We then recalculate the likelihoods using both the detections and upper limits in the analysis but fix the minimum initial mass to $8.5\,{\rm M}_{\odot}$ as derived from the detections alone. This is because the non-detections only provide meaningful information on the maximum initial mass $m_{\rm max}$. In contrast they provide only a weak constraint on $m_{\rm min}$ as when combined with the IMF they would simply favour a low mass due to the rising probability of having more low-mass stars. We suggest it is more reasonable to calculate $m_{\rm min}$ from the detections and effectively this converges towards the lowest masses detected in the progenitor sample. The upper mass limits have a strong impact on the uncertainty on $m_{\rm max}$ and we determine that $m_{\rm max} = 16.5 \pm 1.5\,{\rm M}_{\odot}$. With the error on $m_{\rm max}$ reduced significantly, this suggests that at 95 per cent confidence level the maximum initial mass to produce a Type II-P is $21\,{\rm M}_{\odot}$.

In all of the above we have assumed a Salpeter IMF and it is reasonable to question the validity of this assumption. Elmegreen (2009) has recently reviewed evidence for the variation in the IMF slope in local star-forming environments such as Galactic and Local Group Galaxy clusters and field populations within the Galaxy and the Magellanic Clouds. In clusters and OB associations with total masses between 10^2 and $10^4\,{\rm M}_{\odot}$ there is little evidence for strong and real deviations from the Salpeter slope of $\Gamma = -1.35$ above and beyond the rms measurement errors determined in each region of high-mass stars (with typical uncertainties of the order of ± 0.1 to ± 0.3). That is not to say that such real variations do not exist, only that stochastic effects mean that determining the true IMF in

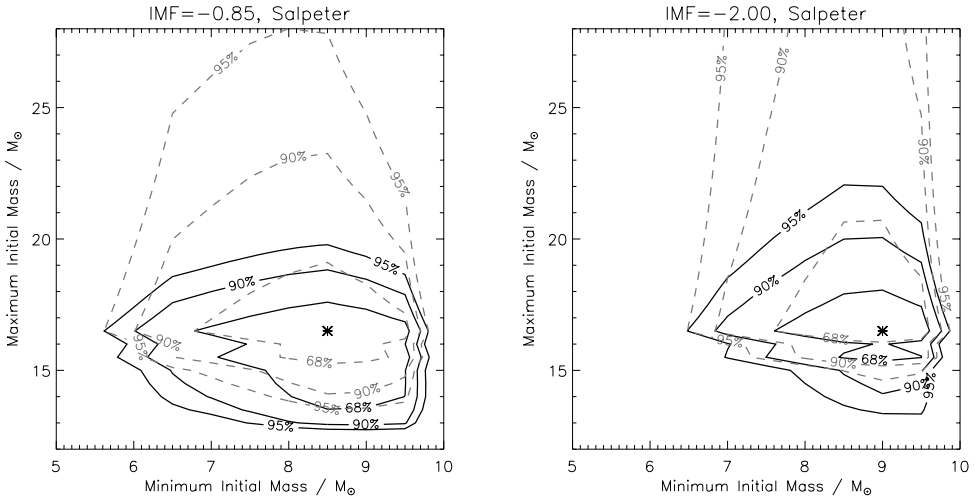

Figure 7. As in Fig. 6 but with a shallower (left-hand panel) and steeper (right-hand panel) IMF.

localized regions can at best reach the accuracy of a few tenths. There is some evidence that flatter IMF slopes exist in very dense star-forming regions such as NGC 3603 ($\Gamma = -0.9 \pm 0.15$; Stolte et al. 2006) and the Galactic Centre ($\Gamma = -1.05 \pm 0.05$; Kim et al. 2006). Also there is evidence that the field population may show much steeper slopes, with $\Gamma = -1.80 \pm 0.09$ applicable for a large sample of field stars lying outside clusters and associations in the LMC (Parker et al. 1998). Extreme values of around 3–4 have even been found (Gouliermis et al. 2002; Massey 2002) though it is unclear to what extent this is simply due to stellar drift out of low-mass clusters. Elmegreen (2009) surmises that $\Gamma = -1.35$ appears to be fairly typical in moderate mass clusters and star-forming regions and variation around this is, on the whole, limited to approximately ± 0.5. As our SNe, and their progenitors, seem to reside in typical star-forming regions and the field of their host spirals there is no compelling evidence to favour an IMF too dissimilar to Salpeter. In Fig. 7 we have recalculated the maximum likelihood values with the extreme IMFs suggested in Elmegreen (2009) of $\Gamma = -0.85$ and $\Gamma = -2.0$. For the shallow IMF slope of $\Gamma = -0.85$ the best estimates of the minimum and maximum initial mass are unchanged but the uncertainties increase slightly to $m_{\rm min} = 8.5^{+1}_{-2}\,{\rm M}_{\odot}$ and $m_{\rm max} = 16.5^{+1}_{-3}\,{\rm M}_{\odot}$. This shallow IMF is unlikely to be representative of our progenitor environments as they are not (apart from perhaps 2004am and 2004dj) in dense clusters such as seen in NGC 3603 and the Arches cluster at the Galactic Centre. For the steeper IMF, the most likely minimum initial mass increases to $m_{\rm min} = 9^{+0.5}_{-1.5}\,{\rm M}_{\odot}$ and the 95 per cent confidence limit for $m_{\rm max}$ is pushed to the higher value of $22\,{\rm M}_{\odot}$. In summary there is no strong evidence (from Local Group studies as reviewed by Elmegreen 2009) that our progenitor population should come from a massive stellar population with an IMF slope significantly different (i.e. by more than ± 0.5) than Salpeter, and adoption of the either of those extreme values does not significantly affect the values of $m_{\rm min}$ and $m_{\rm max}$.

Two remaining uncertainties are extinction and the value of H_0. As discussed in Section 6.2, if we have underestimated the extinctions towards five events with non-detections and replace them with the slightly higher masses, $m_{\rm min}$ and $m_{\rm max}$ change by less than $0.1\,{\rm M}_{\odot}$. As discussed in Section 5, if we employ $H_0 = 65\,{\rm km\,s^{-1}\,Mpc^{-1}}$, then the luminosity differences of the five progenitors for which we employ only a kinematic host galaxy distance (see Table 2) would change by $+0.22$ dex. This corresponds to approximately 2–3 $\rm M_{\odot}$ in the ZAMS estimate. The value of $m_{\rm min}$ does not change, but the maximum mass increases to $m_{\rm max} = 18.5 \pm 2$. This is due to SN1999ev having the most massive progenitor estimate and the host of SN1999ev has a kinematic distance only. Similarly, using $H_0 = 85\,{\rm km\,s^{-1}\,Mpc^{-1}}$ keeps $m_{\rm min}$ with in 8–9 $\rm M_{\odot}$ (as all the SNe which determine this number have distances from other methods), but the maximum mass reduces to $m_{\rm max} = 15.5^{+1}_{-0.5}\,{\rm M}_{\odot}$. This illustrates that in the future it is important to try to find the Type II-P SNe from the highest mass progenitors to tie down $m_{\rm max}$ as reliably as possible.

8 DISCUSSION

With our analysis of the progenitor observations and mass estimates we are able to consider some outstanding questions on the nature of SN progenitors from a firm observational footing. There has recently been much discussion on the initial masses of progenitor stars of SNe of all types (Smartt et al. 2003; Gal-Yam et al. 2007a; Li et al. 2007) and the nature of faint type II-P SNe (Zampieri, Shapiro & Colpi 1998; Zampieri et al. 2003; Nomoto et al. 2004; Pastorello et al. 2006).

Our maximum likelihood analysis reveals that the progenitors of Type II-P arise from stars with initial masses between $8.5^{+1}_{-1.5}$ and $16.5 \pm 1.5\,{\rm M}_{\odot}$. The derivation of the mass range assumes that the stars are red supergiants, in that to transform the optical or near-IR limiting magnitudes to a luminosity and mass we must assume a stellar progenitor spectrum with a suitable photospheric temperature (or range of temperatures). This is well justified in that five of the detections have colours consistent with them being late K-type to mid M-type supergiants and the requirement that a II-P light-curve results from the explosion of a star which has an extended H-rich envelope ($R_* \sim 500$–$1000\,{\rm R}_{\odot}$; Chevalier 1976; Arnett 1980; Popov 1993). The maximum initial mass is important to constrain the final evolutionary stage of the most massive stars and the lowest initial mass that could produce a type Ib/c, or perhaps II-L and IIn, explosion. The minimum initial mass that can support an SN explosion is of great interest for explosion models, stellar evolution, comparing with massive WD progenitor masses and galactic chemical evolution.

The mass range that we find for the progenitors is much lower than ejecta masses of a sample of II-P SNe suggested by Hamuy (2003). This study estimated ejecta mass of between 14 and $56\,{\rm M}_{\odot}$ from the application of the Nadyozhin (2003) formulae to

determine energy of explosion, radius of progenitor and ejected mass. Even though the error bars on the masses are large there is a clear discrepancy between our results. The determination of the ejecta masses is very sensitive to how the mid-point in the light curve is defined to determine V_{50} (the visual magnitude at 50 d) and v_{50} (the ejecta velocity at the same point). The measurement of the latter is also highly dependent on which ionic species is used to measure the photospheric velocity and Nadyozhin (2003) suggests that the bolometric light curve should be used to define the plateau mid-point. It appears to us that the choice of the point at which to define the measured parameters has a critical effect on the physical values determined and caution should be employed when applying this method. We note that Nadyozhin (2003), with similar data to Hamuy (2003) has determined ejecta masses in the range 10–30 $M_\odot$, closer to our progenitor mass range but still systematically higher. It is likely that the mid-points of the plateau light curves defined by Hamuy (2003) (and the parameters thus arising) were not exactly compatible with those required for the Nadyozhin (2003) equations to be applied. The lower ejecta masses of Nadyozhin (2003) are probably more reliable in that they are estimated with the appropriate input parameters and are a better match to the progenitor masses we determine.

One may ask if a ZAMS mass of 8.5 $M_\odot$ is large enough for a long plateau phase to be sustained. In our model the star would lose 0.5 $M_\odot$ due to stellar winds and with a neutron star remnant of 1.5 $M_\odot$, this leaves about 6.5 $M_\odot$ for the ejected mass. Hendry et al. (2005, 2006) showed that the low progenitor masses of SN2004A and SN2003gd (8–9 $M_\odot$) were consistent with the observed recombination powered plateau duration, but only just within the error bars of both model estimates (see also Smartt et al. 2003). In a future paper we will analyse the light curves of a large subset of the SNe presented here to determine if their progenitor mass estimates are consistent with the ejected masses required to produce their plateau phases.

8.1 The minimum mass of II-P progenitors

Theory predicts that a few of the low-mass progenitors should be massive AGB stars, sometimes referred to as super-AGB stars (Eldridge & Tout 2004b; Siess 2007; Poelarends et al. 2008). The cores of these objects never reach high enough temperatures to produce iron, rather the oxygen–neon core grows to the Chandrasekhar mass and an electron capture SN is triggered. These explosions have been predicted to produce less luminous SN than in normal iron core-collapse (Kitaura, Janka & Hillebrandt 2006), and perhaps this signature could be used to find real candidates and to identify progenitor stars at the lowest mass range (see the Section 8.4 and references therein for a discussion of the lowest luminosity SNe). From their models of super-AGB stars, Poelarends et al. (2008) suggest that the number of these stars at solar metallicity would result in them producing 3 per cent of the local core-collapse SNe. This increases to greater than 10 per cent at metallicities below a tenth solar. From the observational properties, one of the best studied examples of a low-luminosity, low ejecta velocity event is SN2005cs, and indeed we do suggest it had a low progenitor mass of $8 \pm 2\,M_\odot$. However, Eldridge et al. (2007) show that there is a clear observational signal for AGB stars, in that these progenitors should be much cooler than higher mass red supergiants and hence be quite bright at NIR bands. Deep NIR pre-discovery images were available for SN2005cs, and we showed that it was unlikely to be a massive AGB star. Thus we suggest that all of the 20 progenitors were genuine Fe core-collapse events, and we have no evidence for any of them being electron capture events in ONe cores. We also have no evidence to support the idea that stars in the range $\sim$ 7–9 $M_\odot$ go through second dredge-up and end as quite high-luminosity progenitors, either as S-AGB stars with ONe cores or genuine Fe core-collapse events. Our models (and those of Poelarends et al. 2008) would suggest that the luminosity of these events can reach $4.6 \leq \log L/L_\odot \leq 5.1$ which is significantly more luminous than any of the progenitors detected so far. Eldridge & Tout (2004b) and Poelarends et al. (2008) point out that this evolutionary phase is very dependent on the treatment of semiconvective mixing and convective overshooting. The fact that we do not see luminous progenitors with $\log L/L_\odot \gtrsim 4.6$ dex (the highest of our sample: SN2005cs) would apparently disfavour the scenario in which $\sim$7–9 $M_\odot$ stars increase their luminosity due to second dredge-up before collapse. The apparent luminosity of the progenitors (around 4.3–4.6) favours a lower limit than is normally assumed for core-collapse with no luminosity spike.

The lower mass limit we derive from Section 7 of $8.5^{+1}_{-1.5}\,M_\odot$ is interesting to compare with the maximum stellar mass that produces WDs. A compilation of mass estimates of WDs by Dobbie et al. (2006) suggests that, in Milky Way intermediate age clusters, stars up to 6.8–8.6 $M_\odot$ produce WDs and they suggest this as the initial mass range for core-collapse SNe. Rubin et al. (2008) suggest that a homogeneous analysis of WDs in their Lick–Arizona White Dwarf Survey (LAWDS) confidently determines the maximum mass to be no less than 6 $M_\odot$. Further recent evidence suggests that the mass limit is no less than 7.1 $M_\odot$ (Williams, Bolte & Koester 2009). A slightly higher mass limit is not ruled out as there is ongoing work on younger clusters to find WDs and determine their progenitor age (K. Williams, private communication). Hence the two, very different approaches, of SN progenitor mass and WD progenitor masses appear to be converging towards $8 \pm 1\,M_\odot$. Unless both methods are significantly in error it would seem unlikely that the lower mass for a core-collapse SN is outside this range. Theoretically several mass-limits have been determined, ranging from 6 to 11 $M_\odot$ (Ritossa, García-Berro & Iben 1999; Heger et al. 2003; Eldridge & Tout 2004b; Poelarends et al. 2008, and references therein) depending critically on the amount of convective overshooting employed. In our analysis we have used models with convective overshooting as there is growing evidence that extra mixing is required above that predicted by mixing-length theory (e.g. Schroder, Pols & Eggleton 1997; Aerts et al. 2003). We suggest that a minimum initial mass of 10 $M_\odot$ or more can now be ruled out for two reasons. First, we detect five progenitors with best estimated masses below 10 $M_\odot$ although admittedly the individual uncertainties would not rule out a higher mass progenitor. Secondly, in our maximum likelihood analysis masses at 10 $M_\odot$ and above are ruled out at over 95 per cent confidence, even with a steep IMF of $\Gamma = -2$. This value is supported by the fact that Type II-P SNe are not always associated with underlying H II emission line regions in their host galaxies (Anderson & James 2008) which would suggest their progenitors are from a population of less than $\sim$10 $M_\odot$.

We suggest that $8.5^{+1}_{-1.5}\,M_\odot$ is the current best estimate, based on observational constraints, for the lower limit to produce an Fe core-collapse driven SN of type II-P. This is in agreement with the mass range for the most massive progenitors of WDs.

8.2 The maximum mass of II-P progenitors

The maximum mass of a star that can produce a II-P SN is an important threshold to constrain. In Fig. 8 we summarize the initial masses of all the progenitors. Similar plots were first shown by Heger et al. (2003) and Eldridge & Tout (2004b) with a large

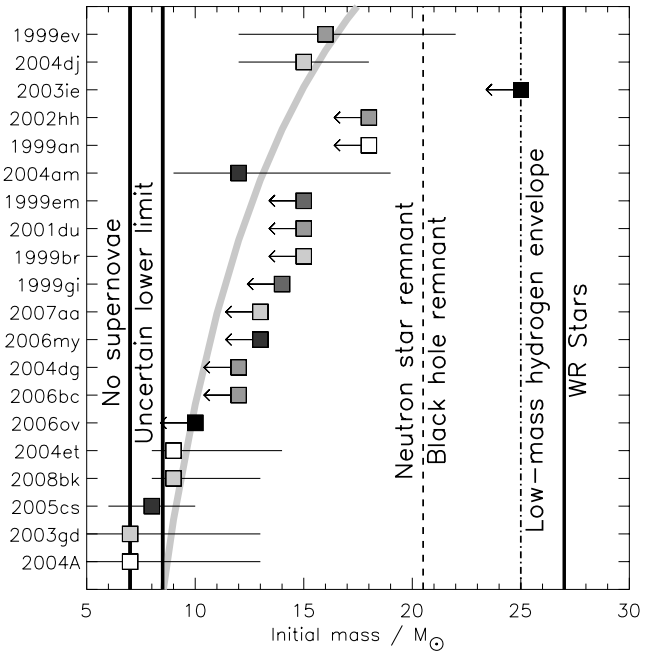

Figure 8. The initial masses of all our Type II-P progenitor stars, compared with our theoretical limits for production of SNe of different types and type of compact remnant. The box symbols are shaded on a metallicity scale, the lighter the shade the lower the metallicity, with the values taken from Table 2.

range of metallicity plotted on the vertical axis, from supersolar to metal-free. As our progenitor stars cover a relatively small range in metallicity, we have removed the axis scale and instead flagged the points with a metallicity coded grey-scale. Clearly the highest mass of a detected progenitor is $16^{+6}_{-4}\,M_{\odot}$ (SN1999ev) with one upper limit above $20\,M_{\odot}$, due to shallow pre-explosion images (SN2003ie). Our estimated maximum initial mass for a II-P (Section 7) is $m_{\rm max} = 16.5 \pm 1.5\,M_{\odot}$, with a 95 per cent confidence limit (assuming Salpeter IMF $\Gamma = -1.35$) of $21\,M_{\odot}$. Fig. 8 is effectively a cumulative frequency distribution (CFD) which is constrained at the lower and upper mass limits and has an IMF with $\Gamma = -1.35$ consistent with the limits in between (the CFD of the Salpeter IMF is plotted as the thick grey line). This Salpeter IMF is a good fit to the distribution of masses and mass limits, if the hard minimum and maximum masses for II-P progenitors hold. Stars more massive than about $20\,M_{\odot}$ would be easily detectable in our archive images, and there is unlikely to be any bias against detecting the most massive progenitors. Hence there does appear to be a real upper limit to the mass of stars that produce normal Type II-P SNe. The one caveat to this is if the progenitor stars suffer large circumstellar extinctions which are photoevaporated in the explosion. We discussed this in Section 6 and while we cannot see a compelling case for such an effect in our population we cannot rule it out.

We can compare this maximum mass limit with the ratios of CCSN types in Table 1. With a maximum possible stellar mass of $150\,M_{\odot}$ (Figer 2005), the fraction of stars born with masses between 8.5–16.5 $M_{\odot}$ (for a Salpeter IMF, $\Gamma = -1.35$) is $\simeq$60 per cent, closely mirroring the Type II-P rate. One might immediately conclude that the agreement suggests that all stars above $\sim 17\,M_{\odot}$ produce the other varieties of CCSNe. However, this is too simplistic and ignores our wealth of knowledge of massive stellar populations from Local Group studies and interacting binaries.

8.2.1 The red supergiant problem

Massive red supergiants have been frequently surveyed in the Milky Way and the Magellanic Clouds, and up until recently their luminosities as determined from model atmospheres implied that they are found at evolutionary masses up to 40–60 $M_{\odot}$ (Humphreys 1978; Massey & Olsen 2003). However, using new MARCS atmosphere models Levesque et al. (2006) have shown that the effective temperatures of these stars have been revised upwards and they have combined this with revised bolometric luminosities based on *K*-band magnitudes. The result is that the highest luminosity red supergiants of Massey & Olsen (2003) and Levesque et al. (2005) now have warmer effective temperatures and luminosities that imply masses of between 12 and 30 $M_{\odot}$. Massey, DeGioia-Eastwood & Waterhouse (2001) and Crowther (2007) suggest stars with an initial mass of around $25\,M_{\odot}$ could evolve to the WN phase in Galactic clusters, at solar metallicity. The mass estimates generally come from the estimated age of the stellar clusters as measured from the turn-off. Only two out of 11 in the Massey et al. study are as low as 20–25 $M_{\odot}$ and one can really only take this as a lower limit. The minimum initial mass to form a WR star in the LMC (and SMC) has been estimated at $30\,M_{\odot}$ (and $45\,M_{\odot}$ respectively) using similar methods (Massey, Waterhouse & DeGioia-Eastwood 2000). Stars above these masses, if they explode as bright SNe, should produce H-deficient (and He-deficient) SNe like the Ib/c we observe. Hence there is good agreement between the maximum observed masses of red supergiants in the Galaxy and the LMC and the minimum mass required to produce a WR star, from the ages and turn-off masses of coeval clusters. Crowther (2007) points out that there are few Milky Way clusters that harbour both RSGs and WR stars which would suggest that there is a definite mass segregation between the two populations. The metallicity ranges of our progenitor sample (Table 2) range between solar and LMC, hence these studies of Local Group stellar populations would suggest the minimum initial mass for a single star to become a WR (probably of type WN) is 25–30 $M_{\odot}$.

The question is what is the fate of the massive red supergiants between 17 and 25–30 $M_{\odot}$? They appear to exist in this mass range and one would expect them to produce SN of type II-P but they are missing from our progenitor population. A single star of initial mass of $17\,M_{\odot}$ does not have a high enough mass-loss rate to strip its outer layers of enough mass to become a WR star and hence a Ib or Ic SN (either observationally or theoretically). If our sample of 20 progenitor stars were really sampled from an underlying population of red supergiants, with initial masses in the region 8.5–25 $M_{\odot}$, then a Salpeter IMF would suggest we should have 4 between 17 and $25\,M_{\odot}$. The probability that we detect none by chance is 0.018 (or 2.4σ significance). For a steeper IMF of $\Gamma = -2.0$ the numbers are three stars, probability of 0.05 and 2σ significance. We term this discrepancy the 'red supergiant problem', in that we have a population of massive stars with no obvious channel of explosion.

One could attempt to fill this mass gap with the other SN types IIn and II-L and IIb. The fraction of stars born with masses between 17 and 25 $M_{\odot}$ (within an underlying population of 8.5–150 $M_{\odot}$) is 18 per cent, and Table 1 suggests the combined rate of II-L, IIn and IIb is 12 per cent. Hence it is perhaps appealing to account for the red supergiant problem by saying that at least some of these stars form II-L, IIn or IIb SNe. But there is evidence arguing against this. Thompson (1982) presented a deep photographic plate of NGC 6946 49 d before the maximum of the II-L SN1980K and found no progenitor or discernible stellar cluster. He suggested an upper mass limit of $< 18\,M_{\odot}$ and using our stellar tracks and more recent

distance we recalculated this as $<20\,M_\odot$ in Smartt et al. (2003). SNe IIb have been suggested to be from interacting binary systems and for SN1993J a viable model is a close pair of 14 and $15\,M_\odot$ stars. The binary companion to SN1993J's progenitor was theoretically predicted and observationally detected (Podsiaklowski et al. 1993; Woosley et al. 1994; Maund et al. 2004). Ryder, Murrowood & Stathakis (2006) suggest a similar scenario explains their detection of a stellar source at the position of the IIb SN 2001ig. A single $28\,M_\odot$ WNL star was favoured as the progenitor of the recent SN IIb 2008ax by Crockett et al. (2008), but a binary system cannot yet be ruled out. There is also evidence that very luminous type IIn arise from very massive LBV type stars, generally thought to be $>40\,M_\odot$ and hence too high mass to solve the problem (see Section 8.2.4).

One could appeal to rotation as a way out and the rotating Geneva models of Hirschi et al. (2004) predict an upper mass limit of $22\,M_\odot$ for a hydrogen rich progenitor (for stars rotating initially at 220 km s^{-1}). Above this mass a single star ends its life as a WR and hence a Ib/c SN. This is well above our estimated maximum initial mass $17\,M_\odot$, but consistent with the 95 per cent confidence limit. However, this would mean every II-P progenitor would have to be rotating initially with speeds around 220 km s^{-1}. This is clearly not what we see in the rotational velocity distributions in the Galaxy, or Magellanic Clouds, (Dufton et al. 2006; Huang & Gies 2006; Hunter et al. 2008), which suggest less than 15 per cent of massive stars should be rotating at such intrinsic rotational velocities.

8.2.2 *Black hole formation*

An intriguing possibility is that the red supergiant problem is due to the vast majority of high-mass stars above $17\,M_\odot$ collapsing to form black holes and either very faint SNe or no explosion at all. Theoretically this has been suggested for some time, e.g. most recently by Fryer (1999), Fryer et al. (2007) and Heger et al. (2003). Our model stars in the mass range of 20–$27\,M_\odot$ end as hydrogen rich red supergiants with helium core masses of $>8\,M_\odot$ and such masses have been suggested to result in the formation black holes (this line is plotted for reference in Fig. 8; Fryer 1999). The models of Limongi & Chieffi (2003, 2007) suggest the maximum mass to produce a Type II-P SN is 30–$35\,M_\odot$ and a minimum initial mass for black hole formation is 25–$30\,M_\odot$. Although Fryer (1999) notes that the mass range to produce black holes is theoretically quite uncertain. For example reducing the mean neutrino energy by 20 per cent could reduce the explosion energy by a factor of 2 and push the minimum mass for black hole formation to as low as $15\,M_\odot$.

As pointed out by Kochanek et al. (2008), the collapsar model in which a GRB is produced along with a Type Ic SN, is likely to be too rare to produce the bulk of the black holes seen in our Galaxy (MacFadyen & Woosley 1999). The collapsar scenario would have problems within massive hydrogen rich progenitors (the jet would have difficulty in escaping from a red supergiant MacFadyen, Woosley & Heger 2001). Young, Smith & Johnson (2005) suggest that bright II-L SNe may be black hole forming events, in which the collapsar mechanism occurs within a massive H-rich star.

Whatever the explanation we have evidence for a lack of progenitors above $17\,M_\odot$ and perhaps the minimum mass to form a black hole could be as low as this. It could be that stars in the 17–$30\,M_\odot$ range produce SNe so faint that they have never been detected by any survey. In this case they would typically be fainter than $M_R \sim -12$. If the limit for black hole formation is low then it bodes well for surveys for disappearing stars. Kochanek et al. (2008) have suggested that a survey of nearby galaxies over several years would have a chance of detecting massive stars that disappear without an accompanying SN. From a similar comparison of a Salpeter IMF with the general progenitor compilation of Li et al. (2007) they also suggest there may be a dearth of massive star progenitors. Their calculation is somewhat inexact in that it includes 1999gi and 2001du as possible detections and is neither volume nor time limited to minimize biases on SN and progenitor selection effects, and the masses come from many inhomogeneous methods. But it does support our quantitative mass range estimate for II-P progenitors.

8.2.3 *Binaries and Ibc SNe*

A further flaw in the argument that the Type II-P rates match the mass range of 8.5–$16.5\,M_\odot$ is that it ignores the consequence of binary evolution. Podsiadlowski, Joss & Hsu (1992) suggested that around 15 per cent of SNe could be from interacting binaries in which mass transfer causes the primary to loose its H (and He) envelope. This assumes that about 30 per cent of all massive stars are in close binaries that will interact in case A, B or C mass transfer. Recent results suggest that $\geq$60 per cent of massive stars could be in close binaries (Kobulnicky & Fryer 2007) leading Fryer et al. (2007) to claim that perhaps all local Ibc SNe could be formed in binary systems and the progenitors could thus have initial masses down to our $m_{\rm min}$ limit of $8.5\,M_\odot$. It appears very likely that at least some Ibc SNe are formed in moderate mass interacting binaries (Crockett et al. 2007; Eldridge, Izzard & Tout 2008).

At around solar metallicity Fryer et al. (2007) and Heger et al. (2003) argue that single, massive WR stars all have core masses large enough to form black holes and that they cannot be the progenitors of the local, normal Ibc SN population. They suggest that these should give weak SNe or no explosion at all. Current observations have not yet confirmed that massive WR stars are definitely the progenitors of Ibc SNe. The bulk of the population may form black holes with no explosion and a fraction (with low metallicity and high rotational velocities) may form black holes in the collapsar model with an accompanying GRB (Woosley & Bloom 2006). The ejecta masses and pre-explosion limits of SNe Ibc (with no associated GRB) are consistent with them being stars of $\sim$10–$20\,M_\odot$ stripped of their envelopes through close binary interaction (Mazzali et al. 2002; Crockett et al. 2007; Valenti et al. 2008a). We do not yet have a firm confirmation of a Ibc explosion (with no associated GRB) directly associated with a massive WR star, or with ejecta masses high enough to suggest a WR progenitor. Those broad lined SNe *with* a GRB associated do have high enough ejecta masses to be consistent with LMC type WC stars (Crowther 2007). However, there is a suggestion of a $28\,M_\odot$ WNL progenitor for the Type IIb SN2008ax (Crockett et al. 2008) and this SN appears to be on the H abundance continuum between Ib and IIb events (Pastorello et al. 2008a). We will discuss the Ibc progenitor scenarios further in the second paper in this series.

8.2.4 *The Type IIn population and their progenitors*

There is clear evidence now that some very massive stars, above 25–$30\,M_\odot$ do explode as very bright SN, SN2005gl is a Type IIn at 65 Mpc and has a very luminous progenitor detected at $M_V \simeq -10.3$ (Gal-Yam et al. 2007a). The latter is evidence that LBVs are direct progenitors of some SNe and this is supported by studies of the energies and spectral evolution of other events (Kotak & Vink

2006; Smith et al. 2007, 2008b; Trundle et al. 2008). The case of SN2006jc showed that an LBV-like outburst occurred directly coincident with a peculiar type of hydrogen deficient SN (Pastorello et al. 2007b). SN2006jc resembles a Type Ic with narrow lines of He arising from a circumstellar He-rich shell (Foley et al. 2007; Pastorello et al. 2008b). Woosley, Blinnikov & Heger (2007) have suggested that both the superbright IIn events (2006gy-like; Smith et al. 2007) and the double outburst events (2006jc-like; Pastorello et al. 2008b) may not be the canonical core-collapse mechanism, but be due to pulsational pair-instability in the cores.

Thus one might venture that above $17\,M_{\odot}$ the vast majority of stars form black holes at core-collapse and cannot produce bright explosions through the canonical neutrino-driven convection mechanism. A fraction of them form collapsars due to a combination of rotation or binarity and low metallicity (see Woosley & Bloom 2006). And a fraction may form H-rich luminous Type IIn SNe through the pulsational pair-instability mechanism.

A caveat to this is the discovery of neutron stars in two young clusters (Muno et al. 2006; Messineo et al. 2008), which suggests the progenitors had initial masses greater than 40 and 20–30 $M_{\odot}$, respectively. These stars should perhaps have formed black holes but Belczynski & Taam (2008) suggests that under certain conditions, binary evolution could result in stars as massive as 50–80 $M_{\odot}$ ending up as neutron stars. A further argument against is that the locations of Ibc SNe tend to be more closely associated with H II regions than II-P SNe, suggesting a higher initial mass range for the progenitors of Ibc (Anderson & James 2008).

The nature of the deaths of the most massive stars, whether in black hole forming events, or other explosion mechanisms, still remains to be determined. The combination of studies of direct progenitor detections, environment evaluation, SN ejecta and remnant properties will be a fertile field for discovery for many years to come.

8.2.5 The progenitor of SN 1987a: Sanduleak −69°202

Although the progenitor of SN 1987A is often quoted to be a $20\,M_{\odot}$ star, one needs to be careful with a simple interpretation of placing the progenitor on an HRD and taking the closest mass track. The spectral type and *UBV* magnitudes from Walborn et al. (1989) suggest a B3-type supergiant ($T_{\rm eff} \simeq 15750$, from the calibration of LMC B-supergiants in Trundle et al. 2007) and hence $\log(L/L_{\odot}) = 5.1 \pm 0.1$. When placed on single-star evolutionary tracks this lies close to a $20\,M_{\odot}$ model just after the end of core H burning. However, it is not valid to assume $20\,M_{\odot}$ as the progenitor initial mass, as the model track is not at its endpoint and is no where near to having an Fe core (or at least at the point of neon burning within a helium core). The luminosity of the He core of an evolved massive star determines the stars luminosity and we estimate the corresponding He core mass to be $5.2^{+2}_{-1.0}\,M_{\odot}$. The initial mass of a single star required to produce this core mass is $15^{+4}_{-1}\,M_{\odot}$. The interacting binary model in Maund et al. (2004) and Podsiaklowski et al. (1993) can produce an SN1987A like progenitor with a pair of 14 and $15\,M_{\odot}$ stars. And a merger involving a lower mass star of 3–6 $M_{\odot}$ with an evolved 15–16 $M_{\odot}$ primary can also account for the luminosity (Podsiadlowski 1992; Morris & Podsiadlowski 2007). In both scenarios an initially less massive star gains mass to explode with a final mass of $20\,M_{\odot}$. However, the helium core mass was that expected for a $15\,M_{\odot}$ star leading to its position in the blue part of the HRD. The ejecta mass has also been estimated at around $15\,M_{\odot}$ (Arnett 1996b). Hence our suggestion of black holes coming from $\sim 17\,M_{\odot}$ stars and above is not directly disproven by the example of Sanduleak −69° 202

8.3 Explosion mechanisms and production of ^{56}Ni

The tail phase of Type II-P SNe are thought to be powered by the radioactive decay of ^{56}Ni and recent studies have shown that there can be a large range in tail-phase luminosities. This would imply that a different mass of ^{56}Ni has been ejected in the explosions. As ^{56}Ni is created by explosive burning of Si and O as the shock wave destroys the star, it can be used as a probe of the explosion mechanism. For example, Turatto et al. (1998), Pastorello et al. (2004) and Nomoto et al. (2004) predict that high-mass stars may undergo fallback in which some of the ^{56}Ni falls back on to a protoneutron star or black hole and, hence, one might get a fainter SN. This has lead to suggestions that plotting initial mass versus ejected mass of ^{56}Ni could lead to a bimodal population. There are estimates of the mass of ^{56}Ni for nine of the SNe in our sample (by ourselves and also from other groups, already published in the literature) and we can investigate this relation in a direct way.

The ^{56}Ni mass can be estimated from the tail-phase magnitudes using several different methods. For example, the bolometric luminosity of the tail phase (Hamuy 2003), a direct comparison with SN 1987A (Turatto et al. 1998) and the 'steepness of decline' correlation (Elmhamdi, Chugai & Danziger 2003). For the two recent SNe 2004A and 2003gd, Hendry et al. (2005, 2006) have compared the three methods and find the first two in good agreement, while the mass from the 'steepness of decline' relation gives somewhat lower results (at least for these two events). It is important that a consistent method is used to determine all the ^{56}Ni masses if any comparison is to be meaningful, particularly as the uncertainties on the estimates are often fairly large. Hence we determine ^{56}Ni masses from one consistent approach. The values for SNe 2004A, 2003gd, 1999gi and 1999em were taken from Hendry (2006) who used the bolometric tail-phase luminosity method of Hamuy (2003), and the distances and reddening already adopted in Table 2. The mass for SN2004dj was taken from Zhang et al. (2006) who found that the bolometric luminosity of the tail-phase gave a value very similar to that from the 'steepness of decline' relation. We take their value from the bolometric tail-phase luminosity to ensure consistency ($0.025 \pm 0.010\,M_{\odot}$). This is very similar to the value determined by Vinko et al. (2006) with a simple radioactive decay model applied to the bolometric tail luminosity ($0.02 \pm 0.010\,M_{\odot}$). By a similar analysis, the value of SN2004et was determined with the Hamuy (2003) formula, to give $0.06 \pm 0.02\,M_{\odot}$, the highest of our estimates.

The value for SN2004dg has been determined from the late-time, tail-phase magnitudes from our *HST* imaging (see Section 5.1.2). We determine $V = 20.8$ and estimate an explosion epoch from spectra and photometry during the plateau phase. Applying the same bolometric tail-phase method as above results in a value of $0.010 \pm 0.005\,M_{\odot}$. A very low ^{56}Ni mass for SN1999br has been reported in Hamuy (2003), although he used a distance of 10.8 ± 2.4 Mpc, and to keep the analysis consistent we scaled his value to our larger adopted distance listed in Table 2, resulting in a value of $0.003 \pm 0.001\,M_{\odot}$. This is in good agreement with the value determined by Pastorello et al. (2004) of $\sim$0.002 who used a similar distance to ours to calculate the mass from a direct comparison with the tail-phase luminosity of SN1987A. The estimates for SN2006ov and SN2006my have been calculated using a similar bolometric tail-phase method as described above to give $0.003 \pm 0.002\,M_{\odot}$

and $0.03 \pm 0.015\,M_\odot$ respectively (Maguire et al., in preparation; Spiro et al., in preparation).

Finally we consider the case of SN2005cs. The early-time spectra have been studied extensively by Pastorello et al. (2006), Takáts & Vinkó (2006) and Brown et al. (2007), who all find it to be a moderately faint II-P with low ejecta velocities. It appears a similar type of event to the faint SNe 1999br and 2002gd (Pastorello et al. 2006), and a measure of its luminosity in the tail phase is especially interesting particularly as it is one of the events with a detected progenitor and well-determined mass (Table 2). Tsvetkov et al. (2006) present several photometric measurements of SN2005cs in the tail phase and suggest a ^{56}Ni mass of $0.018\,M_\odot$, which would be similar to 2003gd. As the progenitors are likely to have been red supergiants of quite similar masses one might be encouraged by this agreement. However, Pastorello et al. (2009) presents new measurements of the tail-phase magnitudes of SN2005cs and finds it to be significantly fainter than reported in Tsvetkov et al. (2006). The difference is likely due to the differing methods employed to determine the luminosity in this faint phase. Pastorello et al. have used image subtraction to remove contamination of the host galaxy, which can be significant as the SN fades. These fainter measured magnitudes suggest an ejected ^{56}Ni mass of $0.003 \pm 0.001\,M_\odot$, and we believe this to be a more realistic estimate. For reference, the determined value of $0.075\,M_\odot$ for SN1987A from Arnett (1996a) is also plotted in Fig. 9.

8.4 The nature of faint II-P SNe

In Fig. 9 we see how the nickel mass created in II-P SNe compares to the initial mass of the progenitor star. Similar diagrams have been produced before but these derive the initial mass by a model dependent two-step process. First of all the ejected mass is estimated from modelling the SN light curve and velocity evolution of the ejecta, and then an initial main-sequence mass is inferred by assuming an estimated remnant mass and accounting for the effects of mass-loss during stellar evolution (Zampieri et al. 2003; Nomoto et al. 2004). Such models have given satisfactory fits to the luminosity and velocity measurements, but our direct pre-explosion measurements can provide valuable independent information. It is certainly clear that there is a population of low-luminosity II-P SNe, which have lower ejecta velocities throughout the photospheric stage and very low tail-phase bolometric luminosities. The first one recognized was SN1997D (Turatto et al. 1998; Zampieri et al. 1998; Benetti et al. 2001) and in our sample 1999br and 2005cs are similar (Pastorello et al. 2004, 2006). The clear implication of the low tail-phase luminosity is that a low mass of ^{56}Ni is produced in the explosion. Hence one might hope to relate this to the explosion mechanism.

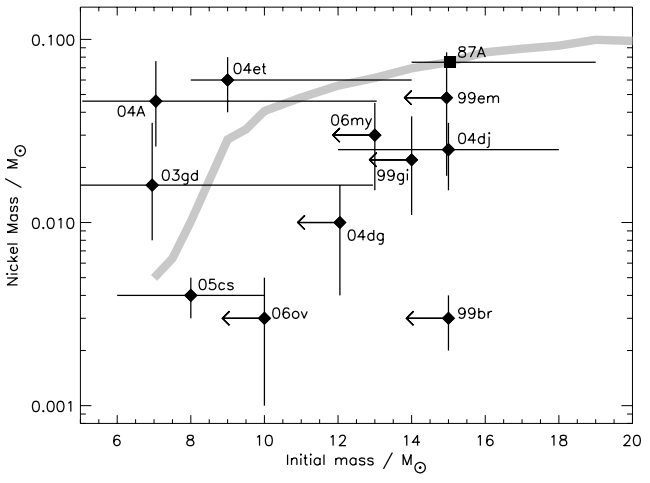

Figure 9. Plots of initial mass versus mass of ^{56}Ni. The grey line is the M_O/M(CO core) normalized to pass through the 1987A nickel mass.

Two alternative suggestions for the faint II-P SNe have been proposed. One is that the SNe formed black holes at core-collapse and the ^{56}Ni produced fell back into the black hole rather than being ejected (Zampieri et al. 2003; Nomoto et al. 2004). An alternative is that they are intrinsically less energetic explosions of lower mass stars. Stars of 9–11 $M_\odot$ can have large density gradients in the O–Si layers around the protoneutron star and the shock may produce lower temperatures than in higher mass counterparts. Statistical equilibrium is only reached in a thinner shell of O- and Si-rich gas, hence low amounts of ^{56}Ni is produced (Mayle & Wilson 1988). Chugai & Utrobin (2000) have also favoured this low-mass star scenario in their fitting of the nebular spectra of SN1997D with a hydrodynamic model. The high-mass stellar origin of Zampieri et al. (2003) and Nomoto et al. (2004) predicts hydrogen rich progenitors of greater than $25\,M_\odot$, but as shown above we do not detect any red supergiant stars of such high masses. These types of stars would be the easiest to detect and in particular for 1999br and 2005cs we favour the low-mass scenario. Fig. 9 argues against the high-mass scenario for the low ^{56}Ni mass SNe, and we find no evidence of the branching of the figure at high masses into low- and high-energy SNe as suggested by both Zampieri et al. (2003) and Nomoto et al. (2004). The low ^{56}Ni SNe have initial masses well below the limit required to produce a massive enough core for black hole formation. In fact rather than being two separate populations there appears to be a continuous trend with lower initial mass producing lower masses of nickel in core-collapse (Maund 2005).

One could advance an argument that the progenitors were actually of higher mass and not detected in our images for some reason. The most obvious reason is high dust extinction as we discussed in Section 6.2. We argued that it is unlikely that we have systematically underestimated the masses due to large extinctions. In addition, the fact that there was no detection of the 2005cs progenitor in deep NIR *JHK* bands argues against a massive progenitor surrounded in dust, of anything up to $A_V \sim 5$ (Maund et al. 2005a). Also SN2008bk was detected in the NIR (*JHK* bands) and hence even a visual extinction of $A_V \sim 10$ would have only a $\sim$1 mag affect in K, increasing the $\log L/L_\odot$ by 0.25 dex. Another possibility is that the stars were not red supergiants, but hotter, blue stars. One could invoke this to explain the non-detections and also argue that the detected red stars are heavily reddened bluer objects. But in this case they would be more compact and the light curves would then tend to resemble SN1987A, and there is no evidence for such peculiarities in any of the SNe presented here. If all, or most, II-P progenitors are not red supergiants this would pose serious problems for stellar evolution theory and models of II-P light curves. We consider this possibility unlikely. As this paper was in the review stage, Utrobin & Chugai (2008) proposed that the ejecta mass of SN2005cs, from hydrodynamic modelling of the light curve and velocity evolution, was around $17.3 \pm 1\,M_\odot$. They also suggest a progenitor mass of 20–25 $M_\odot$ for SN1999em which is again significantly higher than our stellar evolutionary mass. This severe discrepancy between two methods is interesting and should be explored further in the future.

As the ^{56}Ni is produced by explosive silicon and oxygen burning of the mantle material (Woosley, Heger & Weaver 2002), one might imagine that the amount of nickel formed in an SN is related to the amount of oxygen and silicon in the progenitor core. In Fig. 9 we overplot the mass of oxygen in the carbon–oxygen (CO) core

divided by the mass of the CO core from our stellar models against the initial stellar mass. The line is scaled to fit SN 1987A. This simple model follows the general trend of the observations, but with some large scatter. Other factors will affect the amount of nickel produced in an SN but the relation could suggest that the amount of source material is a primary factor in determining how much nickel is produced. Alternatively it could be a reflection of the density and temperature in the explosive burning region in the stars. Whatever the physical reason, we have not detected high-mass stars as progenitors of the faint II-P SNe. Hence we favour the lower mass star progenitor as the origin of these events.

9 LESSONS LEARNED AND FUTURE POSSIBILITIES

This decade long effort to systematically search and detect SN progenitors provides an opportunity to reflect on lessons learned and ways to increase discovery potential. It is perhaps somewhat surprising that unambiguous detections in multiband images have been difficult. As discussed above this could imply that the high-mass, H-rich, bright supergiants up to around 30 $M_{\odot}$ are not the progenitors of Type II-P or Type II-L SNe. Whatever the reason, it seems clear that pursuing this project needs a different approach to make firm detections of progenitors rather than providing many more upper limits. The latter can be interesting if enough are available, but ultimately it is discovery and characterization of objects that will advance the field.

As discussed in Section 5, the three progenitors which are reliably and unambiguously detected (2003gd, 2005cs and 2008bk) and have high-quality multicolour images (giving colour information) are all closer than 10 Mpc. Although the global image archives of nearby galaxies have been *steadily* increasing over the last 10 yr, the total number of galaxies and the quality of the images will not rapidly improve in the near future. For example, it has taken 15 yr of post-SM1 *HST* operations to get to the current archive content. It seems clear that the current *HST* archive does not contain deep enough images of galaxies to enable routine detection of progenitors beyond about 10 Mpc. This does not mean we should give up on searching for progenitors of SNe between ∼10–25 Mpc as one may be fortunate to detect higher mass, and brighter, progenitors than we so far have done (e.g. Gal-Yam et al. 2007a). Each event should certainly be scrutinized for the potential of fortuitous progenitor discovery but when considering how to actively improve the possibilities the following should be noted. In Cycle 10 of *HST* operations (2001 June 01 to 2002 May 31) we were allocated a SNAP proposal (SNAP9042) to enhance the image archive of star-forming galaxies within about 20 Mpc and then to wait for future SNe to occur. We observed approximately 160 galaxies with typical exposure times of 460 s in $F450W$, $F814W$ and $F606W$. These set of images produced pre-explosion environments for SNe 2003jg, 2004A, 2004dg, 2005V, 2006ov, 2007aa, 2007gr and SN2008ax. The progenitors of SN2004A and SN2008ax have been detected (see section 5.1.0, Hendry et al. 2006; Crockett et al. 2008) and the limits on the non-detections have proved very useful. This provides a benchmark for any future studies dedicated to detecting progenitors, retrospectively. The depth reached in these images (typically $m_{F814W} \simeq 25$, 3σ) at a distance of ∼20 Mpc results in sensitivities down to $M_{F814W} \sim -6.8$ [for a typical $E(B-V) \simeq 0.2$].

The most fruitful method of detecting progenitors in the future would be to carry out a deep, wide-field survey of star-forming galaxies within about 10 Mpc with the revived ACS and the new WF3 on *HST* after servicing mission SM4. Reaching AB magnitudes of around 26 would be required to ensure the images go deep enough to detect progenitors down to around 8 $M_{\odot}$. For example, SN2003gd was discovered at $V = 25.8$ ($M_V = -4.4$) and SN2003gd, 2005cs and 2008bk were all discovered at $M_I \sim -6.5 \pm 0.2$ (all Vega based magnitudes). By restricting the distance limit to 10 Mpc would of course result in a lower rate of CCSNe (1–2 per year) in the sample of around 100 major star-forming galaxies (Kennicutt et al. 2008), but the discovery potential would be excellent. One further issue is the size of the star-forming discs of these galaxies which are significantly larger than the 3.4 arcmin diameter of ACS Wide Field Channel. The limited size of the WFPC2 and ACS cameras has resulted in many galaxies having been observed by *HST* before a CCSN occurs but the position falling outside the camera footprints (43 per cent: see Section 2.2). Hence a carefully planned future survey of nearby galaxies must use multiple *HST* pointings to cover the full optical extents of the galaxy discs. A campaign of this extent is already in the arena of 'multicycle treasury proposals'.

A *systematic* survey beyond 10 Mpc that would significantly increase detection probability is probably not the best strategy. A distance limit increase to $r_{10\,\mathrm{Mpc}}$ (where $r_{10\,\mathrm{Mpc}}$ is the distance limit in units of 10 Mpc) would increase the number of galaxies by a factor of approximately $100(r^3_{10\,\mathrm{Mpc}}-1)$ and the time required would increase more than linearly (depending on the $r_{10\,\mathrm{Mpc}}$ distribution and galaxy sizes). The latter is not feasible in any reasonable allocation of time and given the difficulty in detecting progenitors beyond 10 Mpc is not an optimal strategy.

We have found it essential that astrometry of the SNe employs images of the resolution of the *HST* pre-explosion images to avoid large astrometric uncertainties and ambiguous (or spurious) detection of progenitors. Ground-based (natural seeing) images are normally not adequate for providing geometric transformations between pre and post-explosion images to the 10–12 mas level required. Between 2001 and 2006 our group used *HST* to take post-explosion images at the same resolution (or higher, depending the camera pixel scales) as the pre-explosion *HST* images. This proved to be essential as there were several announcements (in IAU Circulars and Central Bureau Electronic Telegrams) of erroneous detections of progenitors using ground-based astrometry (Van Dyk et al. 2003a; Richmond & Modjaz 2005; Li et al. 2007). Using unchecked and absolute astrometry to identify progenitors on ground-based images has also lead to erroneous claims of progenitor detections (SN 2002ap and SN 2004dj: Smartt, Ramirez-Ruiz & Vreeswijk 2002a; Li, Filippenko & van Dyk 2004; Weis et al. 2004). Images with adaptive optics systems on large ground-based telescopes (e.g. the VLT, Gemini and Keck) routinely deliver diffraction limited images in the K band. These images are of sufficient resolution to use instead of *HST* follow-up images (e.g. Gal-Yam et al. 2007a; Crockett et al. 2008). Rapid analysis of images after SNe discoveries and reporting of possible progenitors before extensive analysis has been completed is understandable in a competitive field and helps the community to prioritize potentially interesting events. However, claims of spatial coincidence require detailed *differential* astrometry between post- and pre-explosion images to precisions of around 10 mas and comprehensive error analyses in order to be acceptable. Our experience has shown if this rule of thumb is not followed then erroneous results often follow. The flexibility and rapid reaction time of ground-based AO systems make them an excellent facility to provide precision differential astrometry (at the 10 mas level), and this has been our preferred strategy since 2007.

Finally, we are now at the point at which, for some progenitors, we can return to see if the stars have disappeared. This has been done for only SN 1987A (Gilmozzi et al. 1987) and deep late-time

images of SN 2004et alerted us to likely spurious detection of the progenitor. This area of late-time observations may lead to further surprises, but it is essential it is pursued to verify the results claimed here, and elsewhere, for 2003gd, 2005cs and 2008bk.

10 CONCLUSIONS

This paper presents a consistent and homogeneous analysis of the constraints on progenitor stars of II-P SNe, within a volume- and time-limited search. The work builds on and enhances the discoveries and limits presented in the literature. There are now enough data that a statistical study of progenitor properties is feasible. This represents the culmination of a 10.5-yr search for progenitor stars and the conclusions are as follows.

(i) We have compiled all SNe discovered within a strict volume and time limit and reviewed the SN types reported in the literature. This gives a very good estimate of the relative rate of CCNSe in the local Universe, at metallicities between LMC and solar.

(ii) Of the 55 Type II-P SNe found, 20 have *HST* pre-explosion (or excellent ground-based) images available to search for progenitor stars. We summarize the data presented in the literature to date on these SNe and carry out a consistent and homogeneous analysis of all events. Three groups of events are discussed – those with probable single star progenitors detected, those with upper limits to their luminosities and masses, and those falling on compact, unresolved coeval clusters.

(iii) The masses and mass limits of each are determined using our STARS evolutionary models and a statistical analyses presented of the final masses. A maximum likelihood analysis suggests that the minimum mass for a Type II-P SN is $m_{\rm min} = 8.5^{+1}_{-1.5}\,{\rm M}_{\odot}$. This is consistent with current estimates of the maximum mass that will produce a WD in young clusters.

(iv) We have not detected any progenitors above $16\,{\rm M}_{\odot}$. Assuming a Salpeter IMF, the most likely maximum mass for a II-P SN is $m_{\rm max} = 16.5 \pm 1.5\,{\rm M}_{\odot}$. This is not particularly sensitive to the IMF slope within the typical variations known in the local Universe of ± 0.7.

(v) We suggest that there is a discrepancy between this maximum mass and our knowledge of massive star evolution. Red supergiants between 17 and $30\,{\rm M}_{\odot}$ are not detected as progenitors but are predicted by theory to exist and this is supported by stellar population studies. We term this discrepancy the 'red supergiant problem'. It is unlikely to be due to IMF variations and possible explanations include the possibility that we have systematically under estimated the stellar luminosities and masses due to foreground extinction or that the gap is filled with the other flavours of Type II SNe (e.g. II-L, IIn and IIb). However, neither of these solutions is supported by current data. We suggest that these objects may be forming black holes with faint, or non-existent SN explosions.

(vi) Although low-luminosity SNe are already known (e.g. 1999br, 2005cs) we suggest that these events are not the missing SNe – rather our analysis supports the interpretation that they are stars at the minimum mass limit for SNe.

(vii) We review the information on extinctions towards these SNe and their progenitors and compare it with that towards red supergiant populations in the LMC. We suggest that high extinction towards the SNe progenitors is unlikely to be the cause of the lack of detections of massive supergiants.

(viii) The search for progenitor stars should continue for every nearby SN that has deep, high-resolution pre-explosion images. In particular, the missing high-mass red supergiants should be sought in both optical, NIR and mid-IR images. If the limit for black hole formation is as low as $17\,{\rm M}_{\odot}$ then it bodes well for surveys for disappearing stars as suggested by Kochanek et al. (2008).

ACKNOWLEDGMENTS

This work, conducted as part of the award 'Understanding the lives of massive stars from birth to supernovae' (SJS) made under the European Heads of Research Councils and European Science Foundation EURYI (European Young Investigator) Awards scheme, was supported by funds from the Participating Organizations of EURYI and the EC Sixth Framework Programme. RMC and SJS thank the ESF and Leverhulme Trust for financial support. The research of JRM is supported in part by NSF grant AST-0406740 and NASA grant NNG04GL00G. This paper is based on observations made with the following telescopes: NASA/ESA *HST*, obtained from the data archive at the Space Telescope Institute. STScI is operated by the association of Universities for Research in Astronomy, Inc. under the NASA contract NAS 5-26555 (Programmes GO 10187, 10498, 10803 and SNAP9042). The William Herschel Telescope and data obtained from the Isaac Newton Group Archive are maintained as part of the CASU Astronomical Data Centre at the Institute of Astronomy, Cambridge. We acknowledge the usage of the HyperLeda data base, and this research has made use of the NASA/IPAC Extragalactic Database (NED) which is operated by the Jet Propulsion Laboratory, California Institute of Technology, under contract with the National Aeronautics and Space Administration. We thank Seppo Mattila, Andrea Pastorello, John Danziger, Avishay Gal-Yam, Chris Kochanek for discussions and debate; Mike Irwin and Annette Ferguson for early access to the INT images of NGC 6946; Martin Mobberley for access to an image of SN2003ie; John Beacom for discussions on statistical methods to use, recommending the maximum likelihood approach and discussions on local SNe rates; Mario Hamuy for providing several SNe classifications from private spectra. We thank the referee, David Branch, for comments and suggestions that improved the paper.

REFERENCES

Aerts C., Thoul A., Daszyńska J., Scuflaire R., Waelkens C., Dupret M. A., Niemczura E., Noels A., 2003, Sci, 300, 1926
Agnoletto I., Harutyunyan A., Benetti S., Turatto M., Cappellaro E., Dennefeld M., Adami C., 2007, Cent. Bur. Electron. Telegrams, 1163, 1
Aldering G., Humphreys R. M., Richmond M., 1994, AJ, 107, 662
Aldering G. et al., 2006, The Astronomer's Telegram, 690, 1
Anderson J. P., James P. A., 2008, MNRAS, 390, 1527
Arnett D., 1996a, Supernovae and Nucleosynthesis. Princeton Univ. Press, Princeton, NJ
Arnett D., 1996b, Princeton Series in Astrophysics, Supernovae and Nucleosynthesis. Princeton Univ. Press, Princeton, NJ
Arnett W. D., 1980, ApJ, 237, 541
Asplund M., Grevesse N., Sauval A. J., Allende Prieto C., Kiselman D., 2004, A&A, 417, 751
Asplund M., Grevesse N., Sauval A. J., 2005, in Barnes T. G., III, Bash F. N., eds, ASP Conf. Ser. Vol. 336, Cosmic Abundances as Records of Stellar Evolution and Nucleosynthesis. Astron. Soc. Pac., San Francisco, p. 25
Ayani K., Yamaoka H., 1999, IAU Circ., 7137, 1
Ayani K., Yamaoka H., 2002, IAU Circ., 7976, 3
Ayani K., Kawabata T., Ioroi M., Ohshima O., 2001, IAU Circ., 7683, 2
Ayani K., Kawabata T., Yamaoka H., 2002, IAU Circ., 7864, 4
Ayani K., Hashimoto T., Yamaoka H., 2003, IAU Circ., 8048, 2
Baade W., Zwicky F., 1934, Proc. Natl. Acad. Sci., 20, 254
Baron E. et al., 2000, ApJ, 545, 444

Barth A. J., van Dyk S. D., Filippenko A. V., Leibundgut B., Richmond M. W., 1996, AJ, 111, 2047
Belczynski K., Taam R. E., 2008, ApJ, 685, 400
Benetti S. et al., 2001, MNRAS, 322, 361
Benetti S. et al., 2004, MNRAS, 348, 261
Berger E. et al., 2009, ApJ, submitted (arXiv:0901.0710)
Blackman J., Schmidt B., Kerzendorf W., 2006, Cent. Bur. Electron. Telegrams, 541, 1
Blondin S., Calkins M., 2007a, Cent. Bur. Electron. Telegrams, 1119, 1
Blondin S., Calkins M., 2007b, Cent. Bur. Electron. Telegrams, 800, 2
Blondin S., Masters K., Modjaz M., Kirshner R., Challis P., Matheson T., Berlind P., 2006, Cent. Bur. Electron. Telegrams, 636, 1
Bond H. E., Walter F. M., Velasquez J., 2008, IAU Circ., 8946, 2
Bond H. E., Bonanos A. Z., Humphreys R. M., Berto Monard L. A. G., Prieto J. L., Walter F. M., 2009, ArXiv e-prints
Branch D. et al., 2003, AJ, 126, 1489
Bresolin F., 2008, in Israelian G., Meynet G., eds, The Metal-Rich Universe. Cambridge Univ. Press, Cambridge, p. 155
Bresolin F., Garnett D. R., Kennicutt R. C., Jr, 2004, ApJ, 615, 228
Bressan A., Fagotto F., Bertelli G., Chiosi C., 1993, A&AS, 100, 647
Brown P. J. et al., 2007, ApJ, 659, 1488
Cappellaro E., Evans R., Turatto M., 1999, A&A, 351, 459
Cardelli J. A., Clayton G. C., Mathis J. S., 1989, ApJ, 345, 245
Chevalier R. A., 1976, ApJ, 207, 872
Chevalier R. A., Fransson C., Nymark T. K., 2006, ApJ, 641, 1029
Chornock R., Filippenko A. V., 2001, IAU Circ., 7577, 2
Chugai N. N., Utrobin V. P., 2000, A&A, 354, 557
Connolly A., 2004, IAU Circ., 8359, 1
Contreras C., Morrell N., Gonzalez S., Lee K.-G., 2007, Cent. Bur. Electron. Telegrams, 1068, 1
Crockett R. M. et al., 2009, MNRAS, submitted
Crockett R. M. et al., 2007, MNRAS, 381, 835
Crockett R. M. et al., 2008, MNRAS, 391, L5
Crowther P. A., 2007, ARA&A, 45, 177
Daflon S., Cunha K., Butler K., 2004, ApJ, 604, 362
de Jager C., Nieuwenhuijzen H., van der Hucht K. A., 1988, A&AS, 72, 259
de Vaucouleurs G., 1979, ApJ, 227, 380
Dessart L. et al., 2008, ApJ, 675, 644
Di Carlo E. et al., 2002, ApJ, 573, 144
Dobbie P. D. et al., 2006, MNRAS, 369, 383
Dolphin A. E., 2000, PASP, 112, 1383
Drilling J. S., Landolt A. U., 2000, in Cox A. N., ed., Allen's Astrophysical Quantities, 4th edn. Am. Inst. Phys., New York
Dufton P. L. et al., 2006, A&A, 457, 265
Dwek E., 1983, ApJ, 274, 175
Eggleton P. P., 1971, MNRAS, 151, 351
Eldridge J. J., 2007, Rev. Mex. Astron. Astrofis. Conf. Ser., 27, 35
Eldridge J. J., Tout C. A., 2004a, MNRAS, 348, 201
Eldridge J. J., Tout C. A., 2004b, MNRAS, 353, 87
Eldridge J. J., Mattila S., Smartt S. J., 2007, MNRAS, 376, L52
Eldridge J. J., Izzard R. G., Tout C. A., 2008, MNRAS, 384, 1109
Elias N. et al., 2004, IAU Circ., 8376, 2
Elias-Rosa N. et al., 2004, IAU Circ., 8273, 2
Elias-Rosa N. et al., 2006, MNRAS, 369, 1880
Elias-Rosa N. et al., 2008, MNRAS, 384, 107
Elmegreen B. G., 2009, in Sheth K., Noriega-Crespo A., Ingalls J., Paladini R., eds, The Fourth Spitzer Science Center Conf., The Evolving ISM in the Milky Way and Nearby Galaxies, http://ssc.spitzer.caltech.edu/mtgs/ismevol/
Elmhamdi A., Chugai N. N., Danziger I. J., 2003, A&A, 404, 1077
Fassia A. et al., 2001, MNRAS, 325, 907
Figer D. F., 2005, Nat, 434, 192
Filippenko A. V., 1997, ARA&A, 35, 309
Filippenko A. V., Chornock R., 2000, IAU Circ., 7511, 2
Filippenko A. V., Chornock R., 2001, IAU Circ., 7638, 1
Filippenko A. V., De Breuck C., 1998a, IAU Circ., 6994, 3
Filippenko A. V., De Breuck C., 1998b, IAU Circ., 6997, 2
Filippenko A. V., Foley R. J., 2005, IAU Circ., 8486, 3
Filippenko A. V., Leonard D. C., Riess A. G., 1999a, IAU Circ., 7089, 3
Filippenko A. V., Li W. D., Modjaz M., 1999b, IAU Circ., 7152, 2
Filippenko A. V., Li W. D., Treffers R. R., Modjaz M., 2001, in Paczynski B., Chen W.-P., Lemme C., eds, ASP Conf. Ser. Vol. 246, IAU Colloq. 183, Small Telescope Astronomy on Global Scales. Astron. Soc. Pac., San Francisco, p. 121
Filippenko A. V., Foley R. J., Chornock R., Matheson T., 2004a, IAU Circ., 8420, 2
Filippenko A. V., Ganeshalingam M., Serduke F. J. D., Hoffman J. L., 2004b, IAU Circ., 8404, 1
Filippenko A. V., Silverman J. M., Foley R. J., Modjaz M., Papovich C., Willmer C. N. A., Blondin S., Brown W., 2007, Cent. Bur. Electron. Telegrams, 1101, 1
Folatelli G., Gonzalez S., Morrell N., 2007a, Cent. Bur. Electron. Telegrams, 850, 1
Folatelli G., Morrell N., Phillips M., Hamuy M., 2007b, Cent. Bur. Electron. Telegrams, 862, 1
Folatelli G., Olivares F., Morrell N., 2008, Cent. Bur. Electron. Telegrams, 1227, 1
Foley R. J., Pugh H., Filippenko A. V., 2004a, IAU Circ., 8374, 2
Foley R. J., Wong D. S., Ganeshalingam M., Filippenko A. V., Chornock R., 2004b, IAU Circ., 8339, 2
Foley R. J., Smith N., Ganeshalingam M., Li W., Chornock R., Filippenko A. V., 2007, ApJ, 657, L105
Freedman W. L. et al., 2001, ApJ, 553, 47
Fryer C. L., 1999, ApJ, 522, 413
Fryer C. L. et al., 2007, PASP, 119, 1211
Gal-Yam A. et al., 2005, ApJ, 630, L29
Gal-Yam A. et al., 2007a, ApJ, 656, 372
Gal-Yam A., Cenko S. B., Fox D. B., Leonard D. C., Moon D.-S., Sand D. J., Soderberg A. M., 2007b, in Di Salvo T. et al., eds, AIP Conf. Ser. Vol. 924, The Multicolored Landscape of Compact Objects and Their Explosive Origins: Cefalu 2006. Am. Inst. Phys., New York, p. 297
Gal-Yam A. et al., 2008, ApJ, 685, L117
Garnavich P., Jha S., Kirshner R., Challis P., Berlind P., Holman M., 1999, IAU Circ., 7306, 2
Garnavich P. M. et al., 2004, ApJ, 613, 1120
Garnett D. R., Shields G. A., Skillman E. D., Sagan S. P., Dufour R. J., 1997, ApJ, 489, 63
Gerardy C. L., Fesen R. A., Nomoto K., Maeda K., Hoflich P., Wheeler J. C., 2002, PASJ, 54, 905
Gerardy C. L. et al., 2007, ApJ, 661, 995
Gezari S. et al., 2008, ApJ, 683, L131
Gezari S. et al., 2009, ApJ, 690, 1313
Gilmozzi R. et al., 1987, Nat, 328, 318
Gómez G., López R., 2000, AJ, 120, 367
Gonzalez L., Morrell N., Hamuy M., 2003, IAU Circ., 8173, 3
Gonzalez S., Krzeminski W., Folatelli G., Hamuy M., Morrell N., 2004, IAU Circ., 8409, 2
Gouliermis D., Keller S. C., de Boer K. S., Kontizas M., Kontizas E., 2002, A&A, 381, 862
Guetta D., Della Valle M., 2007, ApJ, 657, L73
Hamuy M., 2001, PhD thesis
Hamuy M., 2003, ApJ, 582, 905
Hamuy M., Roth M., Morrell N., 2002, IAU Circ., 8037, 2
Hamuy M. et al., 2006, PASP, 118, 2
Harutyunyan A., Agnoletto I., Benetti S., Turatto M., Cappellaro E., Lorenzi V., 2007a, Cent. Bur. Electron. Telegrams, 903, 1
Harutyunyan A., Benetti S., Cappellaro E., Patat F., Ghinassi F., 2007b, Cent. Bur. Electron. Telegrams, 1021, 1
Harutyunyan A., Navasardyan H., Benetti S., Turatto M., Pastorello A., Taubenberger S., 2007c, Cent. Bur. Electron. Telegrams, 1184, 1
Harutyunyan A. H. et al., 2008, A&A, 488, 383
Heger A., Langer N., 2000, ApJ, 544, 1016
Heger A., Fryer C. L., Woosley S. E., Langer N., Hartmann D. H., 2003, ApJ, 591, 288
Hendry M. A., 2006, PhD thesis, Univ. Cambridge
Hendry M. A. et al., 2005, MNRAS, 359, 906

Hendry M. A. et al., 2006, MNRAS, 369, 1303
Hernandez M. et al., 2000, MNRAS, 319, 223
Hirschi R., Meynet G., Maeder A., 2004, A&A, 425, 649
Howell D. A., 2003, IAU Circ., 8241, 2
Huang W., Gies D. R., 2006, ApJ, 648, 580
Humphreys R. M., 1978, ApJS, 38, 309
Humphreys R. M., Aaronson M., 1987, AJ, 94, 1156
Hunter I. et al., 2007, A&A, 466, 277
Hunter I., Lennon D. J., Dufton P. L., Trundle C., Simón-Díaz S., Smartt S. J., Ryans R. S. I., Evans C. J., 2008, A&A, 479, 541
Immler S. et al., 2006, ApJ, 648, L119
Irwin M., Lewis J., 2001, New Astron. Rev., 45, 105
James P. A., Anderson J. P., 2006, A&A, 453, 57
Jegerlehner B., Neubig F., Raffelt G., 1996, Phys. Rev. D, 54, 1194
Jha S., Garnavich P., Challis P., Kirshner R., Berlind P., 1999, IAU Circ., 7339, 2
Karachentsev I. D. et al., 2003, A&A, 404, 93
Kelly P. L., Kirshner R. P., Pahre M., 2008, ApJ, 687, 1201
Kennicutt R. C., Jr, Lee J. C., Funes José G. S. J., Sakai S., Akiyama S., 2008, ApJS, 178, 247
Kewley L. J., Dopita M. A., 2002, ApJS, 142, 35
Kim S. S., Figer D. F., Kudritzki R. P., Najarro F., 2006, ApJ, 653, L113
Kistler M. D., Yuksel H., Ando S., Beacom J. F., Suzuki Y., 2008, preprint (arXiv:0810.1959)
Kitaura F. S., Janka H.-T., Hillebrandt W., 2006, A&A, 450, 345
Kniazev A. Y., Arkhyz N., Engels D., Pustilnik S. A., Ugryumov A. V., Masegosa J., 1998, IAU Circ., 6900, 1
Kobulnicky H. A., Fryer C. L., 2007, ApJ, 670, 747
Kochanek C. S., Beacom J. F., Kistler M. D., Prieto J. L., Stanek K. Z., Thompson T. A., Yüksel H., 2008, ApJ, 684, 1336
Kotak R., Vink J. S., 2006, A&A, 460, L5
Krisciunas K. et al., 2003, AJ, 125, 166
Kulkarni S. R. et al., 2007, Nat, 447, 458
Lançon A., Gallagher J. S., III, Mouhcine M., Smith L. J., Ladjal D., de Grijs R., 2008, A&A, 486, 165
Langer N., Maeder A., 1995, A&A, 295, 685
Leaman J., Li W., Filippenko A., 2004, BAAS, 1464
Leitherer C. et al., 1999, ApJS, 123, 3
Lejeune T., Schaerer D., 2001, A&A, 366, 538
Leonard D. C., 2005, IAU Circ., 8579, 2
Leonard D. C. et al., 2002a, PASP, 114, 35
Leonard D. C. et al., 2002b, AJ, 124, 2490
Leonard D. C., Chornock R., Filippenko A. V., 2003a, IAU Circ., 8144, 2
Leonard D. C., Kanbur S. M., Ngeow C. C., Tanvir N. R., 2003b, ApJ, 594, 247
Leonard D. C., Gal-Yam A., Fox D. B., Cameron P. B., Johansson E. M., Kraus A. L., Mignant D. L., van Dam M. A., 2008, PASP, 120, 1259
Levesque E. M., Massey P., Olsen K. A. G., Plez B., Josselin E., Maeder A., Meynet G., 2005, ApJ, 628, 973
Levesque E. M., Massey P., Olsen K. A. G., Plez B., Meynet G., Maeder A., 2006, ApJ, 645, 1102
Li W., Filippenko A. V., van Dyk S. D., 2004, IAU Circ., 8388, 2
Li W., Van Dyk S. D., Filippenko A. V., Cuillandre J.-C., 2005, PASP, 117, 121
Li W., Van Dyk S. D., Filippenko A. V., Cuillandre J.-C., Jha S., Bloom J. S., Riess A. G., Livio M., 2006, ApJ, 641, 1060
Li W., Wang X., Van Dyk S. D., Cuillandre J.-C., Foley R. J., Filippenko A. V., 2007, ApJ, 661, 1013
Li W. D., Modjaz M., Treffers R. R., Filippenko A. V., Leonard D. C., 1998, IAU Circ., 6882, 1
Limongi M., Chieffi A., 2003, ApJ, 592, 404
Limongi M., Chieffi A., 2007, in Di Salvo T. et al., eds, AIP Conf. Ser. Vol. 924, The Multicolored Landscape of Compact Objects and Their Explosive Origins: Cefalu 2006. Am. Inst. Phys., New York, p. 226
Loup C., Zijlstra A. A., Waters L. B. F. M., Groenewegen M. A. T., 1997, A&AS, 125, 419
MacFadyen A. I., Woosley S. E., 1999, ApJ, 524, 262
MacFadyen A. I., Woosley S. E., Heger A., 2001, ApJ, 550, 410
Maíz-Apellániz J., Bond H. E., Siegel M. H., Lipkin Y., Maoz D., Ofek E. O., Poznanski D., 2004, ApJ, 615, L113
Massey P., 2002, ApJS, 141, 81
Massey P., 2003, ARA&A, 41, 15
Massey P., Olsen K. A. G., 2003, AJ, 126, 2867
Massey P., Waterhouse E., DeGioia-Eastwood K., 2000, AJ, 119, 2214
Massey P., DeGioia-Eastwood K., Waterhouse E., 2001, AJ, 121, 1050
Massey P., Plez B., Levesque E. M., Olsen K. A. G., Clayton G. C., Josselin E., 2005, ApJ, 634, 1286
Matheson T., Berlind P., 2001, IAU Circ., 7748, 3
Matheson T., Calkins M., 2001, IAU Circ., 7597, 3
Matheson T., Berlind P., 2002, IAU Circ., 7800, 4
Matheson T., Jha S., Challis P., Kirshner R., Berlind P., 2001a, IAU Circ., 7756, 4
Matheson T., Jha S., Challis P., Kirshner R., Rines K., 2001b, IAU Circ., 7759, 2
Matheson T., Challis P., Kirshner R., Berlind P., 2003, IAU Circ., 8206, 2
Matheson T., Challis P., Kirshner R., Berlind P., 2004a, IAU Circ., 8269, 2
Matheson T., Challis P., Kirshner R., Berlind P., 2004b, IAU Circ., 8304, 4
Matheson T., Challis P., Kirshner R., Berlind P., Huchra J., 2004c, IAU Circ., 8293, 2
Mattila S., Meikle W. P. S., Groeningsson P., Greimel R., Schirmer M., Acosta-Pulido J. A., Li W., 2004, IAU Circ., 8299, 2
Mattila S., Smartt S. J., Eldridge J. J., Maund J. R., Crockett R. M., Danziger I. J., 2008, ApJ, 688, L91
Maund J. R., 2005, PhD thesis, Univ. Cambridge
Maund J. R., Smartt S. J., 2005, MNRAS, 360, 288
Maund J. R., Smartt S. J., Kudritzki R. P., Podsiadlowski P., Gilmore G. F., 2004, Nat, 427, 129
Maund J. R., Smartt S. J., Danziger I. J., 2005a, MNRAS, 364, L33
Maund J. R., Smartt S. J., Schweizer F., 2005b, ApJ, 630, L33
Maund J. R. et al., 2006, MNRAS, 369, 390
Maund J. R., Wheeler J. C., Patat F., Wang L., Baade D., Höflich P. A., 2007, ApJ, 671, 1944
Mayle R., Wilson J. R., 1988, ApJ, 334, 909
Mazzali P. A. et al., 2002, ApJ, 572, L61
Messineo M., Figer D. F., Davies B., Rich R. M., Valenti E., Kudritzki R. P., 2008, ApJ, 683, L155
Meynet G., Maeder A., 2003, A&A, 404, 975
Miller A. A. et al., 2009, ApJ, 690, 1303
Misra K., Pooley D., Chandra P., Bhattacharya D., Ray A. K., Sagar R., Lewin W. H. G., 2007, MNRAS, 381, 280
Misra K., Sahu D. K., Anupama G. C., Pandey K., 2008, MNRAS, 389, 706
Modjaz M., Falco E., 2005, IAU Circ., 8461, 3
Modjaz M. et al., 2008, AJ, 135, 1136
Modjaz M., Kirshner R., Challis P., Calkins M., Hutchins R., 2005, IAU Circ., 8553, 2
Mokiem M. R. et al., 2007, A&A, 473, 603
Moore M., Li W., Filippenko A. V., Chornock R., Foley R. J., 2004, IAU Circ., 8286, 2
Morris T., Podsiadlowski P., 2007, Sci, 315, 1103
Muno M. P. et al., 2006, ApJ, 636, L41
Nadyozhin D. K., 2003, MNRAS, 346, 97
Navasardyan H., Benetti S., Harutyunyan A., Turatto M., 2007, Cent. Bur. Electron. Telegrams, 939, 1
Navasardyan H., Benetti S., Harutyunyan A., Agnoletto I., Bufano F., Cappellaro E., Turatto M., 2008, Cent. Bur. Electron. Telegrams, 1325, 1
Nomoto K., Maeda K., Mazzali P. A., Umeda H., Deng J., Iwamoto K., 2004, in Fryer C. L., ed., Astrophys. Space Sci. Library Vol. 302, Stellar Collapse. Kluwer, Dordrecht, ch. 10
Ofek E. O. et al., 2008, ApJ, 674, 447
Olivares F., Folatelli G., 2007, Cent. Bur. Electron. Telegrams, 1120, 1
Origlia L., Ranalli P., Comastri A., Maiolino R., 2004, ApJ, 606, 862
Parker J. W. et al., 1998, AJ, 116, 180
Pastorello A., 2003, PhD thesis
Pastorello A., Giro E., Altavilla G., Benetti S., 2000, IAU Circ., 7481, 2
Pastorello A. et al., 2004, MNRAS, 347, 74
Pastorello A. et al., 2005, MNRAS, 360, 950

Pastorello A. et al., 2006, MNRAS, 370, 1752
Pastorello A. et al., 2007a, Nat, 449, 1
Pastorello A. et al., 2007b, Nat, 447, 829
Pastorello A. et al., 2007c, MNRAS, 376, 1301
Pastorello A. et al., 2008a, MNRAS, 389, 955
Pastorello A. et al., 2008b, MNRAS, 389, 113
Pastorello A. et al., 2009, MNRAS, 394, 2266
Patat F., Maia M., 1998, IAU Circ., 6888, 1
Patat F., Baade D., Wang L., 2006, Cent. Bur. Electron. Telegrams, 450, 1
Paturel G., Teerikorpi P., Theureau G., Fouqué P., Musella I., Terry J. N., 2002, A&A, 389, 19
Paturel G., Petit C., Prugniel P., Theureau G., Rousseau J., Brouty M., Dubois P., Cambrésy L., 2003, A&A, 412, 45
Pettini M., Pagel B. E. J., 2004, MNRAS, 348, L59
Phillips M., Hamuy M., Roth M., Morrell N., 2003, IAU Circ., 8086, 2
Phillips M. M., Folatelli G., Contreras C., Morrell N., 2006, Cent. Bur. Electron. Telegrams, 729, 1
Pilyugin L. S., Thuan T. X., 2005, ApJ, 631, 231
Pilyugin L. S., Vílchez J. M., Contini T., 2004, A&A, 425, 849
Podsiadlowski P., 1992, PASP, 104, 717
Podsiadlowski P., Joss P. C., Hsu J. J. L., 1992, ApJ, 391, 246
Podsiaklowski P., Hsu J. J. L., Joss P. C., Ross R. R., 1993, Nat, 364, 509
Poelarends A. J. T., Herwig F., Langer N., Heger A., 2008, ApJ, 675, 614
Pols O. R., Tout C. A., Eggleton P. P., Han Z., 1995, MNRAS, 274, 964
Popov D. V., 1993, ApJ, 414, 712
Pozzo M. et al., 2006, MNRAS, 368, 1169
Prantzos N., Boissier S., 2003, A&A, 406, 259
Press W. H., Teukolsky S. A., Vetterling W. T., Flannery B. P., 1992, Numerical Recipes in FORTRAN. The Art of Scientific Computing, 2nd edn. Cambridge Univ. Press, Cambridge
Prieto J., 2006, Cent. Bur. Electron. Telegrams, 731, 1
Prieto J. L. et al., 2008a, ApJ, 681, L9
Prieto J. L., Stanek K. Z., Beacom J. F., 2008b, ApJ, 673, 999
Quimby R. et al., 2004, IAU Circ., 8446, 1
Quimby R. M., Aldering G., Wheeler J. C., Höflich P., Akerlof C. W., Rykoff E. S., 2007, ApJ, 668, L99
Richardson D., Branch D., Casebeer D., Millard J., Thomas R. C., Baron E., 2002, AJ, 123, 745
Richmond M. W., Modjaz M., 2005, IAU Circ., 8555, 2
Ritossa C., García-Berro E., Iben I. J., 1999, ApJ, 515, 381
Roy J.-R., Walsh J. R., 1997, MNRAS, 288, 715
Rubin K. H. R., Williams K. A., Bolte M., Koester D., 2008, AJ, 135, 2163
Ruiz-Lapuente P., Benetti S., Balastegui A., Basa S., Guide D., Mendez J., Raux J., Turatto M., 2002, IAU Circ., 8028, 3
Ryder S. D., Murrowood C. E., Stathakis R. A., 2006, MNRAS, 369, L32
Sahu D. K., Anupama G. C., Srividya S., Muneer S., 2006, MNRAS, 372, 1315
Salvo M., Schmidt B., Keller S., 2004, IAU Circ., 8432, 2
Salvo M., Blackman J., Schmidt B., Bessell M., 2006, Cent. Bur. Electron. Telegrams, 557, 1
Schaller G., Schaerer D., Meynet G., Maeder A., 1992, A&AS, 96, 269
Schawinski K. et al., 2008, Sci, 321, 223
Schlegel D. J., Finkbeiner D. P., Davis M., 1998, ApJ, 500, 525
Schmidt B., Salvo M., 2005, IAU Circ., 8496, 2
Schroder K.-P., Pols O. R., Eggleton P. P., 1997, MNRAS, 285, 696
Siess L., 2006, A&A, 448, 717
Siess L., 2007, A&A, 476, 893
Simon J. D. et al., 2007, ApJ, 671, L25
Simón-Díaz S., Herrero A., Esteban C., Najarro F., 2006, A&A, 448, 351
Singer D., Pugh H., Li W., 2004, IAU Circ., 8297, 2
Smartt S. J., Gilmore G. F., Trentham N., Tout C. A., Frayn C. M., 2001, ApJ, 556, L29
Smartt S. J., Ramirez-Ruiz E., Vreeswijk P., 2002a, IAU Circ., 7816, 3
Smartt S. J., Gilmore G. F., Tout C. A., Hodgkin S. T., 2002b, ApJ, 565, 1089
Smartt S. J., Maund J. R., Gilmore G. F., Tout C. A., Kilkenny D., Benetti S., 2003, MNRAS, 343, 735
Smartt S. J., Maund J. R., Hendry M. A., Tout C. A., Gilmore G. F., Mattila S., Benn C. R., 2004, Sci, 303, 499
Smith L. J., Westmoquette M. S., Gallagher J. S., O'Connell R. W., Rosario D. J., de Grijs R., 2006, MNRAS, 370, 513
Smith N. et al., 2007, ApJ, 666, 1116
Smith N., Chornock R., Li W., Ganeshalingam M., Silverman J. M., Foley R. J., Filippenko A. V., Barth A. J., 2008a, ApJ, 686, 467
Smith N., Chornock R., Li W., Ganeshalingam M., Silverman J. M., Foley R. J., Filippenko A. V., Barth A. J., 2008b, ApJ, 686, 467
Smith N., Ganeshalingam M., Li W., Chornock R., Steele T. N., Silverman J. M., Filippenko A. V., Mobberley M. P., 2008c, ApJL, submitted (arXiv:0811.3929)
Soderberg A. M., Chevalier R. A., Kulkarni S. R., Frail D. A., 2006, ApJ, 651, 1005
Sofia U. J., Meyer D. M., 2001, ApJ, 554, L221
Solanes J. M., Sanchis T., Salvador-Solé E., Giovanelli R., Haynes M. P., 2002, AJ, 124, 2440
Stancliffe R. J., 2006, MNRAS, 370, 1817
Stanishev V., Pastorello A., Pursimo T., 2008, Cent. Bur. Electron. Telegrams, 1235, 1
Stockdale C. J., Williams C. L., Weiler K. W., Panagia N., Sramek R. A., Van Dyk S. D., Kelley M. T., 2007, ApJ, 671, 689
Stolte A., Brandner W., Brandl B., Zinnecker H., 2006, AJ, 132, 253
Takáts K., Vinkó J., 2006, MNRAS, 372, 1735
Taubenberger S., Pastorello A., Benetti S., Aceituno J., 2005a, IAU Circ., 8474, 3
Taubenberger S., Pastorello A., Mazzali P. A., Witham A., Guijarro A., 2005b, Cent. Bur. Electron. Telegrams, 305, 1
Thompson L. A., 1982, ApJ, 257, L63
Thompson T. A., Prieto J. L., Stanek K. Z., Kistler M. D., Beacom J. F., Kochanek C. S., 2009, ApJ, in press (arXiv:0809.0510)
Tonry J. L., Blakeslee J. P., Ajhar E. A., Dressler A., 2000, ApJ, 530, 625
Trundle C., Dufton P. L., Lennon D. J., Smartt S. J., Urbaneja M. A., 2002, A&A, 395, 519
Trundle C., Dufton P. L., Hunter I., Evans C. J., Lennon D. J., Smartt S. J., Ryans R. S. I., 2007, A&A, 471, 625
Trundle C., Kotak R., Vink J. S., Meikle W. P. S., 2008, A&A, 483, L47
Tsvetkov D. Y., 2006, Peremennye Zvezdy, 26, 3
Tsvetkov D. Y., Volnova A. A., Shulga A. P., Korotkiy S. A., Elmhamdi A., Danziger I. J., Ereshko M. V., 2006, A&A, 460, 769
Turatto M., 2000, Mem. Soc. Astron. Ital., 71, 573
Turatto M. et al., 1998, ApJ, 498, L129
Turatto M., Benetti S., Cappellaro E., 2003, in Hillebrandt W., Leibundgut B., eds, in Proc. ESO/MPA/MPE Workshop, From Twilight to Highlight: The Physics of Supernovae Variety in Supernovae. Springer, Heidelberg, p. 200
Umbriaco G., Pietrogrande T., di Mille F., Agnoletto I., Harutyunyan A., Benetti S., 2007, Cent. Bur. Electron. Telegrams, 1174, 1
Utrobin V. P., Chugai N. N., 2008, A&A, 491, 507
Utrobin V. P., Chugai N. N., Pastorello A., 2007, A&A, 475, 973
Valenti S. et al., 2008a, MNRAS, 383, 1485
Valenti S. et al., 2008b, ApJ, 673, L155
Valentini G. et al., 2003, ApJ, 595, 779
van den Bergh S., Li W., Filippenko A. V., 2005, PASP, 117, 773
van Dyk S. D., 1992, AJ, 103, 1788
van Dyk S. D., Hamuy M., Filippenko A. V., 1996, AJ, 111, 2017
Van Dyk S. D., Peng C. Y., Barth A. J., Filippenko A. V., 1999, AJ, 118, 2331
Van Dyk S. D., Garnavich P. M., Filippenko A. V., Höflich P., Kirshner R. P., Kurucz R. L., Challis P., 2002, PASP, 114, 1322
Van Dyk S. D., Li W., Filippenko A. V., 2003a, PASP, 115, 1
Van Dyk S. D., Li W., Filippenko A. V., 2003b, PASP, 115, 448
Van Dyk S. D., Li W., Filippenko A. V., 2003c, PASP, 115, 1289
Van Dyk S. D., Li W., Filippenko A. V., Humphreys R. M., Chornock R., Foley R., Challis P. M., 2006, PASP, submitted (astro-ph/0603025)
van Loon J. T., Hekkert P. T. L., Bujarrabal V., Zijlstra A. A., Nyman L.-A., 1998, A&A, 337, 141

van Loon J. T., Cioni M.-R. L., Zijlstra A. A., Loup C., 2005, A&A, 438, 273
van Loon J. T., Marshall J. R., Cohen M., Matsuura M., Wood P. R., Yamamura I., Zijlstra A. A., 2006, A&A, 447, 971
van Zee L., Salzer J. J., Haynes M. P., O'Donoghue A. A., Balonek T. J., 1998, AJ, 116, 2805
Vink J. S., de Koter A., Lamers H. J. G. L. M., 2001, A&A, 369, 574
Vinko J., Takáts K., Sárneczky K., Szabó G. M. et al., 2006, MNRAS, 369, 1780
Vinko J. et al., 2008, preprint (arXiv:0812.1589)
Voss R., Nelemans G., 2008, Nat, 451, 802
Wagner R. M. et al., 2004, PASP, 116, 326
Walborn N. R., Prevot M. L., Prevot L., Wamsteker W., Gonzalez R., Gilmozzi R., Fitzpatrick E. L., 1989, A&A, 219, 229
Wang X., Yang Y., Zhang T., Ma J., Zhou X., Li W., Lou Y.-Q., Li Z., 2005, ApJ, 626, L89
Wang X. et al., 2008, ApJ, 675, 626
Waxman E., Draine B. T., 2000, ApJ, 537, 796
Wei J. Y., Cao L., Qiu Y. L., Qiao Q. Y., Hu J. Y., Gu Q. S., 1999, IAU Circ., 7124, 1
Weis K., Bomans D. J., 2005, A&A, 429, L13
Weis K., Bomans D. J., Klose S., Spiller F., 2004, IAU Circ., 8384, 4
Williams K. A., Bolte M., Koester D., 2009, ApJ, preprint (arXiv:0811.1577)
Wood-Vasey W. M., Aldering G., Nugent P., Beutler B., Martin P., Papenkova M., Filippenko A. V., Hamuy M., 2002, IAU Circ., 7999, 1
Woosley S. E., Bloom J. S., 2006, ARA&A, 44, 507
Woosley S. E., Eastman R. G., Weaver T. A., Pinto P. A., 1994, ApJ, 429, 300
Woosley S. E., Heger A., Weaver T. A., 2002, Rev. Mod. Phys., 74, 1015
Woosley S. E., Blinnikov S., Heger A., 2007, Nat, 450, 390
Young D. R., Smartt S. J., Mattila S., Tanvir N. R., Bersier D., Chambers K. C., Kaiser N., Tonry J. L., 2008, A&A, 489, 359
Young T. R., Smith D., Johnson T. A., 2005, ApJ, 625, L87
Zampieri L., Shapiro S. L., Colpi M., 1998, ApJ, 502, L149
Zampieri L., Pastorello A., Turatto M., Cappellaro E., Benetti S., Altavilla G., Mazzali P., Hamuy M., 2003, MNRAS, 338, 711
Zaritsky D., Kennicutt R. C., Jr, Huchra J. P., 1994, ApJ, 420, 87
Zhang T., Wang X., Li W., Zhou X., Ma J., Jiang Z., Chen J., 2006, AJ, 131, 2245

APPENDIX A: COMPLETE LIST OF SNe EMPLOYED IN THE SURVEY FOR PROGENITORS

Table A1. SNe discovered between 1998 and 2008.5 in galaxies with recessional velocities less than 2000 km s^{-1}. The *HST* FOV column notes if the host galaxy has been observed by *HST* prior to explosion and if the position of the SN is 'in' or 'out' of the camera FOV. The full table is available in the online appendix.

Supernova	Galaxy	V_{vir}	Type	*HST* FOV	Comments
Core-collapse					
1998A	IC2627	1975.7	IIpec	–	Pastorello et al. (2005), SN1987A-like
1998S	NGC 3877	1114.8	IIn	–	Fassia et al. (2001)
1998bm	IC2458	1809.7	II	–	Li et al. (1998), unknown subtype
1998bv	PGC2302994	1793.7	II-P	–	Kniazev et al. (1998)
1998dl	NGC 1084	1298.2	II-P	–	Filippenko & De Breuck (1998a)
1998dn	NGC 337A	997.1	II	–	Gómez & López (2000), unknown subtype
1999B	UGC7189	1962.1	II	–	Filippenko, Leonard & Riess (1999a), unknown subtype
1999an	IC 755	1607.2	II	in	Wei et al. (1999), unknown subtype
1999bg	IC758	1530	II-P	–	Ayani & Yamaoka (1999), amateur LC
1999br	NGC 4900	1012.6	II-P	in	Pastorello et al. (2004), low-luminosity II-P
1999bw	NGC 3198	850.9	LBV	out	Filippenko et al. (1999b)[a]
1999el	NGC 6951	1704.2	IIn	out	Di Carlo et al. (2002)
1999em	NGC 1637	615.2	II-P	out	Leonard et al. (2002a)

[a] http://etacar.umn.edu/etainfo/related/

SUPPORTING INFORMATION

Additional Supporting Information may be found in the online version of this article.

Table A1. SNe discovered between 1998 and 2008.5 in galaxies with recessional velocities less than 2000 km s^{-1}.

Please note: Wiley-Blackwell are not responsible for the content or functionality of any supporting information supplied by the authors. Any queries (other than missing material) should be directed to the corresponding author for the article.

This paper has been typeset from a TEX/LATEX file prepared by the author.